SYNTHESIS, SPECTROSCOPIC INVESTIGATION AND IMMOBILIZATION OF

COPPER(II) COMPLEXES AS OXIDATION CATALYSTS

Except where reference is made to the work of others, the work described in this dissertation is my own or was done in collaboration with my advisory committee. This dissertation does not include proprietary or classified information.

_____

Moses G. Gichinga

Certificate of approval:

_____

Peter Livant
Associate Professor
Chemistry and Biochemistry

_____

Susanne Striegler, Chair
Assistant Professor
Chemistry and Biochemistry

_____

David Stanbury
Professor
Chemistry and Biochemistry

_____

S. Davis Worley
Professor
Chemistry and Biochemistry

_____

George Flowers
Dean
Graduate School

SYNTHESIS, SPECTROSCOPIC INVESTIGATION AND IMMOBILIZATION OF COPPER(II) COMPLEXES AS OXIDATION CATALYSTS

Moses G. Gichinga

A Dissertation

Submitted to

the Graduate Faculty of

Auburn University

in Partial Fulfillments of the

Requirements for the

Degree of

Doctor of Philosophy

Auburn, AL
August 10, 2009

SYNTHESIS, SPECTROSCOPIC INVESTIGATION AND IMMOBILIZATION OF COPPER(II) COMPLEXES AS OXIDATION CATALYSTS

Moses G. Gichinga

_____

Signature of Author

_____

Date of Graduation

VITA

Moses Gichinga, son of Joseph Gichinga and Hannah Wangui, was born on June 2, 1980 in Kenya. He graduated with a Bachelor of Science degree in Chemistry in May, 2004 from University of Nairobi, Kenya. In the fall of 2004, he entered the Graduate School in the Department of Chemistry and Biochemistry at Auburn University. In January of 2005, he joined the laboratory of Dr. Susanne Striegler and is currently pursuing a Ph.D. degree.

DISSERTATION ABSTRACT

SYNTHESIS, SPECTROSCOPIC INVESTIGATION AND IMMOBILIZATION OF COPPER(II) COMPLEXES AS OXIDATION CATALYSTS

Moses G. Gichinga

Doctor of Philosophy, August 10, 2009
(B. S., University of Nairobi, 2004)

193 Typed Pages

Directed by Susanne Striegler

Schiff-base complexes that function as catalysts in aqueous media have been developed. The design of environmentally benign metal catalysts with multidentate ligands is a field of intense current interest. Transition metal complexes with Schiff-base ligands offer a promising route towards discovery of novel catalysts due to the ease of their synthesis, which allows structural modification for optimization of the catalytic sites. Bis(salicylaldehyde)-based complexes, for example, can be modified by derivatizing the ligand backbone to present desirable properties like enhanced solubility in water. Derivatization of 2,4-dihydroxybenzaldehyde at the more reactive 4-position has generated structurally diverse precursor aldehydes for synthesis of pentadentate Schiff-base ligands. Polyethylene glycol side chains attached at the 4-hydroxyl group of 2,4-dihydroxybenzaldehydes has resulted in new water-soluble ligands. These ligands coordinate to copper(II) acetate resulting in binuclear copper(II) Schiff-base complexes

that have been shown to catalyze the aerobic oxidation of model catechol, 3,5-ditertbutyl catechol, faster in aqueous methanol than in pure methanol. Derivatization of 2,4-dihydroxybenzaldehyde with *p*-vinylbenzyl group resulted in a polymerizable precursor aldehyde that led to synthesis of a polymerizable Schiff-base ligand. A homogeneous catalytic system was developed in which this polymerizable ligand was anchored on a polymer support derived from styrene and butyl acrylate by miniemulsion polymerization. The macromolecular polymeric catalyst was found to have superior catalytic properties over small molecular weight analogues.

Reduced Schiff-base complexes based on bis-pyridyl ligands were also explored as catalysts because they provide flexible metal-binding properties due to reduction of the rigid azomethine bond to a less constrained amine moiety. These bis(pyridyl)-based catalysts were found to have higher glycosidase activity than bis(salicyaldehyde)-based catatalysts at pH 10.5.

To further modify the catalytic sites of the catalysts and provide possible selectivity, asymmetric binuclear copper(II) complexes were synthesized by modifying the precursor diamine from symmetric 1,3-diamino-2-propanol to asymmetric 1,4-diamino-2-butanol.

ACKNOWLEDGMENTS

First and foremost, I would like to express my appreciation and thanks to my advisor, Dr. Susanne Striegler, for her guidance and encouragement throughout my studies here at Auburn University. My dissertation would not be possible without her advice and undying devotion to this research. Secondly, I thank my committee members Dr. Peter Livant, Dr. S. Davis Worley, Dr. David Stanbury and Dr. Gisela Büschle-Diller for their helpful discussions and constructive suggestions to my dissertation.

I especially express my gratitude to my parents Joseph Gichinga and Hannah Wangui, my brothers and sisters Njoki, Githuka, Kiarie and Muthoni for their support and encouragement during my graduate studies. And last, but certainly not least, I thank the Department of Chemistry and Biochemistry and the National Science Foundation for their monetary support.

Style manual used: Journal of the American Chemical Society

Computer software used: Microsoft Word 2007, ChemDraw 11.0, Origin 7.0, Win-NMR 5.1

TABLE OF CONTENTS

LIST OF TABLES

LIST OF SCHEMES

LIST OF FIGURES

LIST OF PUBLICATIONS

This work has resulted in the following publications.

1. Gichinga, M. G.; Striegler, S. *Tetrahedron* **2009**, *65(25)*, 4917-4922.

2. Gichinga, M. G.; Striegler, S, *Catalysis of Organic Reactions, (M. L. Prunier, Ed.)* **2008**, 53, 473-477.

3. Striegler, S.; Gichinga, M. G. *Chem. Commun.* **2008**, 5930-5932.

4. Gichinga, M. G.; Striegler, S. *J. Am. Chem. Soc.* **2008**, *130(15)*, 5150-5156.

5. Striegler, S.; Gichinga, M. G.; Dittel, M. *Org. Lett.* **2008**, *10(2)*, 241-244.

CHAPTER ONE

INTRODUCTION

1.1 Schiff-base complexes

Schiff base complexes, named after Hugo Schiff (1834 – 1931), have over the years played an important role in coordination chemistry because they form stable complexes with most transition metals in different oxidation states.[1] They are also straight forward to prepare; hence, a library of structurally diverse complexes can easily be generated allowing adjustments in steric and electronic properties.

Schiff-bases have been used for various applications including catalysis, as antiviral agents, and for corrosion protection.[2-4] Furthermore, they have been immobilized on solid supports for various applications in two distinct ways. One method involves immobilization on organic polymeric structures such as polystyrene where a monomer is covalently linked to the ligand used for polymerization.[5] The second method involves use of inorganic supports like silica or alumina.[6,7] Some inorganic supports like silica, however, have acidic groups that cause deactivation of the catalysts.[8,9] Supported Schiff-base complexes have been shown to have higher catalytic activities and selectivity than non-immobilized complexes. Zhou et al. showed that an immobilized chromium(III) Schiff-base complex exhibited significantly higher enantioselectivity towards epoxidation of alkenes than unsupported complexes.[8] Similarly, Gupta and Sutar showed that polymer

anchored Schiff-base complexes of iron(III), nickel(II) and cobalt(II) were more catalytically active than unsupported catalysts towards phenol oxidation.[9] The remarkable stereoselectivity, and rate acceleration of the immobilized complexes can be attributed to well-organized three dimensional structures with both catalytic and binding sites for the substrates.

Development of polymeric catalyst supports like microgels that function as water-soluble homogeneous catalysts is a big step towards green chemistry. This can be achieved by use of miniemulsion polymerization. Miniemulsion polymerization provides improved control over properties such as size, shape and surface functionalities of polymeric particles. Although Schiff-bases are the most widely used ligands in coordination chemistry, there are no studies involving immobilization of Schiff-base complexes into microgels by miniemulsion polymerization.[10] In this work, we assembled a Schiff-base complex into a microgel and investigated oxidative catalytic activities in aqueous media.

1.2 Organic reactions in water

Water is obviously the most abundant and environmentally benign solvent. In Nature, formation of chemical bonds occurs in aqueous media and at relatively low temperatures. Inspired by Nature, many organic chemists think of water as a versatile solvent for organic reactions. Since Breslow and Rideout reported that Diels-Alder reaction could be accelerated by using water instead of organic solvents, there has been considerable interest in development of organic reactions in water.[11] The underlying

principle behind chemical reactions in water is the hydrophobic effect that occurs when organic compounds are dissolved in water. The effect of water as a solvent has been studied in various organic transformations including Claisen-rearrangements, aldol reactions, hydrogenations and oxidations.[12]

1.3 Alcohol oxidation

Transformation of alcohols into carbonyl compounds is one of the most important organic reactions both in the laboratory and in industry. Traditionally, this transformation is done in environmentally unfavorable conditions like in chlorinated solvents and is based on stoichiometric or substoichiometric transition metal reagents like Cr and Mn, or moisture sensitive oxidants such as *N,N'*-dicyclohexylcarbodiimide (DCC) and oxalyl chloride.[13-23] Use of these transition metals leads to creation of many toxic wastes that are problematic to dispose. Numerous research efforts are therefore geared towards search for better alternatives using transition metals like Ru, Cu, V, Ni, Co and Pd in catalytic amounts to transform alcohols into aldehydes using molecular oxygen as an oxidant (Scheme 1.1).[24-32]

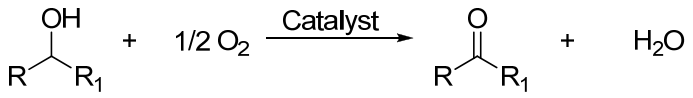

Scheme 1.1. Oxidation of alcohols using molecular oxygen

Molecular oxygen as an oxidant is clean, inexpensive and environmentally desirable.[33] However, these catalytic systems have some drawbacks like deactivation of the catalysts

by formation of metallic polymers, instability of the carbonyl compounds formed in the reaction mixture, and formation of stable complexes between the metal salts and alcohol substrates.[34] Design of efficient catalysts that are capable of transforming a wide range of alcohol substrates including primary, secondary, phenolic and allylic alcohols is a desirable step in development of synthetic organic chemistry. In this work, we designed, synthesized and characterized Schiff-base type copper(II) complexes and used them to study the oxidation of phenols in aqueous media.

1.4 Catalytic oxidation of alcohols in water

There are recently tremendous efforts geared towards development of efficient immobilized catalysts for oxidation of alcohols in aqueous media.[35] These catalytic systems are mainly composed of transition metal complexes. Biffis et al. described microgel-stabilized gold clusters that exhibit remarkable catalytic activity in aerobic oxidation of aliphatic and benzylic alcohols.[36] In another example, Yiochi et al. reported a dispersion of platinum particles that catalyzes the aerobic oxidation of alcohols in water. This catalyst was applicable in a wide range of alcohol substrates including benzylic, allylic, alicyclic and aliphatic alcohols. In similar studies, Uozumi and Nakao reported a palladium catalyst for alcohol oxidation in water.[23] Liu et al. described a catalytic system for oxidation of benzylic alcohols in water without the use of transition metals. The catalyst was comprised of nitroxyl radical 2,2,6,6-tetramethylpiperidyl-1-oxy (TEMPO), Br_2 and $NaNO_2$ as co-catalysts.[37] This catalytic system was capable of transforming alcohols to corresponding aldehydes or ketones using oxygen as the

oxidant. Although much work has been done to find an efficient catalyst for oxidation of alcohols, development of regioselective "green" catalysts remains a challenge. Moreover, most of the reported catalytic alcohol oxidations in water exhibit low turnovers which are usually compensated by addition of less "green" additives like strong bases and phase transfer catalysts.[38]

Development of catalysts for transformation of biomolecules like carbohydrates calls for a regioselective catalyst capable of transforming only one functionality in a molecule with several functionalities.[39] This approach would circumvent tedious use of protecting groups. A long term goal in our laboratory is to design catalytic systems capable of transforming underivatized carbohydrates into hexose-6-carbaldehydes as precursors for unnatural carbohydrates. The first step towards achieving this goal involves immobilization of Schiff-base complexes into microgels to tailor water-soluble homogeneous catalysts.

1.5 Water soluble Schiff-base complexes

Schiff-base complexes are typically insoluble in water because they lack sufficiently polar or ionic groups. In 1955, Mukherjee described the synthesis of a water-soluble Schiff-base complex by sulfonating the ligand backbone using concentrated sulfuric acid (Scheme 1.2).[40]

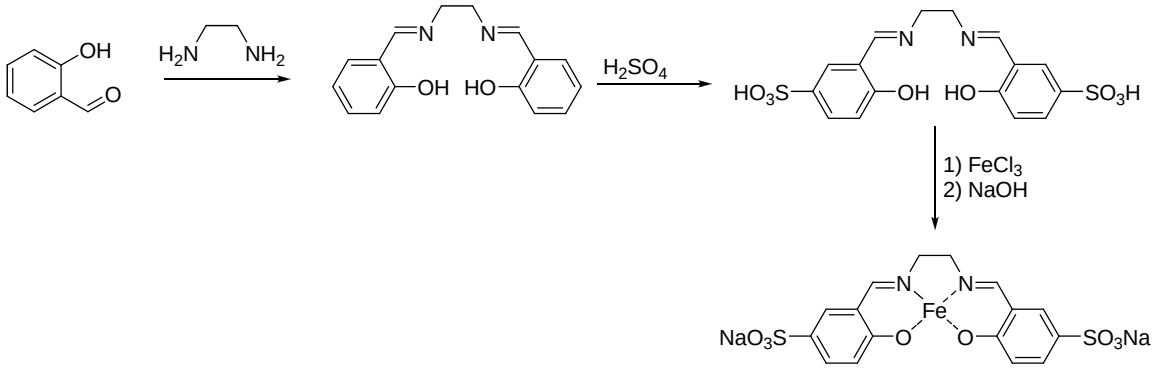

Scheme 1.2. Synthesis of a water-soluble Schiff base complex

The sulfonated ligand was complexed with ferric chloride followed by neutralization of the sulfonic acid group using sodium hydroxide. Schiff bases are, however, prone to undergo hydrolysis in acidic conditions. This synthetic pathway is therefore likely to result in poor yields. An alternative pathway that is commonly used begins with sulfonation of the starting salicylaldehyde followed by condensation with an amine to form a water-soluble ligand.[41-43] The ligand is finally reacted with a metal salt like vanadyl sulfate or manganese(II) acetate to obtain the desired Schiff-base complex. Another common functional group used to promote water solubility in Schiff-bases is the phosphonium group.[44] Use of poly(ethylene glycol) (PEG) to enhance water solubility in Schiff-bases is rare despite their favorable properties. Attachment of PEGs to small-molecule drugs is known to enhance their water-solubility, reduce toxicity and decrease enzymatic degradation.[45]

1.6 Miniemulsion polymerization

The principle of miniemulsion polymerization was first described by Ugelstad et al.[46] in the early 1970s and since then has become a very promising technique for polymerization in aqueous disperse systems.[47,48] Miniemulsion polymerization is a method of polymerization within stabilized dispersions with particle diameters ranging between 50 and 500 nm. Miniemulsions are formed by application of high shear to a system composed of water, oil (monomer), surfactant and a cosurfactant.[49]

In a typical miniemulsion polymerization, the surfactant is dissolved in water, the costabilizer is dissolved in the monomers and the solutions mixed by strirring. The mixture is then subjected to a high shear by means of shear devices like sonifiers that generate ultrasound waves (Figure 1.1).

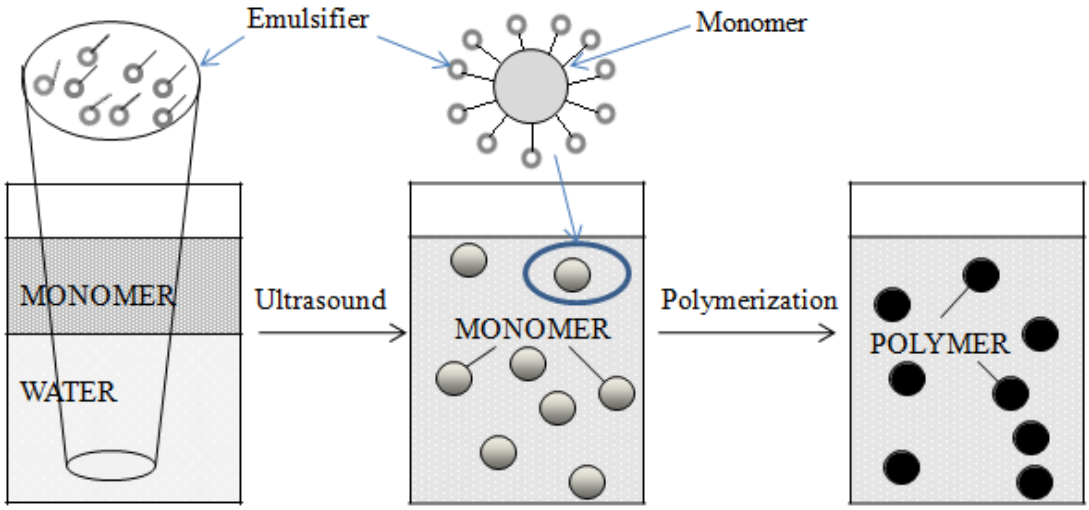

Figure 1.1. Process of miniemulsion polymerization

The high shear causes formation of small monomer droplets that are polymerized by addition of an appropriate initiator to form miniemulsion polymers. Since

polymerization is initiated in the stabilized monomer droplets, the size of miniemulsion polymer droplets is identical to the size of monomer droplets.[50] The stability of the miniemulsion is achieved by use of a surfactant and a small amount of hydrophobic agent called co-surfactant or hydrophobe. The hydrophobe prevents the monomer from diffusing into the aqueous phase leading to droplet degradations or Ostwald ripening while surfactant prevents the droplets from coalescence upon collision.[51]

A wide variety of miniemulsion formulations have been developed to generate miniemulsion polymers with different properties for certain applications.[52-59] Different monomers including styrene, methyl acrylate, butyl acrylate, vinyl acetate and methyl methacrylate with a wide range of properties can be polymerized by miniemulsion polymerization (Table 1.1).

Table 1.1. Examples of literature formulations used for miniemulsion polymerization

Monomer[a]	Surfactant[b]	Cosurfactant[c]	Initiator[d]	Reference
Styrene	SLS	HD	AIBN	Huang et al.[53]
Styrene	SDS	PU	^{60}Co γ–ray	Wang et al.[48]
Styrene	SDS	LPB	KPS	Jia et al.[54]
Styrene	SDS	HD	HRP	Qi et al.[60]
Styrene/ Butyl acrylate	SDS	SM	KPS	Cai et al.[52]
Methyl acrylate	SLS	DM	KPS	Mouran et al.[56]
Butyl acrylate	SDS	HD	KPS	Luo et al.[55]
Styrene/ MMA	SLS	HD	AIBN	Rodriguez et al.[59]
Styrene/MPS	SDS	HD	KPS	Ni et al.[57]
Butyl acrylate/MMA	PVA	HD	APS	Kim et al.[61]
Butyl acrylate/MMA	SDS	None	US	Bradley et al.[62]
VAc	SDS	HD	APS	Graillat and Guyot.[63]
Butyl acrylate/ Vac	SDS	HD	KPS	Oh et al.[64]

[a] *Monomers*. MMA: Methyl methacrylate; MPS: 3-trimethoxysilylpropylmethacrylate silane; Vac: Vinyl acetate.
[b] *Surfactant*. SLS: Sodium lauryl sulfate; SDS: sodium dodecyl sulfate; PVA Poly(vinyl alcohol).
[c] *Cosurfactant*. HD: Hexadecane; PU: polyurethane; DM: dodecyl methacrylate; LPB: Liquid polybutadiene;
[d] *Initiator*. AIBN: 2,2′-Azobis(isobutyronitrile); HRP: Horseradish peroxidase; KPS: Potassium persulfate; US: Ultrasound; APS: Ammonium persulfate.

In addition, monomer mixtures like styrene and butyl acrylate have been employed in preparation of polymers by miniemulsion polymerization.[52] Hexadecane is

one the most commonly used co-surfactant for stabilization of miniemulsions.[65] Different kinds of initiators have been employed for miniemulsion polymerization including gamma radiation,[48] enzymatic initiators,[60] ultrasound,[62] and free radical initiators like potassium persulfate[54,56,57] and 2,2′-azobis(isobutyronitrile).[53] Most of the recipes described in preparation of miniemulsions are based on the use of an anionic surfactant sodium dodecyl sulfate (SDS).[48,52,54,55,57,58,62-64] Non-ionic polymeric surfactants like poly(vinyl alcohol) are able to modify rheological properties and enhance mechanical stability of the miniemulsions in applications such as paints and inks.[61]

1.7 Applications of miniemulsion polymerization

The method of miniemulsion polymerization has generated substantial interest because of its versatile nature (Table 1.1).[52-59,61-64] Polymers obtained by miniemulsion polymerization are stable and isotropic. Miniemulsion polymerization has been used to develop new polymeric products that are not accessible by conventional emulsion polymerization methods. The principle behind making stable miniemulsions i.e. introduction of a hydrophobe into the monomer droplet has been extended to encapsulate inorganic particles into polymer matrices for application in pharmaceuticals, paint production and cosmetics.[65] Landfester et al. showed that magnetite particles can be dispersed in monomer miniemulsion droplets becoming encapsulated upon polymerization.[66] These polymer-coated magnetic particles can be used for biomedical applications such as magnetic drug targeting.

Inorganic and organic particles in emulsions have received a lot of attention in recent years for application in adhesives, paints, drug-delivery, and in catalysis.[67] TiO_2 particles have been encapsulated through miniemulsion polymerization into polystyrene[68] and styrene/*n*-butylacrylate copolymers[69] in order to overcome aggregation and to provide uniform particles. Liu et al. showed that TiO_2 miniemulsion droplets immobilized in polyurea were catalytically active towards degradation of methyl orange, a non-biodegradable industrial pollutant.[70] They also showed that the immobilized TiO_2 polymeric catalyst was reusable three times with no loss of activity.

Naundorf et al. designed a polymeric support based on miniemulsion polymerization that is functionalized with pyridine and poly(ethylene oxide) moieties for immobilization of a titanium complex (bis[*N*-(3-*t*-butylsalicylidene)cycloheptylaminato] titanium(IV) dichloride) (Figure 1.2).[71]

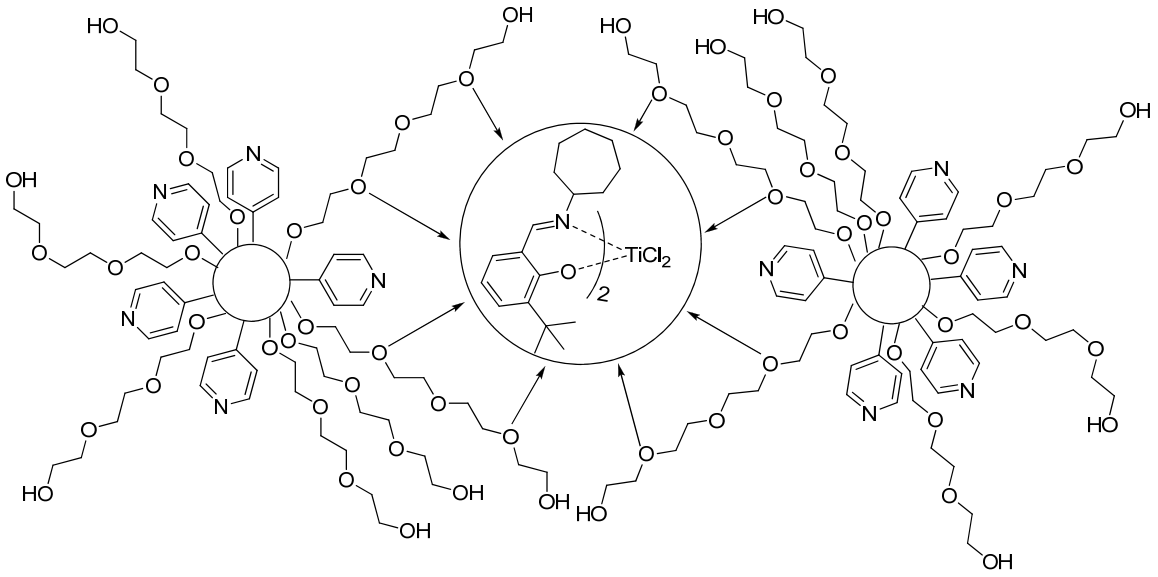

Figure 1.2. Immobilization of bis[*N*-(3-*t*-butylsalicylidene)cycloheptylaminato]titanium(IV) dichloride complex

The nucleophilic substituents on the surface of the polymer were shown to support the bis(phenoxy-imine) titanium complex through non-covalent bonding. The immobilized complex was used to catalyze ethylene polymerization. By adjusting the concentration of the pyridyl groups on the surface of the latex particles and optimizing the crosslinking of the support, the catalyst resulted in the formation of polyethylene with a weight-average molecular weight (M_w) of more than 6,000,000. In another study Jang et al. showed that miniemulsion polymerization of styrene, divinylbenzene and polypropylene oxide functionalized styrene afforded polymer particles that support a metallocene zirconium complex (Figure 1.3).[72]

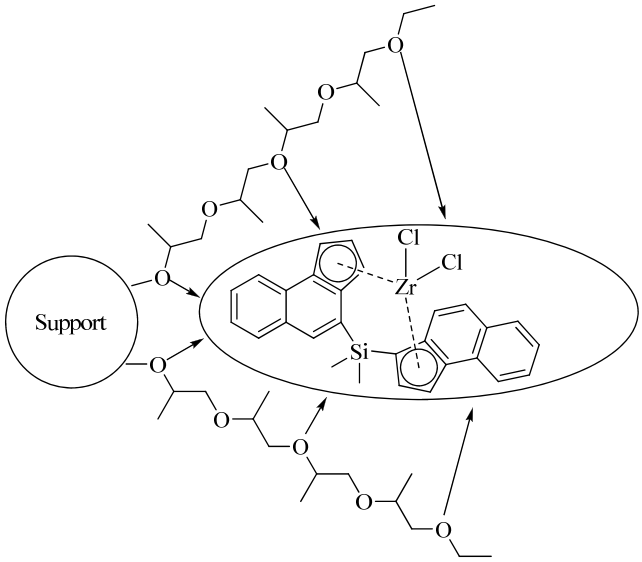

Figure1.3. Immobilization of zirconium complex

This supported metallocene complex was shown to catalyze the homopolymerization of ethylene and copolymerization of ethylene with several comonomers like 1-octene and 1-hexane. Mecking et al. immobilized a phenoxy-imine nickel complex into a polymeric matrix by miniemulsion polymerization that was shown to catalyze the polymerization of ethylene.[73]

CHAPTER TWO

CATALYST DESIGN

2.1 Design of water-soluble catalysts

The design of an efficient catalyst for the oxidation of alcohols was inspired by enzymes. Enzymes typically operate in an aqueous medium and at low temperatures.[74] Enzymatic catalysis in organic solvents has however been shown to provide some technological advantages over catalysis in water, like enhanced solubility of the enzymes in organic solvents, easy recovery of products, and has led to successful commercial processes.[75] However, catalytic activity in an organic solvent is often drastically lower than that in water.[76,77] It was therefore proposed to design catalysts that are applicable in aqueous media and hence soluble in water. Schiff-base complexes were chosen because they are easy to prepare,[2] stable[78] and applicable in various fields such as catalysis and materials chemistry.[79]

A large number of Schiff-base complexes have been reported that are based on the salicylaldehyde moiety.[80-83] Typically, the salicyldehyde is reacted with an aromatic or aliphatic amine to form a Schiff-base ligand. The ligand is then coordinated to a metal salt to form a metal complex.

In order to make the Schiff-base complexes soluble in water and applicable in aqueous media just like enzymes, it was proposed to introduce water

solubility promoting groups into the Schiff-base ligand backbone. Commercially available 2,4-dihydroxybenzaldehyde was envisioned to be a suitable starting aldehyde because its 4-hydroxyl group could be selectively functionalized while leaving the 2-hydroxyl group intact and available for coordination to metal ions (Scheme 2.1).

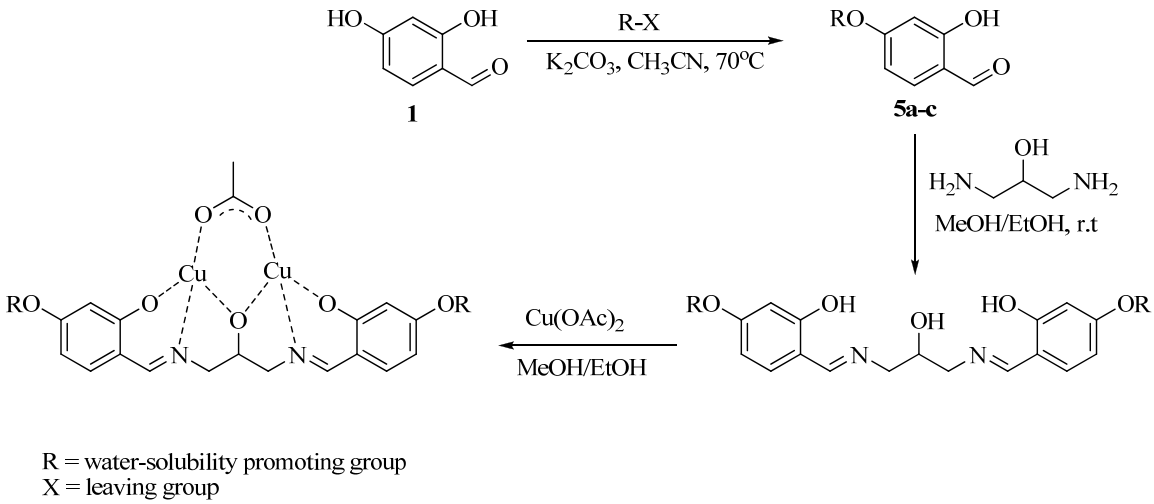

Scheme 2.1.General scheme for the synthesis of copper(II) complexes

2.2 Derivatization of 2,4-dihydroxybenzaldehyde

In the early stages of this work, selective benzylation of 2,4-dihydroxybenzaldehyde (**1**) at the 4-hydroxy group with benzyl chlorides or bromides was achieved in moderate to good yields by using catalytic amount of potassium iodide[84,85] (Table 2.1). The monosubstituted salicylaldehydes were characterized using ^{1}H and ^{13}C NMR spectroscopy.

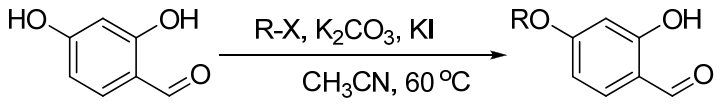

1 **2a-e**

Table 2.1. Summary of benzylation reactions with 2,4-dihydroxybenzaldehyde

Compound	R-X	Yield [%]
2a	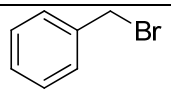	64
2b	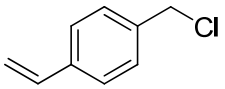	74
2c	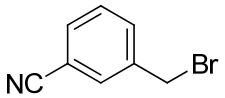	85
2d	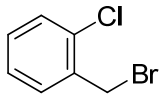	50
2e	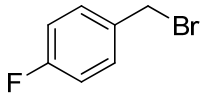	55*

X is Cl or Br. * The yield was determined by ^{1}H NMR analysis.

In an isolated case, benzylation of **1** with 4-fluorobenzylbromide yielded a mixture of monobenzylated product **2e** in 55% yield and a dibenzylated product in 4% yield. This mixture was inseparable using column chromatography. We were thus prompted to investigate the intramolecular hydrogen bonding of the 2-hydroxyl group to the adjacent aldehyde function that is reported to minimize reaction at this site compared to reaction at the 4-hydroxyl group.[86]

To investigate the intramolecular H-bonding, **1** was exposed to excess potassium carbonate in dry acetonitrile at 60 ^{o}C for 48 h. IR spectra were obtained for this mixture and compared with IR spectra of untreated **1** (Figure 2.1).

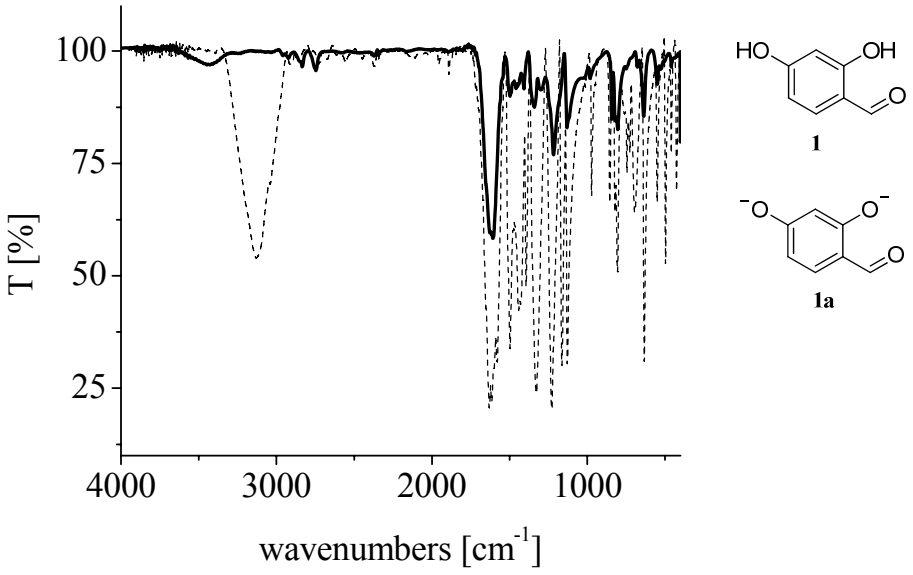

Figure 2.1. IR spectra of **1** (dotted line) and **1a** (solid line)

An overlay of the two IR spectra revealed the absence of any hydroxyl group and consequently H-bonding, which supports the formation of a dianion **1a** as the first step in the reaction. Benzylation of **1** should therefore be equally probable at both 2 and 4-hydroxyl positions. The observed regioselective benzylation of **1** is therefore remarkable and set a stage for alkylation of **1** with functionalities that enhance water solubility.

Following the successful derivatization of sacylaldehyde **1** using benzyl bromides and chlorides, we sought to extend the same methodology to attach

poly(ethylene glycol) side chains. Long chain polyethylene glycols would not only enhance water solubility but would also contribute to the overall macromolecular nature of the complexes. Initial attempts to react variously sized ethylene glycol chlorides (**3a-c,** Table 2.2) with 2,4-dihydroxybenzaldehyde (**1)** in acetonitrile at 60 ^{o}C in the presence of a potassium iodide catalyst yielded only recovery of starting material. Attempts to protect the hydroxyl group of the ethylene glycol chlorides with tetrahydropyran and consequently react compounds **3d - f** with **1** were futile.

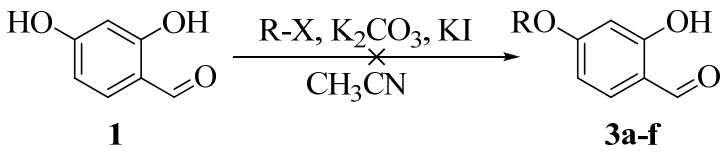

Table 2.2. Summary of failed alkylation reactions of 2,4-dihydroxybenzaldehyde

Entry	Compound	R-X
1	**3a**	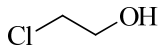
2	**3b**	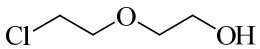
3	**3c**	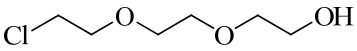
4	**3d**	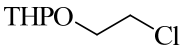
5	**3e**	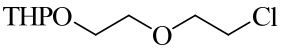
6	**3f**	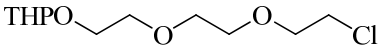

Efforts to increase the reaction temperature from 60 ^{o}C to reflux, extend reaction times from 24 h to 96 h, and even use a one mole equivalent of potassium iodide catalyst were without success. Changing the solvent from acetonitrile to dimethylformamide and even using a strong base like potassium *tert*-butoxide did not yield the desired product.

Nevertheless, activation of various alkyl alcohols by tosylation and consequent reaction with **1** gave the desired monosubstituted salicylaldehyde after chromatographic separation in moderate yields (Table 2.3).[87]

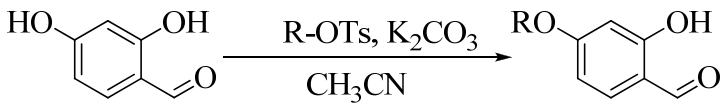

1 **5a-g**

Table 2.3. 4-Alkoxy-salicylaldehydes obtained by the reaction of **1** with tosylates **4a-g**.

	Tosylate **4**		Product **5**	Yield [%]
a	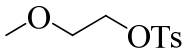	**a**	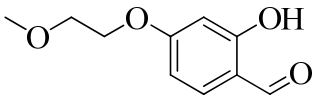	21
b	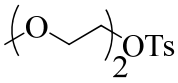	**b**	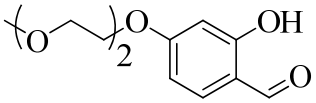	37
c	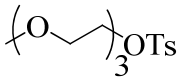	**c**	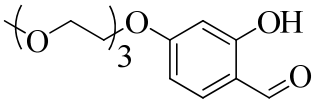	55
d	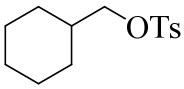	**d**	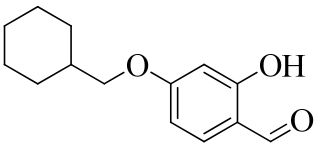	17
e	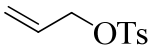	**e**	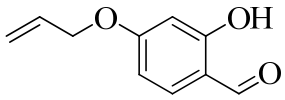	48
f	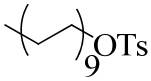	**f**	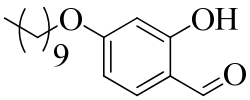	42
g	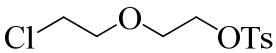	**g**	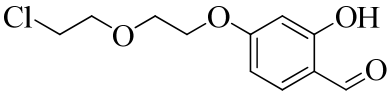	50

The compounds **5a-g** serve as new building blocks for the synthesis of pentadentate

Schiff-base ligands that coordinate to transition metal ions to form Schiff-base complexes. These complexes were envisioned to catalyze the oxidation of alcohols or phenol groups in biomolecules such as carbohydrates or lignin in the long-term.

2.3 Study of de-alkylation reaction

To probe the cause of the generally moderate yields obtained for the mono-alkylation of 2,4-dihydroxybenzaldehyde (**1**) with alkyl tosylates **4a-g**, we looked into the possibility of cleaving the ether bond of the product in the rather basic reaction conditions. Although an ether bond is generally resistant to base cleavage, there are well known exceptions that occur when the alkoxide leaving group is stable, as in the case of a phenoxide.[88] Cleavage of 4-alkoxysalicylaldehydes **5a-g** would lead to formation of a stable phenoxide **1b** (Figure 2.2).

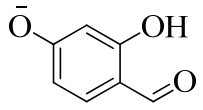

1b

Figure 2.2. Structure of phenoxide **1b**

To explore the possibility of a dealkylation, 4-cyclohexylmethoxy-2-hydroxybenzaldehyde **5d** was heated at 70 ^{o}C in the presence of potassium carbonate and potassium chloride for 48 h in acetonitrile. The reaction mixture was then analyzed by HPLC and compared to the product **5d** (Figure 2.3).

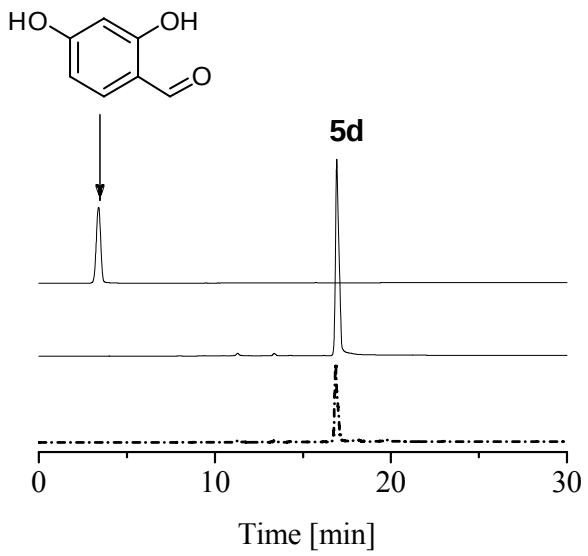

Figure 2.3: HPLC chromatograms for compounds **5d**, 2,4-dihydroxybenzaldehyde and the product after attempted de-alkylation reaction (dotted line).

The HPLC chromatographs obtained revealed that the ether functionality in **5d** is stable under the reaction conditions and does not undergo dealkylation.

2.4 Analysis of reaction products from the alkylation of 2,4-dihydroxybenzaldehyde.

In order to further probe the cause of the moderate yields obtained when salicylaldehyde **1** was reacted with alkyl tosylates **4a - g**, the raw product of the reaction was analyzed using HPLC. Reaction of cyclohexylmethyl tosylate **4d** was chosen because of its low yield of only 17%. Upon reaction of **1** with **4d** in acetonitrile in the presence of potassium carbonate for 48 h at 70 ^{o}C, the crude product was filtered over a short silica gel column and eluted using dichloromethane/methanol 90/10. The eluate was analyzed on semi-preparative HPLC column to separate the reaction products. The chromatograph obtained showed a mixture of four compounds (Figure 2.4).

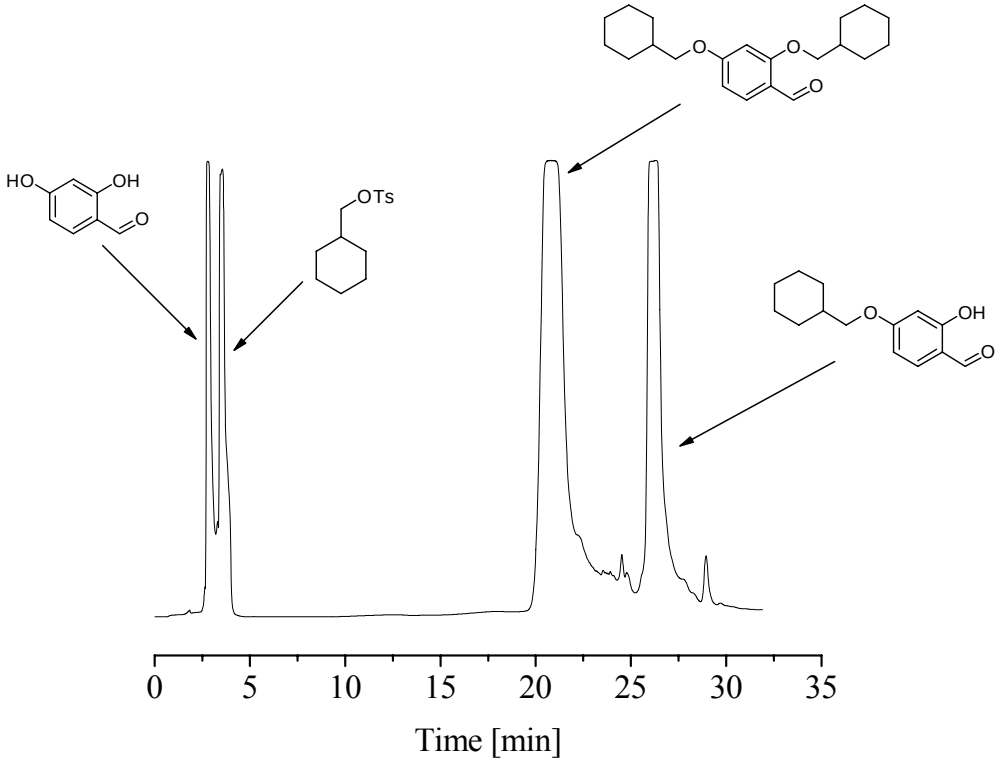

Figure 2.4: HPLC chromatogram for the mixture obtained from reaction of salicylaldehyde **1** with tosylate **4d**. For details of the chromatographic conditions, see experimental section.

The compounds were isolated and characterized using ^{1}H and ^{13}C NMR spectroscopy and mass spectrometry for the new compounds. The isolated compounds were identified as the staring salicylaldehyde **1**, starting tosylate **4d**, desired product 4-alkoxysalicylaldehyde **5d**, and a 2,4-di-alkoxysalicylaldehyde **5d′** (Figure 2.5).

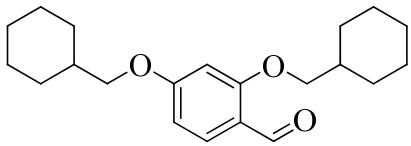

5d'

Figure 2.5. Structure of 2,4-bis(cyclohexylmethoxy)benzaldehyde **5d′**

Chromatographic analysis of this reaction mixture revealed that dialkylation of **1** with **4d** occurred forming **5d′** as the major product and thus leading to the overall low yield of the desired product **5d**. This confirmed our earlier observation that the base (potassium carbonate) deprotonates both hydroxyl groups in **1** leading to phenoxide **1a**.

2.5 Derivatization of other salicylaldehydes

Having investigated the alkylation of **1**, it was necessary to extend our study and explore other closely related salicylaldehydes. Commercially available 2,3-dihydroxybenzaldehyde **6** which differs from **1** simply by position of the 4-hydroxyl group was reacted with allyl tosylate **4e** in acetonitrile at 60 ^{o}C in the presence of potassium carbonate (Scheme 2.2). A dialkylated product 2,4-bis(vinyloxy)benzaldehyde **7** was separated in 31% yield after chromatographic purification.

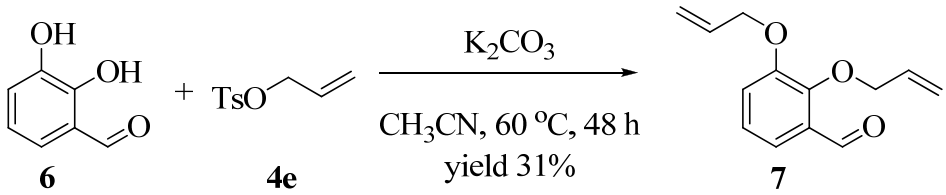

Scheme 2.2. Reaction of 2,3-dihydroxybenzaldehyde **6** with allyl tosylate **4e**.

The desired mono-alkylated product was not realized. The dialkylated product was identified by absence of a hydroxyl peak in the ^{1}H NMR and a shift in the carbonyl carbon peak in the ^{13}C NMR spectrum from 196 ppm in **6** to 190 ppm in **7**. It is however worthwhile to mention that the desired monoalkylated product 3-(allyloxy)-2-hydroxybenzaldehyde has been reported in the literature and was synthesized by reaction of allyl bromide with **6** in DMSO at ambient temperature in the presence of sodium hydride.[89,90]

In another example, 2-(2-chloroethoxy)ethyl tosylate **4g** was reacted with 2,3-dihydroxybenzaldehyde **6** in acetonitrile at 70 ^{o}C for 48 h. After chromatographic separation, a dialkylation product 2,3-bis(2-(2-chloroethoxy)ethoxy)benzaldehyde **8** (Figure 2.6) was isolated in 20% yield.

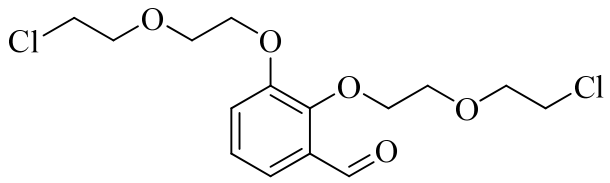

8

Figure 2.6. Structure of 2,3-bis(2-(2-chloroethoxy)ethoxy)benzaldehyde **8**.

It was therefore concluded that **6** is not a good substitute for salicylaldehyde **1** because of its lack of regioselectivity when reacted with alkyl tosylates.

Another closely related salicylaldehyde, 2,5-dihydroxybenzaldehyde **9**, was reacted with allyl tosylate **4e** in identical conditions as **7** to yield an inseparable

mixture of dialkylated product **10** and monoalkylated product **11** and in 11% and 16% yield, respectively (Scheme 2.3).

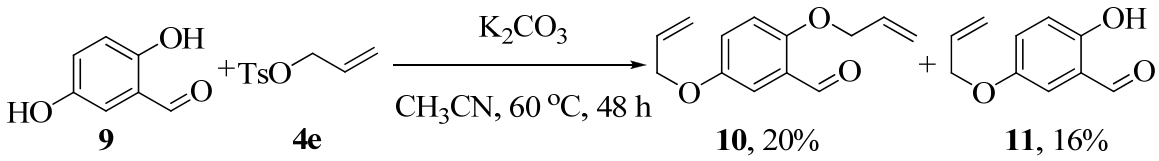

Scheme 2.3. Reaction of 2,5-dihydroxybenzaldehyde **9** with allyl tosylate **4e**.

To further probe the alkylation of **9**, 2-(2-chloroethoxy)ethyl tosylate **4g** was reacted with **9** in acetonitrile at 70 ^{o}C. The reaction mixture was filtered over a short silica gel column and eluted using a 1:1 mixture of cyclohexane and ethyl acetate. The eluate was then separated using a semi-preparative HPLC column to obtain a mixture of three compounds (Figure 2.7).

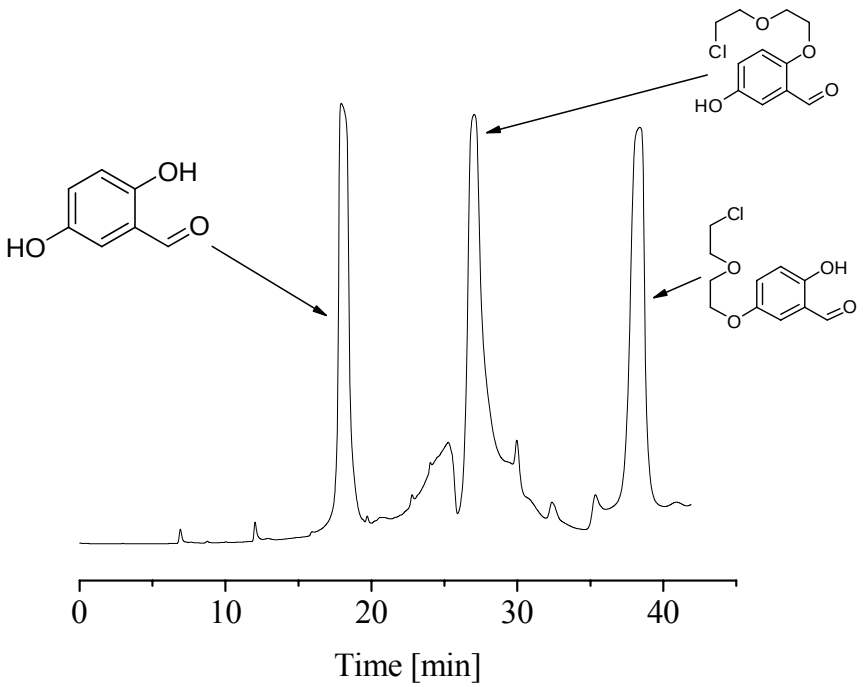

Figure 2.7. HPLC chromatogram for the mixture obtained from the alkylation of salicylaldehyde **9** with alkyl tosylate **4g**. For details of the chromatographic conditions, see experimental section.

Analysis of the fractions collected using ^{1}H and ^{13}C NMR spectroscopy revealed the chromatograph peaks to be aldehyde **9**, 5-alkoxy-salicylaldehyde **12** and 2-alkoxysalicylaldehyde **13** (Scheme 2.4).

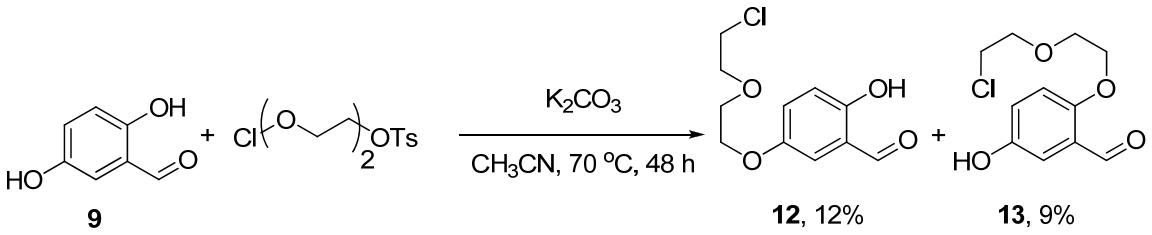

Scheme 2.4. Reaction of 2,5-dihydroxybenzaldehyde **9** with tosylate **4g**.

The identity of compounds **12** and **13** was determined using NMR spectroscopy and confirmed by mass spectrometry analysis. Due to the generally low yields and peralkylation, salicylaldehydes **6** and **9** were not investigated further.

2.6 Summary for alkylation of hydroxysalicylaldehyde

In summary, alkylation of 2,4-dihydroxybenzaldehyde **1** at the 4-hydroxy position was achieved by reaction of **1** with alkyltosylates **4a-g** in moderate to good yields. The tosylates **4a-g** were prepared from commercially available aliphatic alcohols and tosyl chloride using literature procedures. Careful investigation of the alkylation reaction eliminated the possibility of ether cleavage by dealkylation of the reaction products. Although monoalkylation of **1** at 2-hydroxy position was not observed, IR spectroscopy analysis ruled out the possibility of intramolecular hydrogen bonding of the 2-hydroxy group to the adjacent aldehyde function under the basic reaction conditions.

CHAPTER THREE

BINUCLEAR COPPER(II) COMPLEXES

3.1 Synthesis of Schiff-base copper(II) complexes

Enzymes that contain copper play an important role in many biological processes.[91] Galactose oxidase, for example, is an enzyme containing one copper(II) ion that catalyzes the oxidation of primary alcohols to the corresponding aldehydes.[92,93] In our ongoing efforts to develop catalysts for oxidation of alcohol groups in biomolecules such as carbohydrates or lignin, we designed copper(II) Schiff-base complexes that were shown to transform catechols into quinones in aqueous media (Chapter IV).

To prepare the complexes, 2,4-dihydroxybenzaldehyde (**1**) was alkylated as described in Chapter II. The alkylated aldehydes **5a-c** (page 19) were reacted with commercially available 1,3-diaminopropanol (**13**) at ambient temperature in ethanol/methanol (1/1, v/v) to yield the Schiff-base ligands **14a-c** (Scheme 3.1).

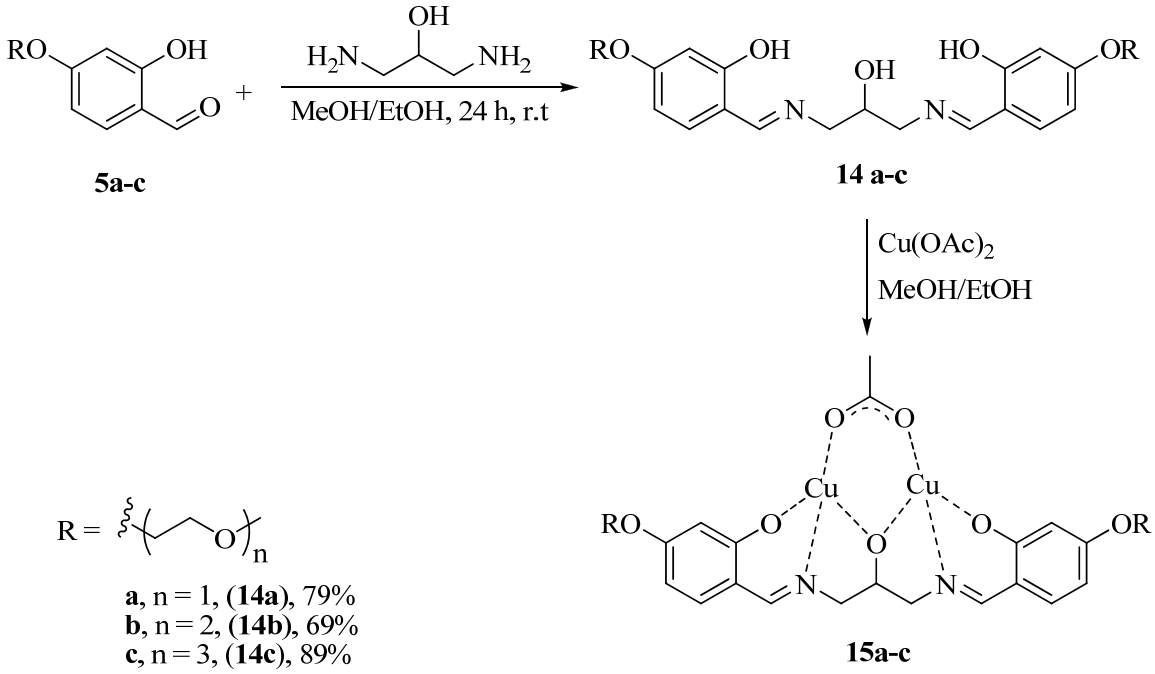

Scheme 3.1. Synthesis of binuclear copper(II) catalysts

Upon condensation of salicylaldehydes **5a-c** with **13**, the aldehyde ^{1}H NMR peak that occurs around 9.6 ppm is replaced by the azomethine proton peak at around 8.2 ppm, and there was a shift in the ^{13}C NMR from ~196 ppm for the carbonyl carbon to ~166 ppm for the azomethine carbon.

After reaction of ligands **14a-c** with copper(II) acetate, binuclear copper(II) complexes **15a-c** were obtained. Spectroscopic species distribution studies revealed the composition of the complexes in solution. In solid state, the complexes were characterized using IR spectroscopy, elemental analysis and X-ray diffraction.

3.2 Characterization of binuclear complexe **15a** in solid state

In order to obtain the composition of the binuclear copper(II) complexes **15a-c** in solid state, complex **15a** (Scheme 3.2) was studied in detail because unlike **15b** and **c,** it formed crystals suitable for X-ray diffractometry**.**

When ligand **14a** was reacted with copper(II) acetate monohydrate in DMF at 60 ^{o}C in the presence of triethylamine, crystals of **15a** were obtained after recrystallization from ethanol. Elemental analysis revealed the composition of complex **15a** to be $Cu_2[(L_{-3H})(OAc)]$ where L is structure **14a** (Scheme 3.2).

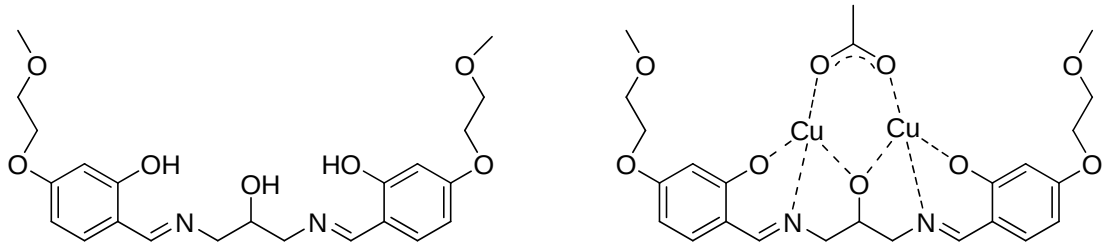

14a **15a**

Scheme 3.2. Structures of ligand **14a** and binuclear copper(II) complex **15a**

Upon coordination of Cu(II) into **14a**, IR spectroscopic analysis showed a shift in the azomethine band from 1636 cm^{-1} in ligand **14a** to 1630 cm^{-1} in **15a** (Figure 3.1).

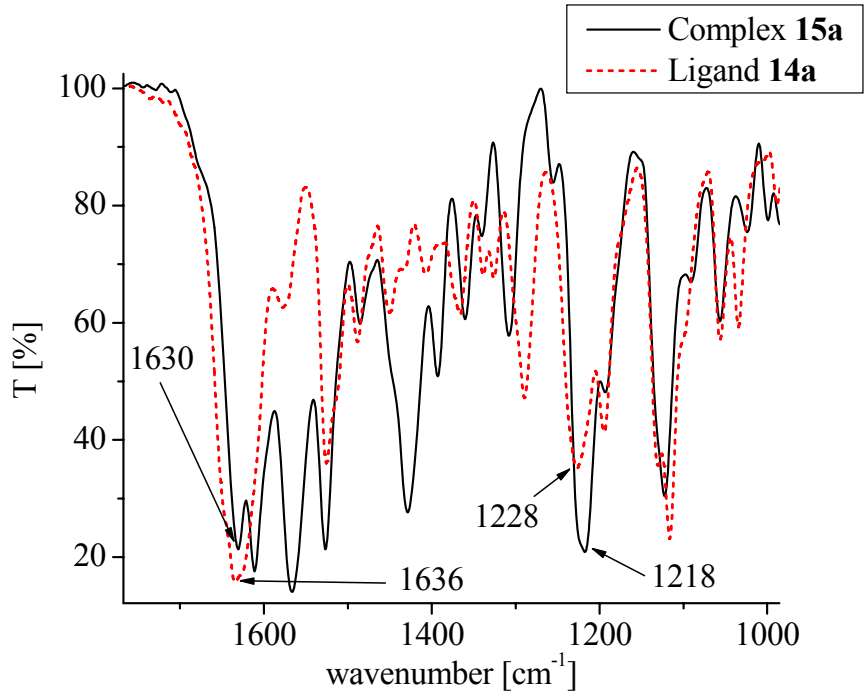

Figure 3.1 IR spectra of ligand **14a** (dotted line) and complex **15a** (solid line) recorded in KBr pellets.

The shift to lower frequency (compared to the free ligand **14a**) indicates that the lone pair on the azomethine nitrogen is donated to the Cu(II) ion upon coordination.[94] Further proof of the complex formation is the shift in phenoxy C–O stretch from 1228 cm^{-1} in ligand **14a** to 1218 cm^{-1} in complex **15a**. These shifts to lower frequency are characteristic of Schiff-base complex formation.[95]

3.3 X-ray Crystallography

Single crystal X-ray analysis of **15a** reveals square planar coordination environments for both Cu(II) centers. The two copper atoms are bridged by an endogenous μ–alkoxo-oxygen atom and by an exogenous μ-1,3-bridged acetate group (Figure 3.2).

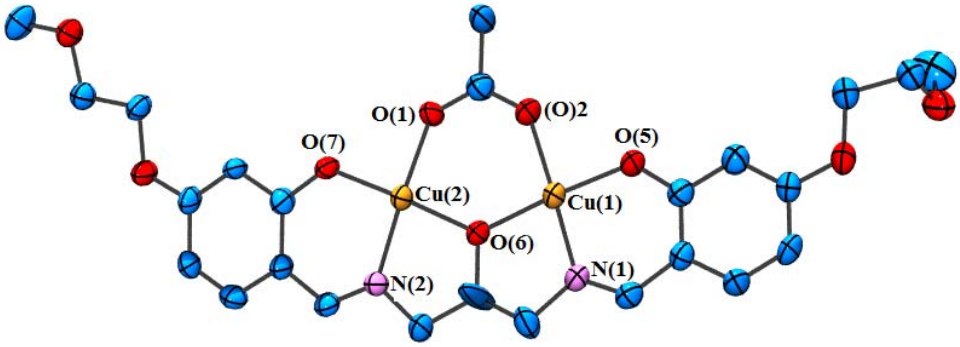

Figure 3.2. ORTEP[96] representation of complex **15a** (70 % probability ellipsoids)

The coordination sphere around each Cu(II) ion is completed by coordination of copper to the nitrogen atom of the pentadentate ligand leading to the formation of N_1O_3 donor set. The resulting intermetallic Cu···Cu bond distance is 3.508 Å. Selected bond angles and bond distances for complex **15a** are listed in Table 3.2.

Table 3.1. Selected bond lengths [Å] and angles [º] for **15a**

Cu(1)–O(5)	1.897(3)	Cu(2)–O(7)	1.893(2)
Cu(1)–O(6)	1.910(3)	Cu(2)–O(6)	1.921(2)
Cu(1)–N(1)	1.921(3)	Cu(2)–N(2)	1.925(3)
Cu(1)–O(2)	1.931(3)	Cu(2)–O(1)	1.942(3)
O(5)–Cu(1)–N(1)	93.6(12)	O(7)–Cu(2)–O(1)	87.6(11)
O(6)–Cu(1)–N(1)	84.8(12)	O(6)–Cu(2)–O(1)	94.6(11)
O(5)–Cu(1)–O(2)	87.8(11)	O(7)–Cu(2)–N(2)	93.3(12)
O(6)–Cu(1)–O(2)	94.5(11)	O(6)–Cu(2)–N(2)	83.9(12)

It was postulated that the geometry of the coordination sphere around Cu(II) ions in **15b** and **15c** would be identical to that of **15a** since the only difference between the three complexes is the length of the PEG side chain. Understanding the geometry of the metal complexes was important in determining the binding interaction of the metal complexes to substrates.

3.4 Characterization of complex **15c** in solution

The composition of a metal complex in solid state may differ from that in solution. To design an efficient catalyst, it is important to investigate its composition in solution in order to understand how it interacts with substrates. To investigate the composition of metal complexes **15a-c** in solution, **15c** was studied in detail because of its good solubility in water. This complex was characterized in three different solutions;

in 100% methanol, 80/20 (methanol/water, v/v) and 60/40 (methanol/water, v/v). This was for the purpose of a careful study aimed at probing the effect of water on the catalytic activity of complex **15c**. A pH profile of **15c** was also determined between pH 4 and 13 since the complex was later used as a catalyst in glycosidase hydrolysis (Chapter IV).

To investigate the composition of **15c** in methanol, complex formation was monitored using a series of spectroscopic UV-Vis titrations and the data analyzed by using fitting procedures provided by the program Specfit.[97] Titration of **14c** with copper(II) acetate in methanol shows formation of an absorption band at 600 nm which shifts to 650 nm (Figure 3.3) with increased copper(II) acetate concentration. This band at 650 nm is characteristic of a $^2T_{2g} \rightarrow {}^2E_g$ (G) transition of square planar copper(II) complexes.[98] A square planar geometry was confirmed by a structurally related complex **15a** whose structure analysis (Figure 3.2) showed square planar coordination geometry around the two copper(II) ions.

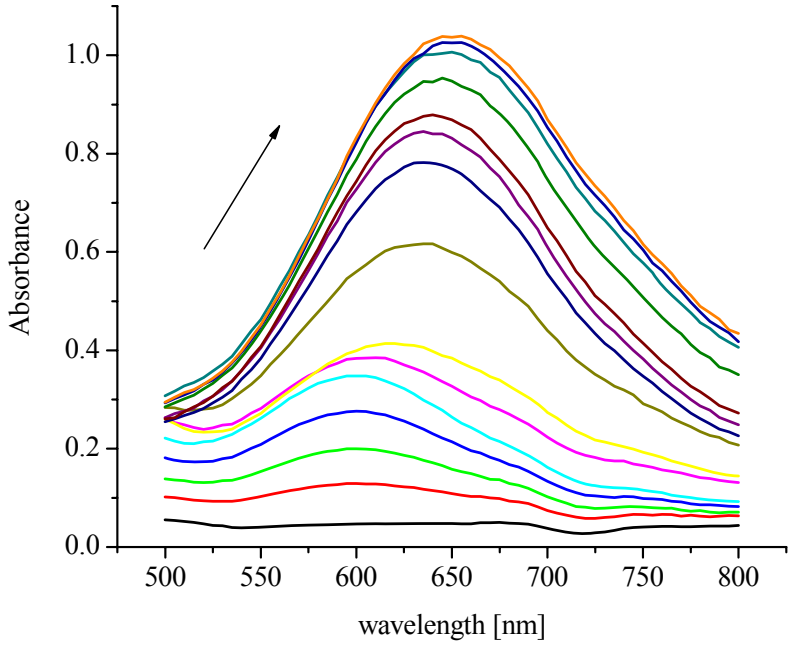

Figure 3.3. UV-Vis absorption spectra obtained from titration of ligand **14c** (2 mM) with 10 μL aliquots of copper(II) acetate (0.3 M) in methanol. Conditions: I = 0.1M ($NaClO_4$), T = 30 ^{o}C, $Cu(OA)_2$ = 2 mM, Ligand **14c** = 1 mM.

After fitting the UV-Vis spectroscopic data using the Specfit program, species distribution curves were obtained that revealed that a 100% formation of a binuclear copper(II) complex **15c** (Figure 3.4) above a 1:2 molar ratio of ligand **14c** to copper(II) acetate (Figure 3.5).

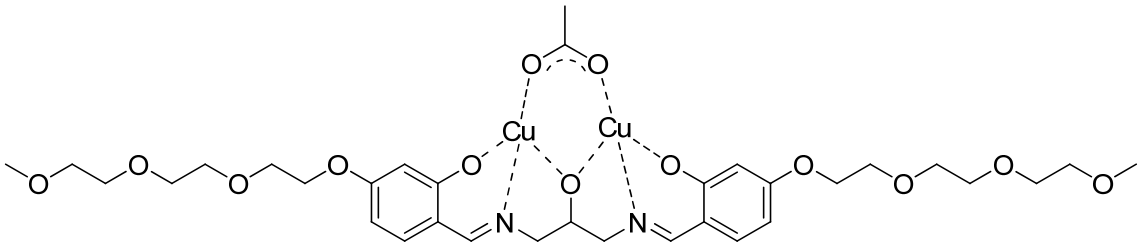

15c

Figure 3.4. Binuclear copper(II) species $Cu_2L_{-3H}(OAc)$.

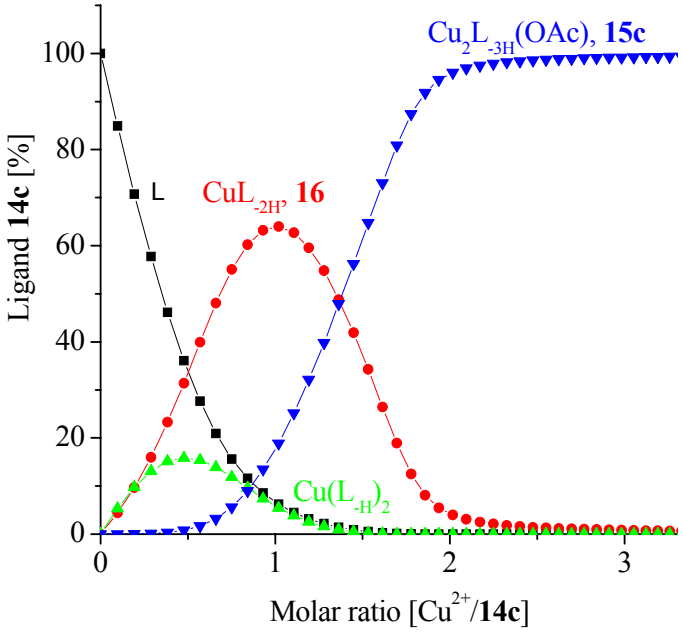

Figure 3.5. Species distribution obtained from spectroscopic titration of **14c** with copper(II) acetate in methanol.

A mononuclear copper(II) species CuL_{-2H} (**16**) was formed at a 1:1 molar ratio of **14c** and copper(II) acetate (Figure 3.6).

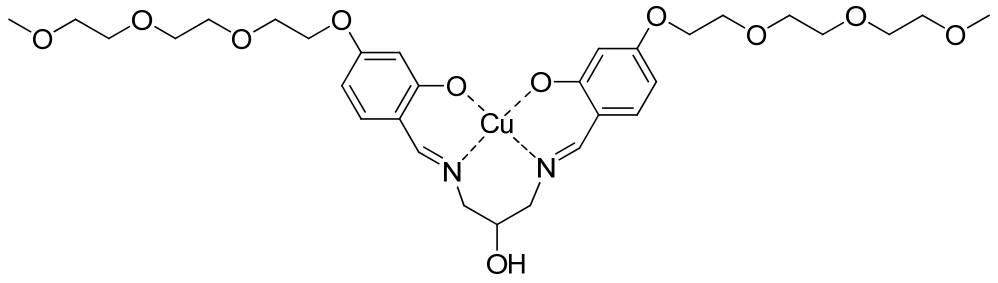

16

Figure 3.6. Mononuclear copper(II) species CuL_{-2H}.

A control experiment was designed to confirm the assignment of the structures deduced from the species distribution curve. To confirm that the acetate is bound in methanol and is not replaced by solvent molecules, a UV-Vis spectrum of ligand **14c** with copper(II) chloride was recorded between 500 and 800 nm in methanol (Figure 3.7)

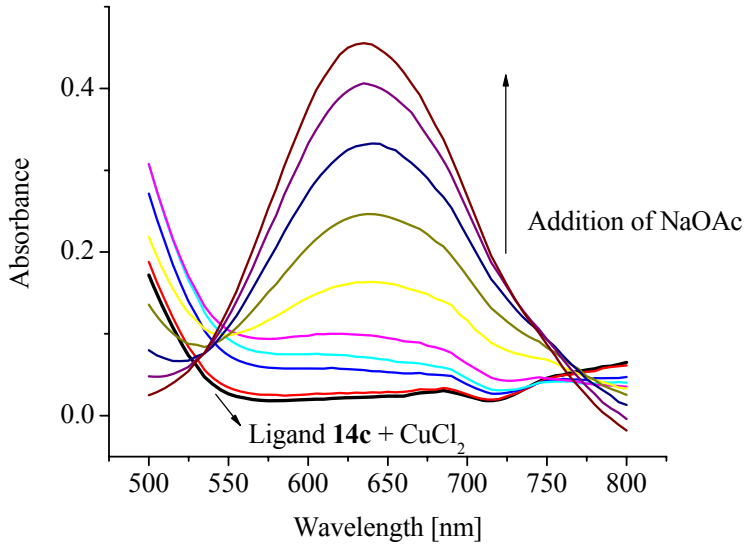

Figure 3.7. UV-Vis spectra of **14c** and copper(II) chloride with consecutive addition of anhydrous sodium acetate in MeOH. For experimental details, see Section 6.5.

A spectrum of **14c** and $CuCl_2$ showed no absorbance between 500 and 800 nm meaning that there was no formation of a complex. Upon successive addition of anhydrous sodium acetate to a solution of **14c** and $CuCl_2$, an absorption band with λ_{max} at 650 nm is obseved which is attributed to formation of a binuclear copper(II) complex derived from **14c**. The acetate ion is therefore necessary for formation of a binuclear copper(II) complex in methanol and the hence composition of **15c** is preserved in methanol.

In aqueous methanol ($MeOH/H_2O$ = 80/20 and $MeOH/H_2O$ = 60/40), the complex formed from ligand **14c** and copper(II) acetate is structurally different from that in pure methanol. The solvent molecules exchange the bridging acetate anion as deduced from spectroscopic experiments. Water and hydroxide ions replace the bridging acetate anion resulting in binuclear copper(II) species $Cu_2L_{-3H}(OH)$ (**17**). The hydroxide ion can either form an intramolecular bridge between the two copper(II) ions to form **17b** or it can be terminally bound to form **17a** (Figure 3.8).

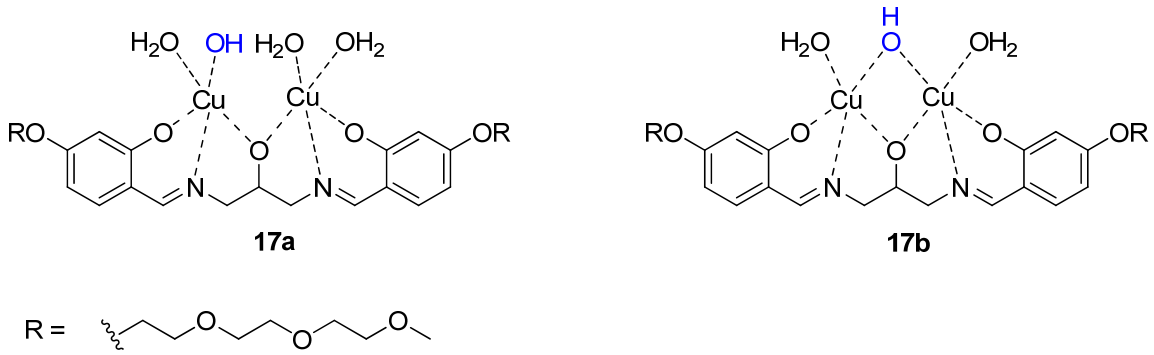

Figure 3.8. Suggested structure of $Cu_2L_{-3H}(OH)$ (**17**) with hydroxide ion (a) bound terminally and (b) forming intra-molecular bridge.

Based on the large Cu···Cu distance (3.508 Å) obtained from X-ray analysis of **15a**, it was suggested that the hydroxide is terminally bound to form catalytically active species **17a**. Species distribution analysis of ligand **14c** and copper(II) acetate in MeOH/H_2O 80/20 (v/v) showed 59% formation of **17** at 2:1 molar ratio of copper(II) acetate to **14c** (Figure 3.9). This decrease from theoretical value of 100% is attributed to formation of a mononuclear complex **16**.

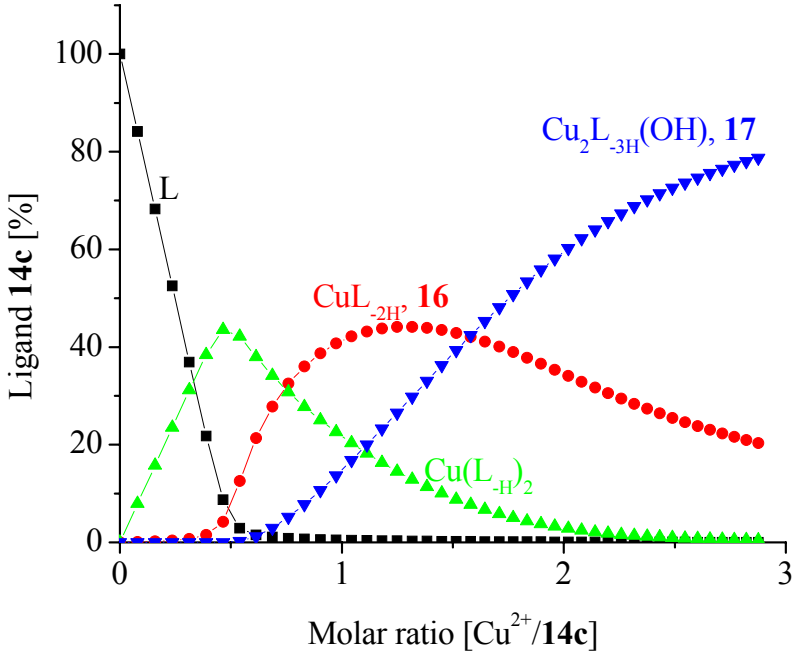

Figure 3.9. Species distribution curves obtained from spectroscopic titration data of ligand **14c** and copper(II) acetate in MeOH/H_2O 80/20 (v/v)

When the solvent system was changed to MeOH/H_2O 60/40 (v/v), the formation of **17** increased to 72% at 2:1 molar ratio of Cu(II) to ligand **14c** At this point, the mononuclear complex **16** formation is 27% (Figure 3.10).

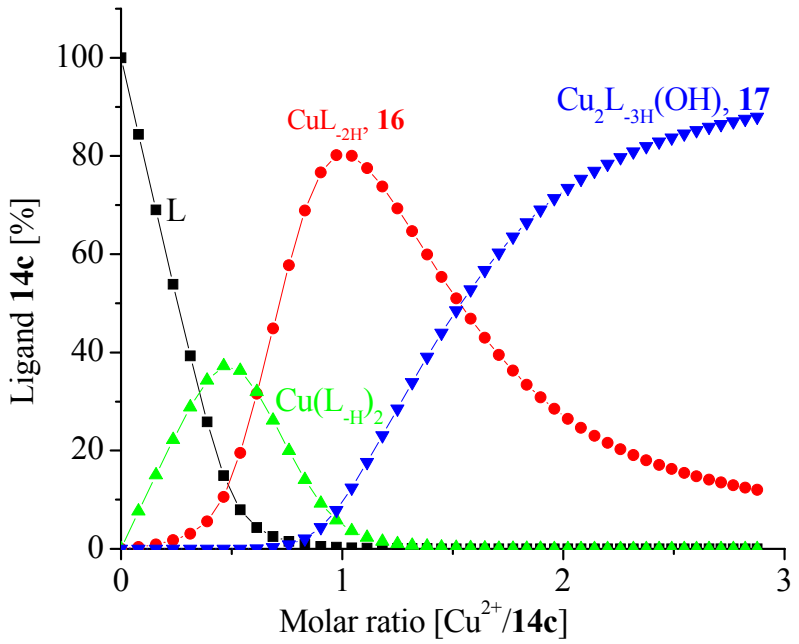

Figure 3.10. Species distribution curves obtained from spectrophotometric titration data of ligand **14c** with copper(II) acetate in MeOH/H_2O 60/40 (v/v).

In summary, the species in solution for complex **15c** were determined and shown to vary according to the solvent system. In methanol, only one species is formed at 1:2 molar ratio of **14c** to Cu(II) ions, while in aqueous methanol, a mononuclear complex competes with formation of a binuclear species. The apparent concentration of the complex used for determination of kinetic parameters was therefore adjusted according to the results of species distribution.

3.5 pH profile of complex **15c** in water.

In a typical experiment, a solution of copper(II) chloride, sodium acetate and ligand **14c** was titrated with sodium hydroxide solution and the pH recorded. UV-Vis spectra were then taken as a function of the pH and the spectroscopic data obtained computed by fitting procedures provided by the program Specfit.[97] The ionic strength of the aqueous solution was maintained constant with 0.1 M $NaClO_4$ at 30 ^oC.

Four species were obtained between pH 4 and 13 for the system consisting of ligand (L) and copper(II) chloride in 1:2 molar ratio. Ligand (L) was found to be the predominant species at pH 4 to 7.4. As the concentration of sodium hydroxide was increased, the L was deprotonated to form a binuclear complex $[Cu_2L_{-3H}]$ between pH 9 and 11.5 (Figure 3.11).

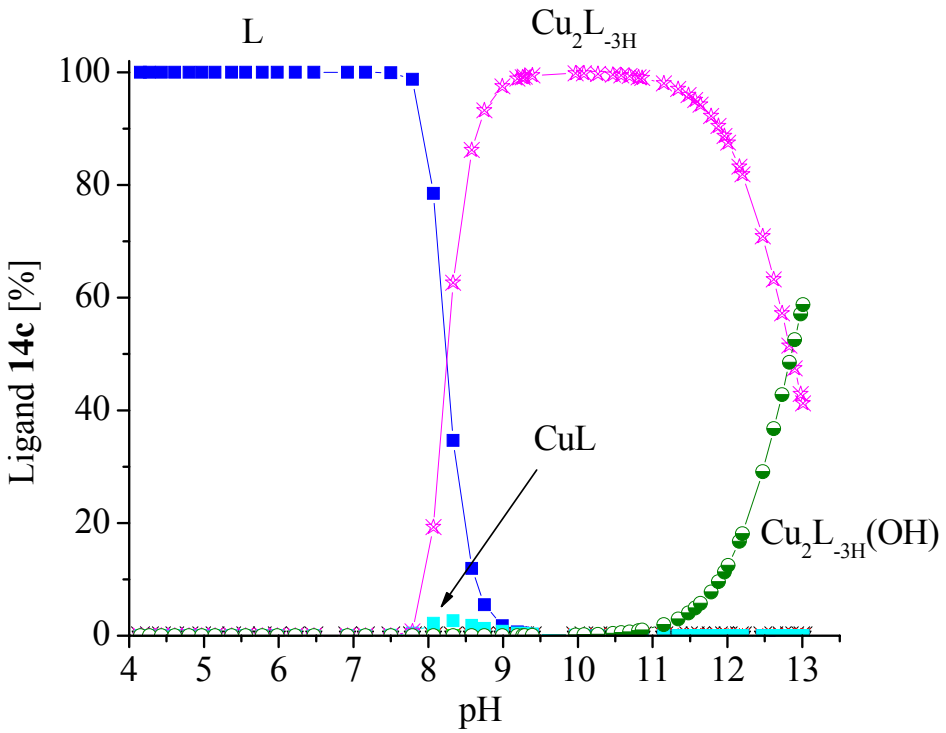

Figure 3.11. Distribution of species at pH 4–13 for a 1:2 molar ratio of ligand to $CuCl_2$ in water at 30 ºC. For experimental details see Section 6.3.

Further deprotonation of Cu_2L_{-3H} was assigned to loss of a proton from bound water molecule to form complex $Cu_2L_{-3H}(OH)$ as shown in Scheme 3.3.

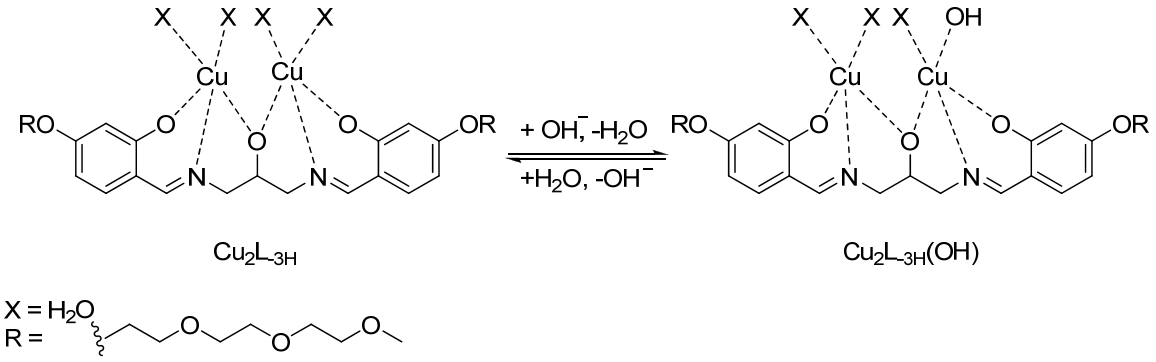

Scheme 3.3. Schematic structures of Cu_2L_{-3H} and $Cu_2L_{-3H}(OH)$.

3.6 Bis-pyridyl copper(II) complexes

Previously in our laboratory, a bis-pyridyl complex **18** (Figure 3.12) was shown to catalyze the oxidation of benzyl alcohol (**19**), into benzaldehyde (**20**) in the presence of TEMPO (Scheme 3.4).[39,99]

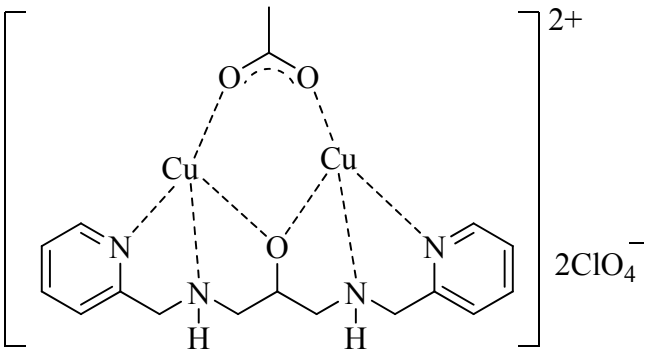

Figure 3.12: Structure of complex **18**

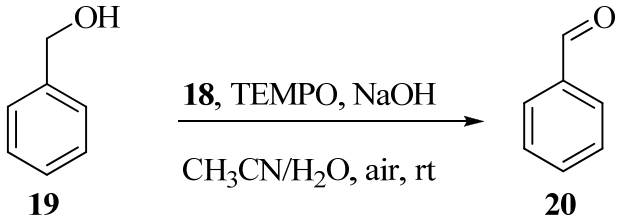

Scheme 3.4. Oxidation of benzyl alcohol to benzaldehyde promoted by **18**.

Based on the encouraging catalytic activity of **18** and the fact that pyridyl groups are known to enhance water solubility which would allow application in water, we sought to modify the catalytic site for complex **18**.[100] A simple way to alter the catalytic site would be to change the intermetallic Cu···Cu distance by varying the length of the

diamine that bridges the two pyridyl groups. In this regard, 1,4-diaminopropanol **23** was synthesized from commercially available 1,4-dibromobutanol **21** using the Gabriel synthesis as described by Kida et al.[101] **21** was reacted with potassium phthalimide in dry DMF to yield phthalide **22** (Scheme 3.5).

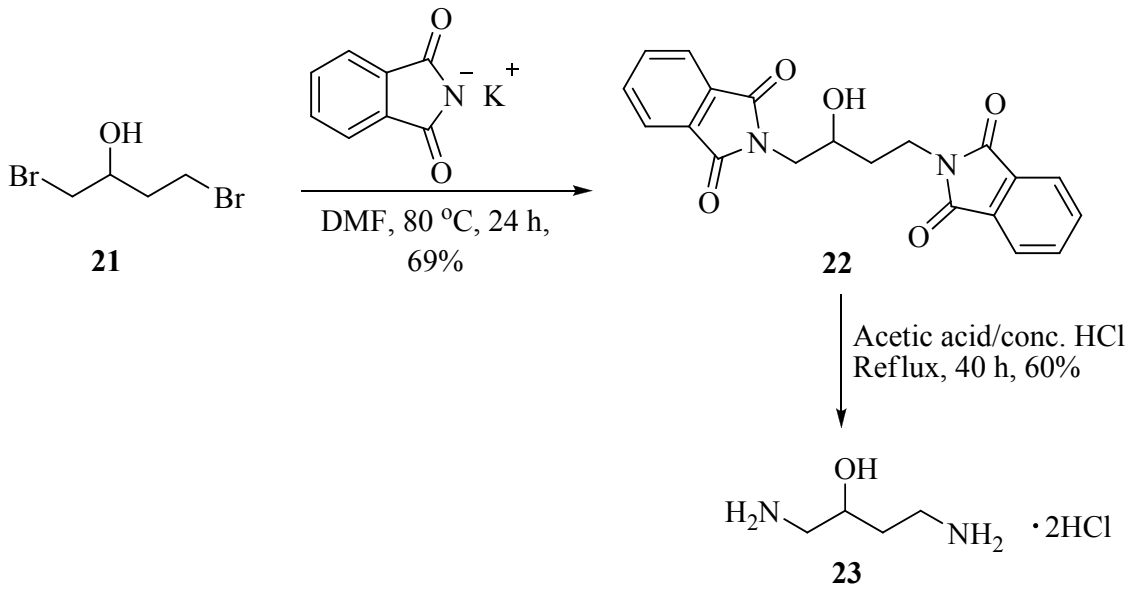

Scheme 3.5. Synthesis of 1,4-diaminobutanol dihydrochloride **23**.[101]

The phthalide was cleaved by heating **22** in a mixture of acetic acid and concentrated hydrochloric acid to yield the desired diamine **23**.

Binuclear complex **26** was prepared by condensing commercially available 2-pyridine carboxaldehyde **24** with 1,4-diaminobutan-2-ol dihydrochloride **23** in the presence of sodium hydroxide at ambient temperature (Scheme 3.6). The Schiff base obtained was consequently reduced using sodium borohydride to obtain ligand **25** in 40 % yield. Reaction of **25** with copper(II) acetate monohydrate in the presence of

sodium perchlorate in aqueous ethanol/methanol mixture yielded crystals of **26** after slow evaporation of the solvent.

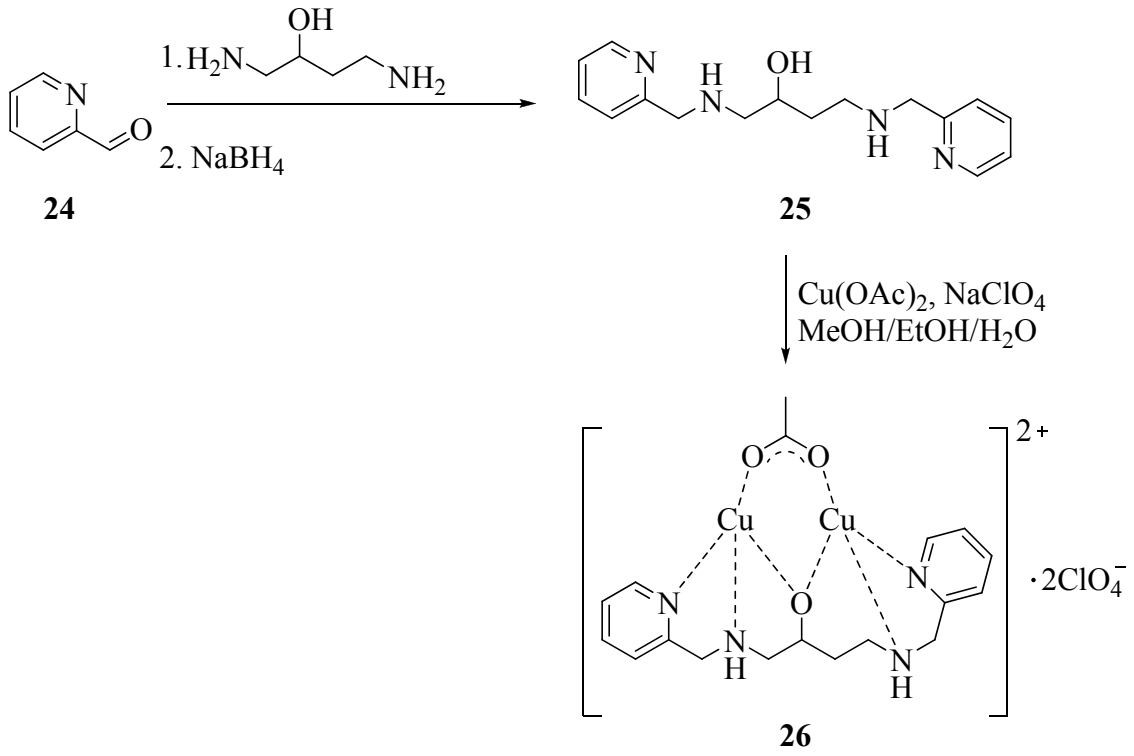

Scheme 3.6. Synthesis of complex **26**.

Elemental analysis revealed the composition of **26** to be $[Cu_2(L_{-H})(OAc)(H_2O)(ClO_4)]ClO_4$. Upon coordination of copper(II) acetate to **25,** the C–O stretching vibration frequency was shifted from 1095 cm^{-1} in **25** to 1120 cm^{-1} in complex **26** (Figure 3.13).

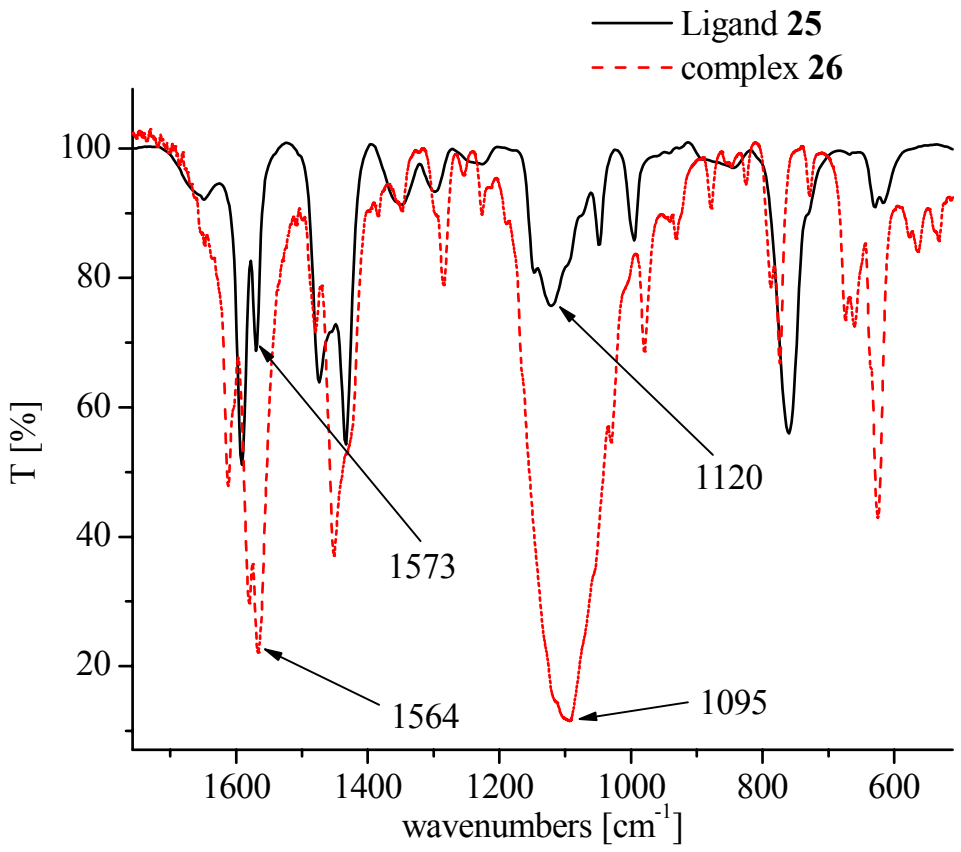

Figure 3.13: IR spectra of ligand **25** and binuclear copper(II) complex **26** recorded in KBr pellets.

3.7 X-ray analysis of **26**.

The X-ray analysis of **26** showed that each Cu(II) ion is chelated to the ligand in a tridentate coordination environment. The two Cu(II) ions are bridged by the endogenous μ–alkoxo-oxygen atom and by the exogenous μ-1,3-bridged acetate group (Figure 3.14).

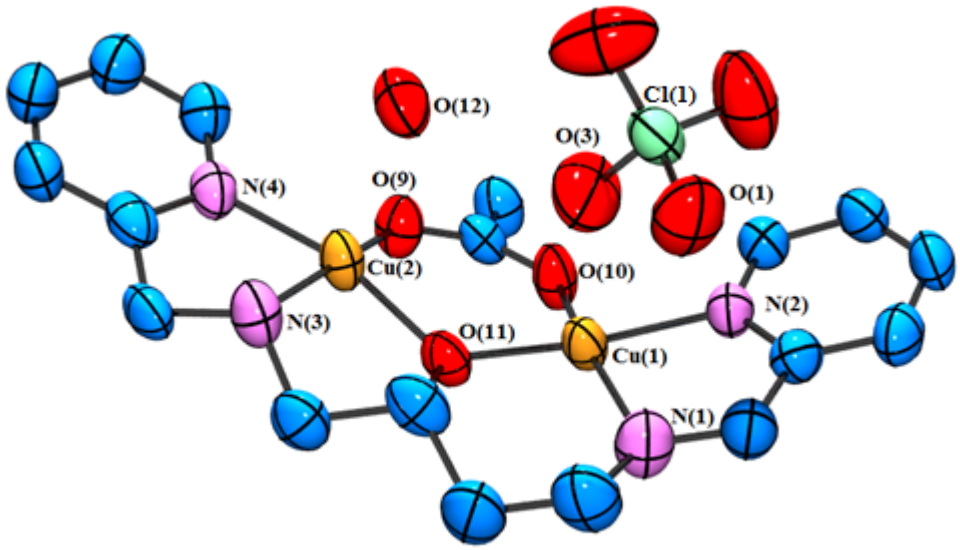

Figure 3.14. ORTEP3 representation of complex **26** (70 % probability ellipsoids). The second perchlorate has been omitted for clarity.

Due to the asymmetric nature of the ligand, the two centers of $[Cu_2(L_{-H})(OAc)(H_2O)(ClO_4)]ClO_4$ have different geometries. The geometry of Cu(1) is distorted square planar with a N_2O_2 donor set. Cu(2) is coordinated to oxygen atom (O12) from the bound water molecule forming square pyramidal structure with a N_2O_3 donor set. Selected bond angles and bond distances for complex **26** are listed in Table 3.3.

Table 3.2. Selected bond lengths [Å] and angles [º] for **26**

Cu(1)–O(11)	1.908(3)	Cu(2)–O(9)	1.929(3)
Cu(1)–O(10)	1.935(3)	Cu(2)–O(11)	1.941(3)
Cu(1)–N(1)	1.987(4)	Cu(2)–N(3)	1.985(4)
Cu(1)–N(2)	2.008(4)	Cu(2)–N(4)	2.002(4)
Cu(2)-O(12)	2.303(4)		
O(11)–Cu(1)–O(10)	94.9(13)	O(9)–Cu(2)–O(11)	98.7(13)
O(11)–Cu(1)–N(1)	97.1(15)	N(3)–Cu(2)–O(12)	98.3(16)
O(9)–Cu(2)–O(12)	92.7(14)	O(11)–Cu(2)–N(3)	86.3(15)
O(11)–Cu(2)–O(12)	98.4(13)	O(9)–Cu(2)–N(4)	91.4(14)
O(10)–Cu(1)–N(2)	88.5(14)	N(4)–Cu(2)–O(12)	91.8(14)
N(1)–Cu(1)–N(2)	81.8(17)	N(3)–Cu(2)–N(4)	81.8(16)

3.8 Composition of complex **26** in aqueous solution

A pH profile for complex **26** was obtained over the pH range 5 to 13. Spectroscopic titration of a solution containing backbone ligand **25**, copper(II) chloride, sodium acetate and sodium perchlorate with sodium hydroxide solution revealed formation of a binuclear complex **27** at pH 7.5 to 12.5 (Figure 3.13). At pH 5 to 6.5, the predominant species was the ligand **25** (L) which was deprotonated as the pH was increased to form complex **27**. (Figure 3.15).[102]

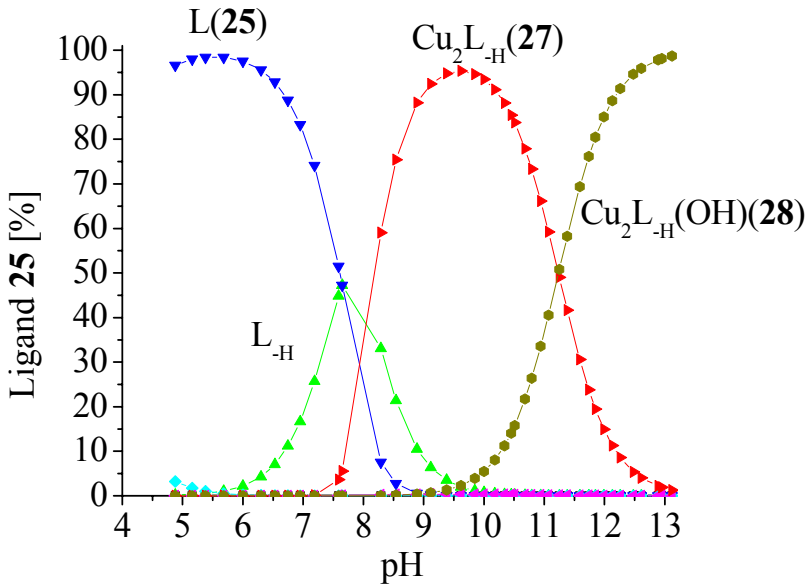

Figure 3.15. Distribution of species at pH 5–13 for a 1:2 molar ratio of ligand **25** and $CuCl_2$ in water at 30 ºC. For experimental details, see Section 6.3.

The second deprotonation in Cu_2L_{-H} was assigned to proton loss from a coordinated water molecule resulting in the species $Cu_2L_{-H}(OH)$ **28**, a structure that has been suggested for related complexes (Scheme 3.7).[103-104]

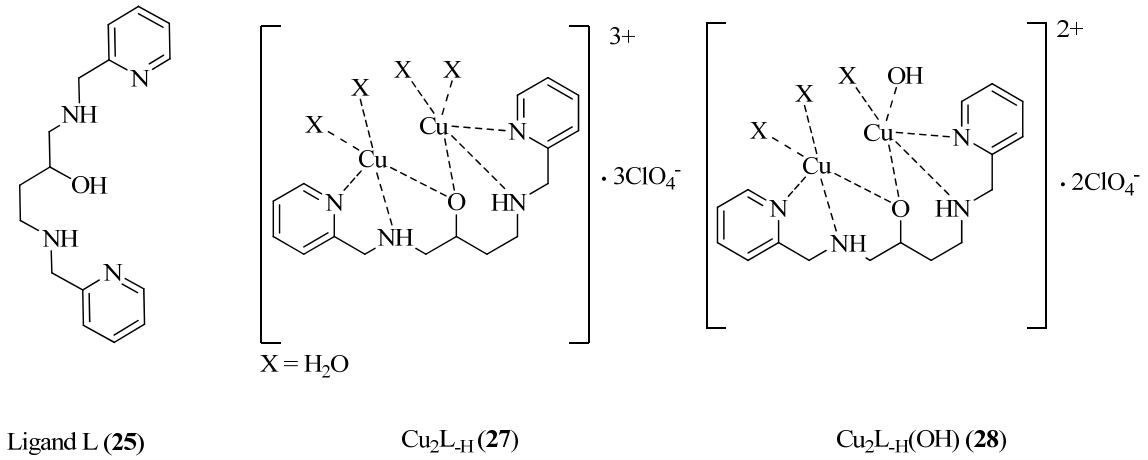

Scheme 3.7. Schematic representation of ligand **25**, Cu_2L_{-H} (**27**) and $Cu_2L_{-H}(OH)$ (**28**)

3.9 Asymmetric bis-salicylaldehyde based ligands

Following the enhanced catalytic activity of complex **15**c towards catechol oxidation in aqueous solutions (Chapter IV), we sought to modify its active site by altering the ligand backbone. Towards this end, ligands **29a** and **29c** were synthesized by condensation of 1,4-diaminopropanol **23** with salicylaldehydes **5a** and **5c** in a methanol mixture at ambient temperature (Scheme 3.8).

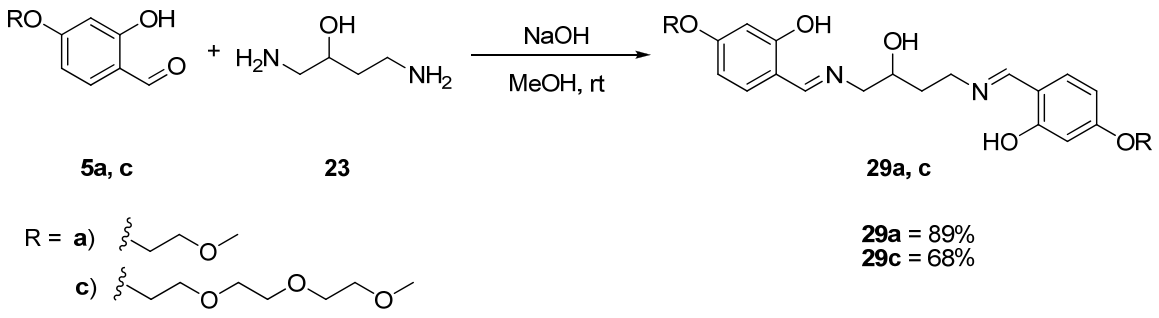

Scheme 3.8. Synthesis of ligands **29a** and **29c**

Surprisingly, ligands **29a** and **29c** were not only insoluble in water but also in common organic solvents including methanol, chloroform, acetone, dimethyl formamide and dimethyl sulfoxide. Ligands **29a** and **29c** were characterized by ^{1}H NMR in DMSO-d_6 at elevated temperatures in order to dissolve the ligands. Due to the poor solubility of these asymmetric ligands, we did not pursue their study any further.

CHAPTER FOUR

CATECHOL OXIDATION

4.1 Copper(II) complexes as catechol oxidation catalysts

Catecholase activity of model binuclear copper(II) complexes with different structural features have received a great deal of attention.[105-110] Binuclear copper centers are commonly found in metalloenzymes and play an important role in enzyme activity.[111] Hemocyanin, tyrosinase and catechol oxidase are all classified as type 3 copper proteins and have magnetically coupled binuclear copper(II) centers at their active sites. These metalloenzymes perform functions such as dioxygen transport (hemocyanin), *o*-phenol aromatic hydroxylations (tyrosinase) and catechol oxidation (catechol oxidase). In an effort to design an efficient oxidation catalyst that is functional in aqueous medium, water soluble binuclear copper(II) complex **15c** was used to investigate catechol oxidation. Catechols were chosen because complex **15c** is structurally similar to known catechol oxidase mimics.[112,113] Among various catechols used in model studies, 3,5-di-*tert*-butylcatechol was chosen because its low redox potential makes it easy to oxidize and the bulky substituents make further oxidation reactions such as ring opening slower.[114-116]

In order to investigate the effect of water, an environmentally benign solvent, on the catalytic effect of complex **15c**, three different solvent systems were

studied in detail. Catalysis was investigated in 100% methanol, MeOH/water 80/20 (v/v) and MeOH/water 60/40 (v/v) for the transformation of 3,5-di-*tert*-butylcatechol (DTBC) **19** into 3,5-di-*tert*-butylquinone (DTBQ) **20** (Scheme 4.1). It is worthwhile to mention that the reaction in 100% water could not be attained because the substrate 3,5-di-*tert*-butylcatechol **19** is insoluble in water.

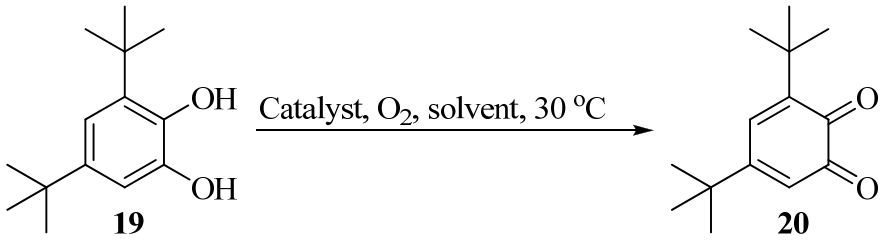

Scheme 4.1. Model reaction

4.2 Catalytic oxidation of DTBC in methanol

Catalyst **15c** was prepared by mixing methanol solutions of copper(II) acetate and ligand **14c** in 2:1 molar ratio. At this ratio, a binuclear complex is formed as concluded from species distribution data (Figure 3.6). The transformation of DTBC into DTBQ was monitored by UV-Vis spectroscopy at 420 nm. The initial rates method was used to determine the kinetic parameters for the oxidation of DTBC that follow Michaelis-Menten model. A typical kinetic trace used to determine an initial rate is shown in Appendix 4. A control experiment showed that the reaction rates increase linearly with the catalyst concentration at constant substrate concentration.

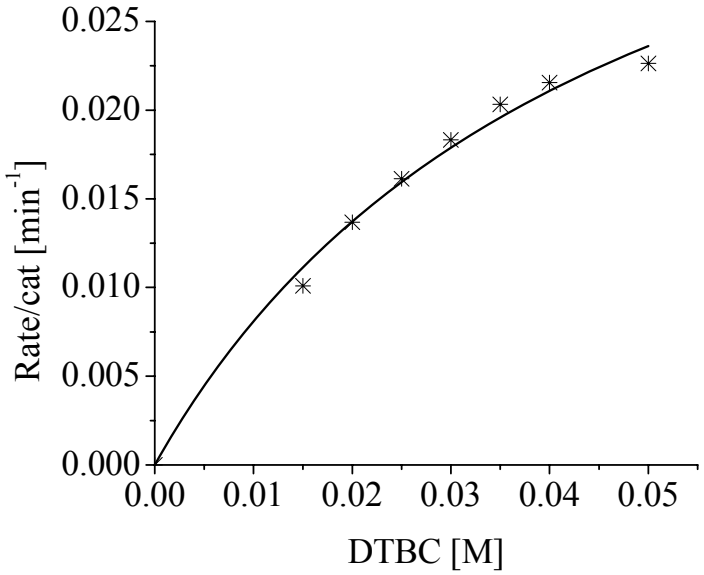

Figure 4.1. Kinetic profile for the aerobic oxidation of **19** into **20** promoted by **15c** in methanol.

To determine the kinetic parameters for the transformation of **19** into **20** in methanol, the substrate concentration was varied from 15 to 50 mM at a 200 μM concentration of **15c**. The catalytic rate constant k_{cat} was found to be 0.04 min^{-1} and the Michaelis-Menten constant K_m was found to be 40 mM at 30 ^oC (Figure 4.1). The rate constant k_{non} for spontaneous (uncatalyzed) oxidation of **19** into **20** was determined to be 6 x 10^{-7} min^{-1} under otherwise identical conditions. The rate acceleration (k_{cat}/k_{non}) deduced from these values is 60,000-fold.

4.3 Catalytic oxidation of DTBQ in 80% aqueous methanol

Catalyst **17** was prepared by mixing 80% aqueous methanol solutions of copper(II) acetate and ligand **14c** in 2:1 molar ratio and the apparent catalyst

concentration determined from the percentage formation (59%) obtained by species distribution analysis (Figure 3.9). Kinetic parameters for the oxidation of **19** were determined at substrate concentration range of 0.05 to 0.4 mM with catalyst concentration of 12 μM.

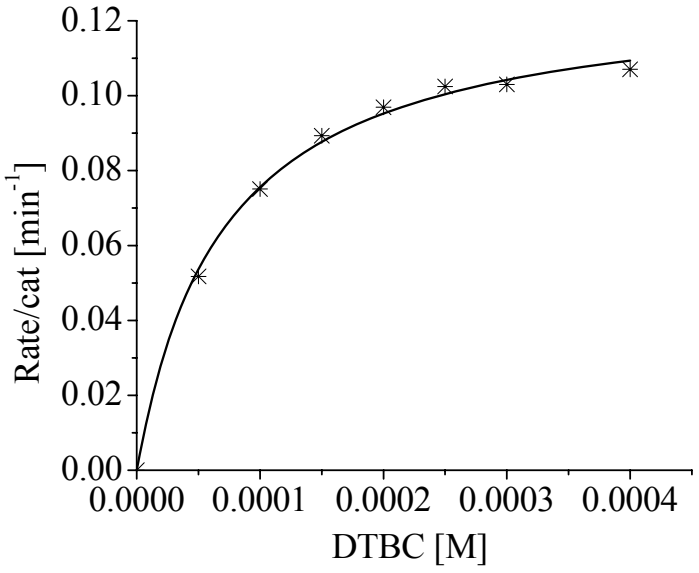

Figure 4.2. Kinetic profile for the aerobic oxidation of **19** into **20** promoted by **17** in MeOH/H_2O 80:20 (v/v)

The catalytic rate constant in 80% aqueous methanol was determined to be 0.13 min^{-1} which is higher than that in pure methanol (Figure 4.2). The Michaelis-Menten constant K_m was found to be 0.07 mM which shows a higher affinity of the substrate to the metal complex in aqueous methanol than in pure methanol. The transformation of DTBC into DTBQ is 140,000-fold accelerated over background under these conditions which is double the acceleration in methanol.

4.4 Catalytic oxidation of DTBQ in 60% aqueous methanol

The kinetic parameters for the catalytic oxidation of **19** into **20** were determined by varying the substrate concentration from 0.1 to 0.8 mM with apparent catalyst concentration of 15 μM. The apparent catalyst concentration was based on species distribution data (Figure 3.10) which indicates 72% catalyst formation at 2:1 molar ratio of Cu(II) to ligand **14c**. The catalytic rate constant was determined to be 0.16 min^{-1} and the Michaelis-Menten constant K_m as 0.41 mM (Figure 4.3). The rate constant for the spontaneous reaction k_{non} was determined as 1×10^{-6} min^{-1}. The rate acceleration (k_{cat}/k_{non}) was deduced from these values as 160,000-fold which is about 3 times higher than in pure methanol.

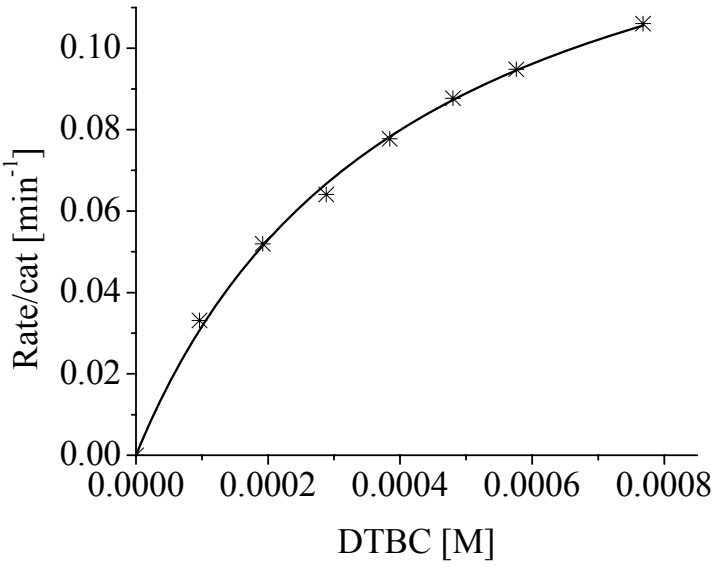

Figure 4.3. Kinetic profile for the aerobic oxidation of **19** to **20** promoted by **17** in MeOH/ H_2O 60/40 (v/v)

4.5 Contribution of mononuclear complex **16**.

Investigation of the contribution of complex **16** towards oxidation of 3,5-di-*tert*-butylcatechol **19**, was done in 60% methanol where formation of complex **16** was 80% at 1:1 molar ratio of Cu(II) to **14c** (Figure 3.10). Under these conditions, the rate constant k_{cat} and Michaelis-Menten constant K_m were found to be 0.0037 min^{-1} and 0.24 mM, respectively (Figure 4.4).

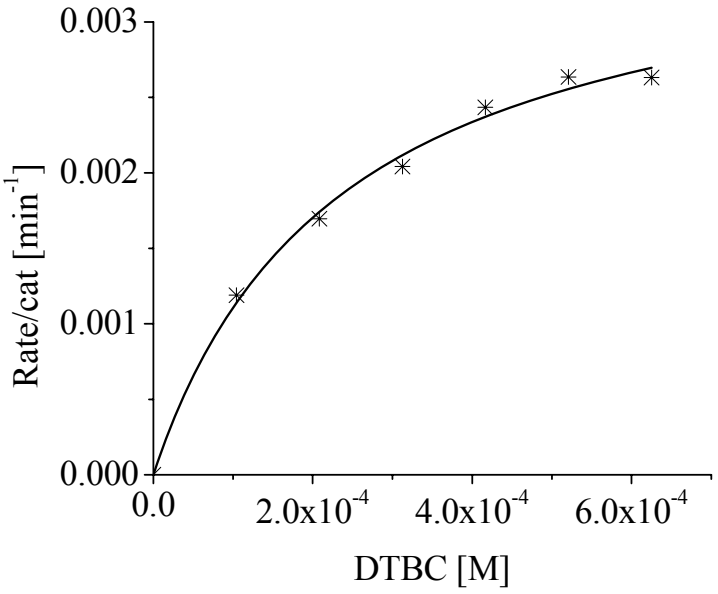

Figure 4.4. Kinetic profile for the aerobic oxidation of **19** to **20** by complex **16** in MeOH/ H_2O 60:40 (v/v)

At 2:1 molar ratio of Cu(II) ions to **14c**, the formation of mononuclear complex **16** is 25% (Figure 3.10). At this molar ratio, the contribution of the mononuclear complex was estimated to be k_{cat} = 0.001 min^{-1}. This contribution is about 1% of the rate

constant for the binuclear complex (k_{cat} = 0.16 min^{-1}) and was therefore considered to be negligible.

4.6 Role of oxygen in the transformation of DTBC into DTBQ

It is generally accepted that the first step of catechol oxidation occurs anaerobically and involves stoichiometric oxidation of catechol by dicopper(II) center leading to the formation of quinone and a dicopper(I) center.[117,118] We therefore probed the dependence on oxygen for the catalytic transformation of DTBC into DTBQ in anaerobic conditions in order to understand the catalytic mechanism. Anaerobic oxidation was followed spectroscopically in methanol and in 60% aqueous methanol at 420 nm and the absorbance recorded over time (Figure 4.5).

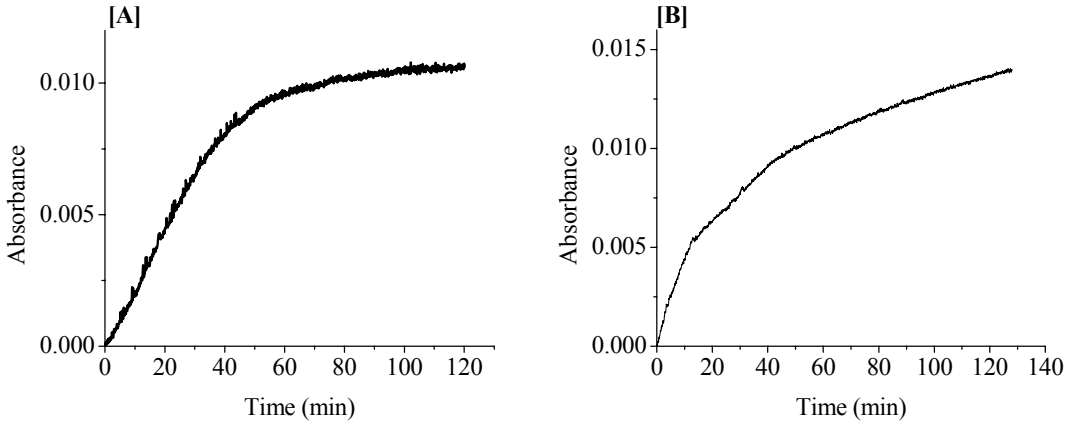

Figure 4.5. Anaerobic catalytic oxidation of DTBC in A) 60% MeOH and B) 100% MeOH

The anaerobic reaction was found to occur very slowly for about 1 h in both MeOH and 60% aqueous MeOH then leveled out after one hour. At the end of 2 h, less than half the stoichiometric amount of product DTBQ with respect to the catalyst concentration was formed in both MeOH and 60% aqueous MeOH. The reaction however proceeded after a 10 min lag time when the flask was opened to allow oxygen intake (Figure 4.6).

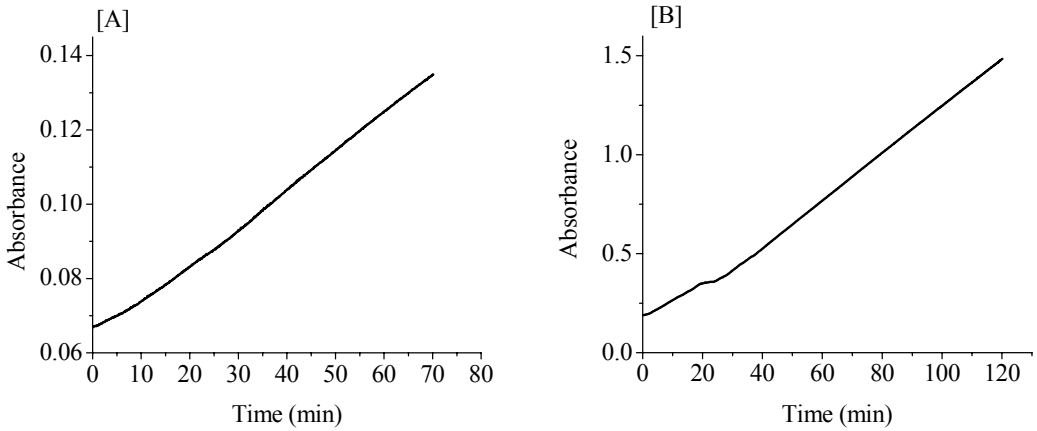

Figure 4.6: Aerobic oxidation of DTBC after opening the flask in A) 60% MeOH and B) 100% MeOH

These results show that the overall catalytic reaction is dependent on the presence of molecular oxygen. We propose formation of a dicopper(II)–catechol intermediate in the first step followed by a one-electron transfer from the catechol to the copper(II) center resulting in a semiquinone intermediate.[119]

4.7 Determination of hydrogen peroxide formation

Formation of hydrogen peroxide is often observed in catechol oxidation reactions catalyzed by binuclear copper(II) complexes.[120] Determination of hydrogen peroxide was performed iodometrically by UV-Vis at 352 nm (ε = 26400 $M^{-1}cm^{-1}$).[121] This iodide method of detecting hydrogen peroxide has a detection limit of ~10^{-6} M and allows differentiation between H_2O_2 and organic peroxides. To determine the formation of hydrogen peroxide, product solution for oxidation of **19** in 60% MeOH using catalyst **17** was tested and compared with a 0.04 mM H_2O_2 solution as a blind test (Figure 4.7).

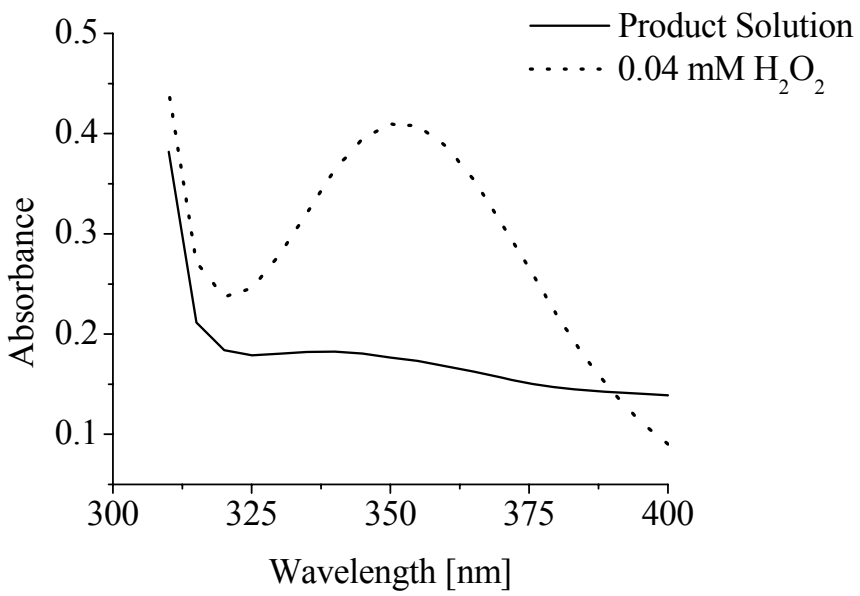

Figure 4.7: UV-Vis analysis of hydrogen peroxide in the catalytic oxidation of **19** using catalyst **17** in 60% methanol.

The test shows formation of a band at 352 nm for 0.04 mM H_2O_2 confirming the validity of the hydrogen peroxide detection method. The product solution

does not however form any detectable amount of hydrogen peroxide during the catalytic cycle. We therefore conclude that oxygen is reduced to water as the final product and not hydrogen peroxide.

4.8 Glycoside Hydrolysis

Schiff-base complexes have been used as catalysts for various transformations including aerobic oxidation of alcohols,[119] epoxidation of olefins,[122] ethylene polymerization,[123] hydrogenation[124] and hydrolysis of phosphate esters.[125] Very little attention has been given to the design of complexes that catalyze the very widespread and important biological process of glycosyl transfer. Glycosyl transfer is a very important biochemical reaction since around two-thirds of the carbon in the biosphere exists as carbohydrate.[126] The simplest nonenzymatic glycosyl transfer reaction is the hydrolysis of a glycoside. Glycoside hydrolysis has been performed extensively using cyclodextrin based catalysts including dicyanohydrins,[127,128] diacids,[129] trifluoromethylated cyclodextrin derivatives[130] and metal ions like copper(II), nickel(II), cobalt(II) and aluminum(III).[131,132] Although cyclodextrins have some desirable properties like solubility in water and good water binding properties, they have several drawbacks such as decomposition during catalysis and lack of catalytic activity after small alteration of the substrate from 4-nitrophenyl to 2-nitrophenyl glycoside.[129,133] So far, studies on hydrolysis of glycosides using metal ions have focused on substrates that provide a binding site for the metal ion close to the glycosidic bond in order to allow for electrophilic catalysis. This has narrowed the pool of substrates to glycosides with metal

ligating properties. To circumvent this, we envisioned having metal ions coordinated to a Schiff-base ligand and studying the catalytic activity of the resulting complexes towards cleavage of glycosidic bonds. Three water soluble complexes **15c**, **26** and **18** (Figure 4.8) were used to study the catalytic hydrolysis of model aryl glycosides in water.

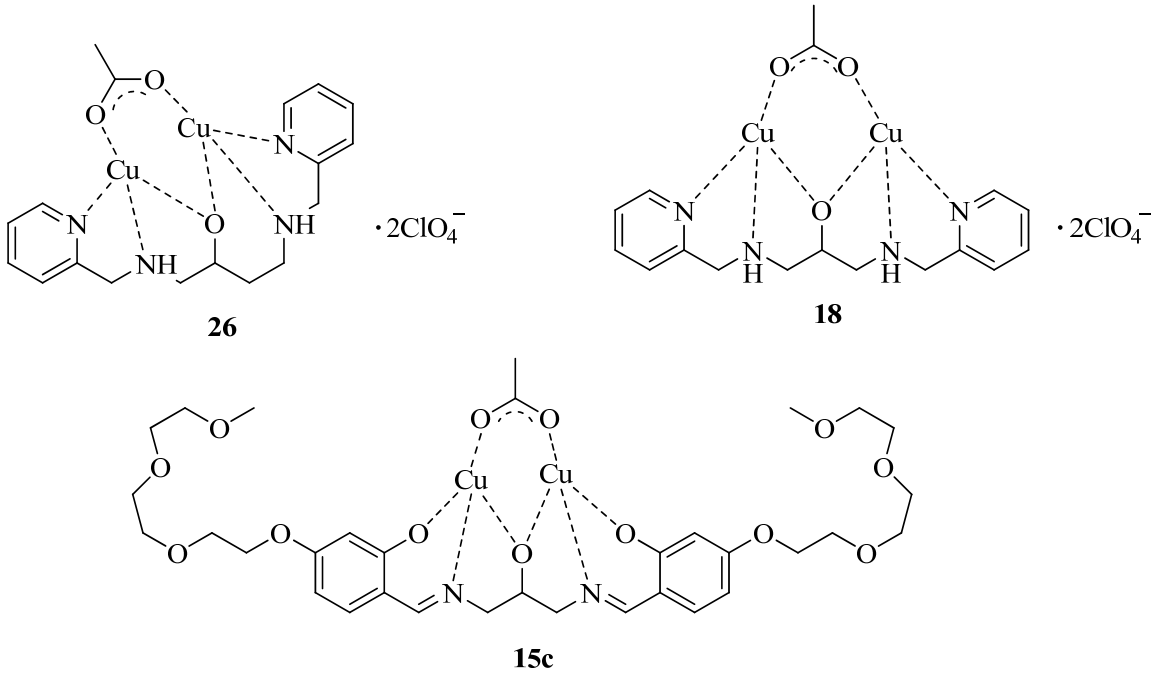

Figure 4.8. Structures of binuclear copper(II) complexes **15c**, **26** and **18**.

While complexes **15c**, **26** and **18** have similar intermetallic distances of around 3.5 Å, they have some structural differences that might impact their catalytic activities. Complexes **26** and **18** are reduced Schiff-base complexes based on pyridyl functionality while complex **15c** is a salicylaldehyde-based Schiff-base complex. Moreover, complexes **15c** and **18** are symmetrical while complex **26** is asymmetrical.

4.9 Hydrolysis of model glycoside

To probe the structural effects of the ligand backbone for catalysts **15c, 26** and **18** that have similar intermetallic distances (~ 3.5 Å), we studied the hydrolysis of model glycoside *p*-nitrophenyl-α-D-galactopyranoside (**30**) (Scheme 4.2). The hydrolytic product of this reaction, the *p*-nitrophenoxide anion (**32**) is colored, allowing the hydrolysis to be monitored by UV-Vis spectroscopy.

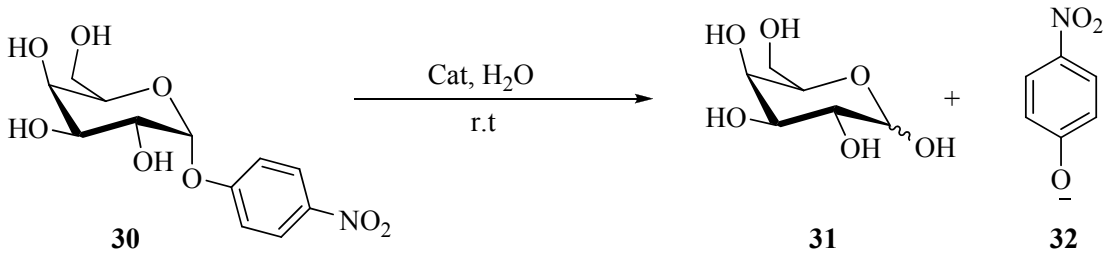

Scheme 4.2. Hydrolysis of *p*-nitrophenyl-α-D-galactopyranoside (**30)**.

In order to determine the wavelength at which to monitor the reaction, UV-Vis absorption spectra were measured at 30 min time intervals for a solution of **30** (22.4 mM) and catalyst **26** (0.1 mM) in CAPS (3-(cyclohexylamino)-1-propane sulfonic acid**)** buffer at pH 10.5 thermostated at 30 ºC. A steady increase in absorbance in the range 350–450 nm was observed with the greatest change occurring around 410 nm as shown in Figure 4.9.

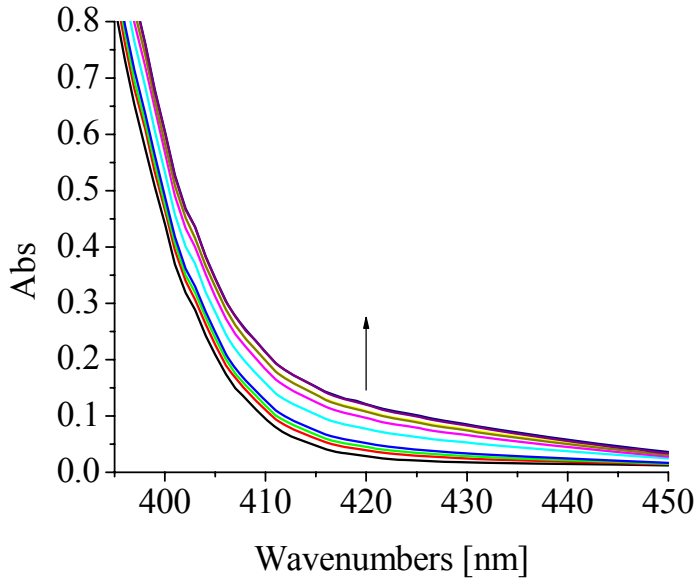

Figure 4.9. Time-dependent UV-Vis spectra of 4-nitrophenyl-α-D-galactopyranoside (**30**) and catalyst **26** in CAPS buffer at pH 10.5 and 30 ºC.

The reaction was monitored at 410 nm. The kinetic profile obtained for hydrolysis of 4-nitrophenyl-α-D-galactopyranoside (**30**) promoted by **26** and **15c** is linear in the 4 mM – 50 mM substrate concentration range as shown in Figure 4.10. Further increase of the substrate concentration to reach saturation was limited by low solubility of **30** in aqueous solution.

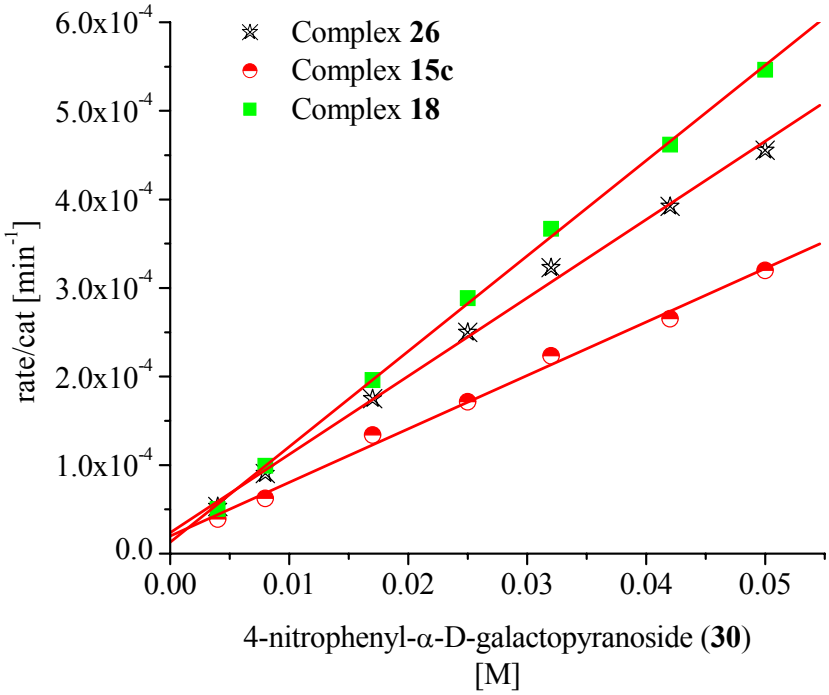

Figure 4.10. Kinetic profile for hydrolysis of 4-nitrophenyl-α-D-galactopyranoside (**30**) in the presence of 0.1 mM catalyst in CAPS buffer at pH 10.5 and 30 ºC.

The catalytic efficiency (k_{cat}/K_m) of catalyst **26** was found to be 1.5 times higher than for catalyst **15c** at pH 10.5 (Table 4.1). Kinetic parameters for non-catalytic hydrolysis of **30** were obtained in borate buffer at pH 9.0 and CAPS buffer at pH 10.5 (Appendix 6). Complex **18**, which is a structurally similar to **26**, was found to be slightly more efficient than **26** (1.2-fold) but almost twice as fast as the structurally different bis-salicylaldehyde complex **15c**. When tested at a lower pH of 9.0, the efficiency of catalyst **26** was found to decrease dramatically (10-fold).

Table 4.1. Summary of catalytic efficiencies for hydrolysis of **30** in CAPS buffer at pH 10.5 (ε = 16,200 $M^{-1}cm^{-1}$) and borate buffer at pH 9.0 (ε = 17,600 $M^{-1}cm^{-1}$) at 30 ^{o}C.

Catalyst	pH	k_{cat}/K_m [M^{-1} min^{-1}]	$k_{cat}/(K_m \times k_{non})$ [M^{-1}]
26	9.0	6.15×10^{-4}	11200
26	10.5	8.84×10^{-3}	16400
15c	10.5	6.02×10^{-3}	11200
18	10.5	10.7×10^{-3}	19800

In conclusion, the binuclear copper(II) complexes **15c**, **18**, and **26** were shown to activate the model glycoside **30** and effect its hydrolysis. The rate of hydrolysis was found to depend on the pH of the reaction and the structural nature of the ligand backbone of the complex.

CHAPTER FIVE

MACROMOLECULAR SCHIFF-BASE COMPLEX

5.1 Immobilized Schiff-base copper(II) complex

The macromolecular nature of enzymes plays a huge role in their high activity and selectivity.[134] The underlying principle of enzyme selectivity is based on molecular recognition of the catalyzed substrates to the macromolecular structure of the enzyme. This concept of molecular recognition is also responsible for a host of other important biological processes such as recognition of hormones by receptors and binding of antigens with antibodies.[135] It is therefore important to adapt the principle of molecular recognition in design of efficient catalysts. This can be achieved by producing macromolecular catalysts designed to specifically interact with the substrate, rather than making small molecular weight analogues.

It was envisioned to make enzyme-like catalysts by immobilizing Schiff-base catalysts into a microgel. Microgels are crosslinked polymers that form stable solutions in an appropriate solvent.[136] Microgels, unlike linear non-crosslinked polymers, have a low viscosity even at high concentrations which makes them easy to work with.[137] In order to incorporate Schiff-base catalysts into a microgel, structural modification of the ligand backbone was necessary to allow polymerization.

5.2 Miniemusion polymerization

In the first step toward immobilization of a Schiff-base ligand into a polymeric support, the ligand backbone was altered by introduction of polymerizable styrene sidechains using a method developed by Dittel et al. to obtain ligand **33** (Scheme 5.1).[138]

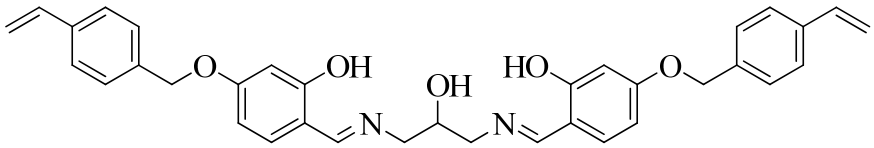

33

Scheme 5.1. Structure of polymerizable ligand **33**.

Several monomers were then explored in an attempt to develop stable miniemulsions. First, a 0.5:1 molar ratio of methyl acrylate to pentaerythritol triacrylate was used to prepare a miniemulsion, but upon polymerization for 10 minutes, a gummy solid was obtained that made it impossible to continue stirring the polymerization mixture. The monomers were changed to a 1:1 molar ratio of 2-hydroxyethyl acrylate to pentaerythritol triacrylate. This similarly led to formation of a solid after polymerization for 2 minutes. Attempts to substitute pentaerythritol triacrylate with methyl acrylate or styrene, and even to use 2-hydroxyethyl acrylate as the only monomer, were futile. Eventually, a stable emulsion was formed from a 1:1 mixture of styrene and butyl acrylate.

The miniemulsion polymer (PolL) was prepared using butyl acrylate, styrene, and ligand **30** as the monomers. Sodium dodecyl sulfate (SDS) was used as the surfactant and decane as the hydrophobic agent to prevent Ostwald ripening of the miniemulsion.[139] A representative miniemulsion recipe is shown in Table 5.1. Due to poor solubility of Ligand **33** in water and other common organic solvents, **33** was first dissolved in a minimum amount of DMSO before mixing it with the other monomers. The miniemulsion polymer was prepared by mixing a solution of the monomers with a solution of SDS in water. The resulting mixture was stirred vigorously for 1 h and then sonicated for 2 min to form a stable miniemulsion.

Table 5.1. Recipe for miniemulsion polymerization of styrene, butyl acrylate and ligand **33**.

Miniemusion recipe	Amount
Styrene (**34**)	3 g
Butyl acrylate (**35**)	3 g
SDS (emulsifier)	140 mg
Water	48 g
Ligand **33** (dissolved in 1 g DMSO)	140 mg
Decane	500 mg
KPS (initiator)	200 mg

Polymerization was initiated using potassium persulfate at 72 ^{o}C. The resulting miniemulsion polymer was washed with chloroform and purified by either ultracentrifugation or through dialysis.

After polymerization, the polymer unit consisted of styrene, butyl acrylate and pentadentate Schiff-base ligand **33** (Scheme 5.2). The elemental composition of the polymer was determined to be C, 77.47, H, 8.30 and N, 0.26%.

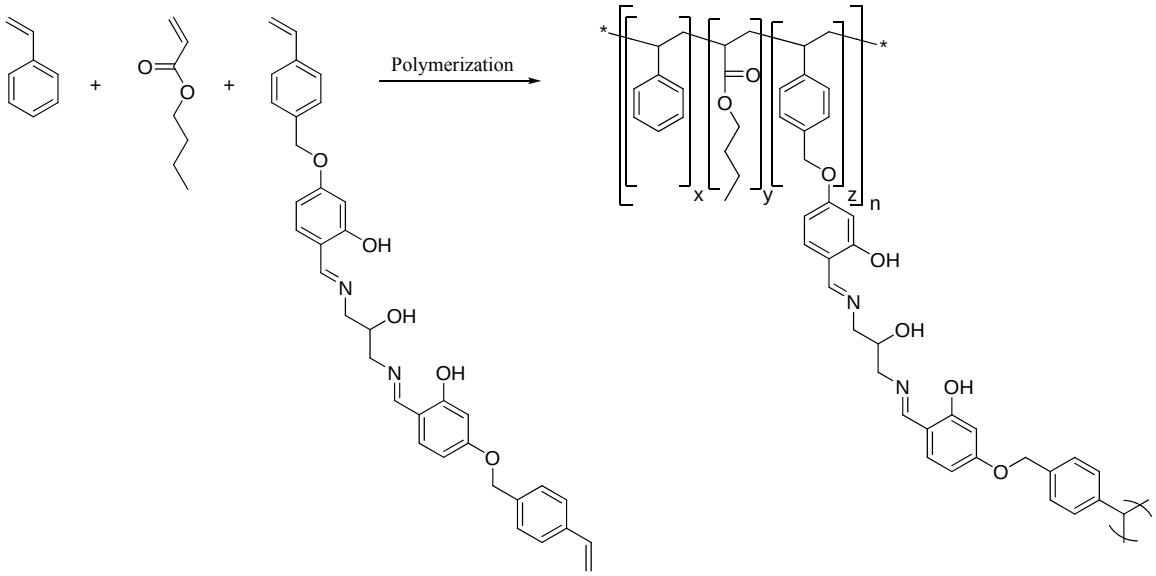

Scheme 5.2. Synthesis of poly(styrene-*co*-butyl acrylate-*co*-ligand **33**) (polL)

A control polymer (PolB) was also synthesized in exactly the same way as PolL with only exclusion of ligand **33** (Figure 5.1**)**.

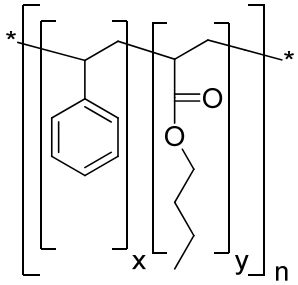

Figure 5.1. Structure of poly(styrene-*co*-butyl acrylate) (polB)

The elemental composition of polB was determined to be C, 77.34, H, 8.41 and N, 0.0%. Since the only possible source of N in polL is from ligand **33**, the percentage amount of N was used to determine the amount of ligand **33** loaded into polL. The theoretical amount of N in polL was 0.11 % which is slightly lower than the experimental value of 0.26%.

5.3 Determination of degree of conversion

The degree of conversion was determined gravimetrically for both polL and polB by using the equation:

$$\% \text{ Conversion} = \frac{M_{solid}}{M_{mo}} \times \frac{1}{1 + \frac{M_e}{M_{mo}}} \times \frac{M_{total}}{M_{aliquot}} \times 100$$

Where,

M_{solid} is the mass of solid

M_e is the mass of emulsifier

M_{mo} is the mass of monomers

M_{total} is total mass of all components of the miniemulsion

$M_{aliquot}$ is the mass of aliquot

Sample aliquots of the polymerization solution were taken at regular time intervals during polymerization, and pyrocatechol was added in order terminate the polymerization. The samples were allowed to air dry and the mass of solid residue obtained after correcting for the amount of pyrocatechol added. This corrected value gave the amount of microgel formed (M_{solid}) in the polymerization sample solution. From M_{solid} and the total amount of aliquot, the degree of conversion was calculated and plotted as a function of time (Figure 5.2). A maximum percentage conversion of 97% was realized after 160 minutes for both polL and the control polymer.

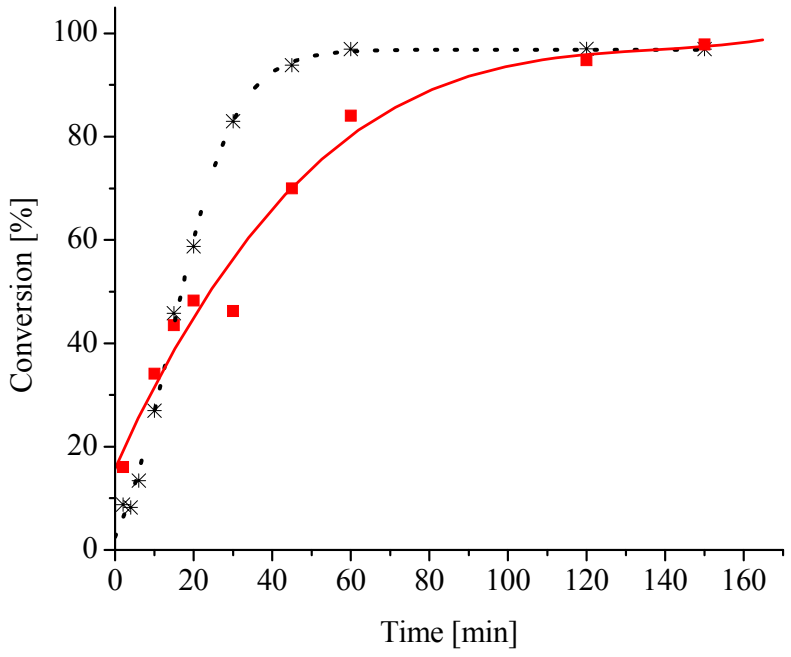

Figure 5.2. Monomer conversion vs time plot for polB (dotted line) and polL (solid line).

In order to achieve the highest monomer conversions possible, all polymerizations were performed for 180 min.

5.4 Characterization of the microgels

Miniemulsion polymers obtained by copolymerization of styrene (**34**), butyl acrylate (**35**) and ligand **33** and control polymer obtained by copolymerization of styrene and butyl acrylate were characterized by NMR, IR spectroscopy, transmission electron microscopy, dynamic light scattering and by gel permeation chromatography analysis.

IR spectra obtained for a freeze-dried miniemulsion polymer sample showed all major characteristic peaks of the polymer unit. The bands at 1452 and 1493 cm^{-1} are assigned to benzene ring vibrations (ν_{C-C}) of the styrene unit and ligand **33** (Figure 5.3). The absorption peak at 1728 cm^{-1} corresponds to C=O stretching vibration of the carbonyl in the butyl acrylate unit of the miniemulsion, polymer and the peaks at 2872 and 2956 cm^{-1} can be attributed to ν_{C-H} of saturated –C-H groups, while the band at 3026 is assigned to ν_{C-H} of the benzene ring.

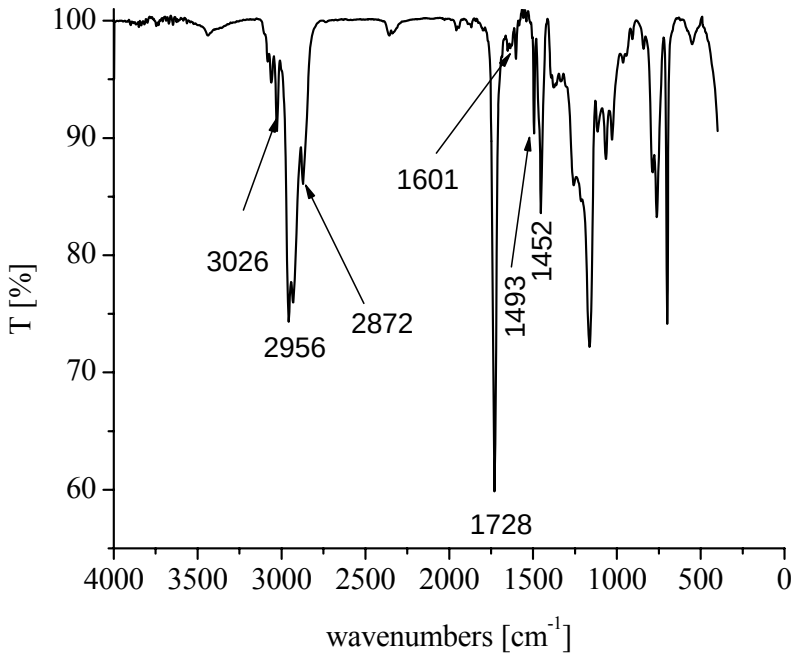

Figure 5.3. IR spectrum of a freeze-dried polymer sample (polL) obtained as a thin film in CCl_4.

The IR spectra of polL was compared to the spectra of monomers styrene and butylacrylate. The bands for the C=C stretching vibration in styrene (1630 cm^{-1}) and butyl acrylate (1636 cm^{-1} and 1617 cm^{-1}) were not observed in polL (Figure 5.4). It was therefore concluded that a negligible amount of C=C double bonds remained in the miniemulsion polymer.

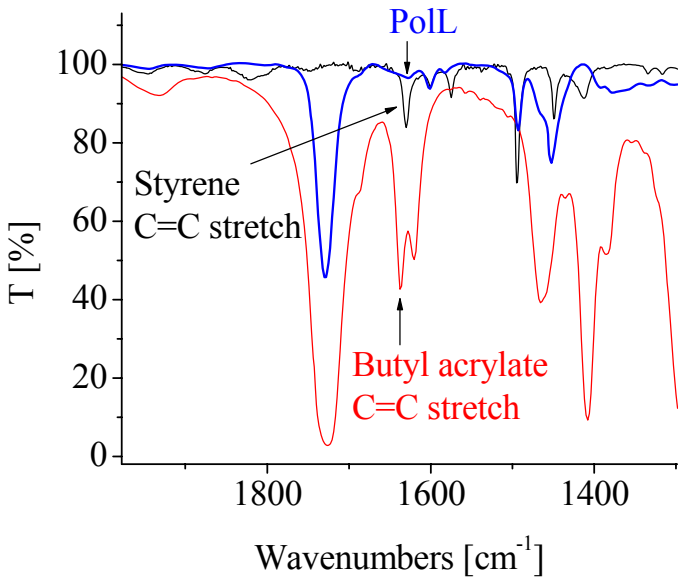

Figure 5.4: IR spectra of polL, styrene (**34**) and butyl acrylate (**35**)

5.5 NMR analysis of polL

^{1}H and ^{13}C NMR spectra for polL were obtained from a freeze dried sample of the miniemulsion polymer using deuterated acetone as the solvent. An overlay of ^{1}H NMR spectra for a freeze-dried polymer sample polL with a 1/1 (v/v) mixture of **34** and **35** shows disappearance of bands due to vinyl protons of **34** and **35** that appear between 5.2 ppm to 6.8 ppm upon polymerization (Figure 5.5).

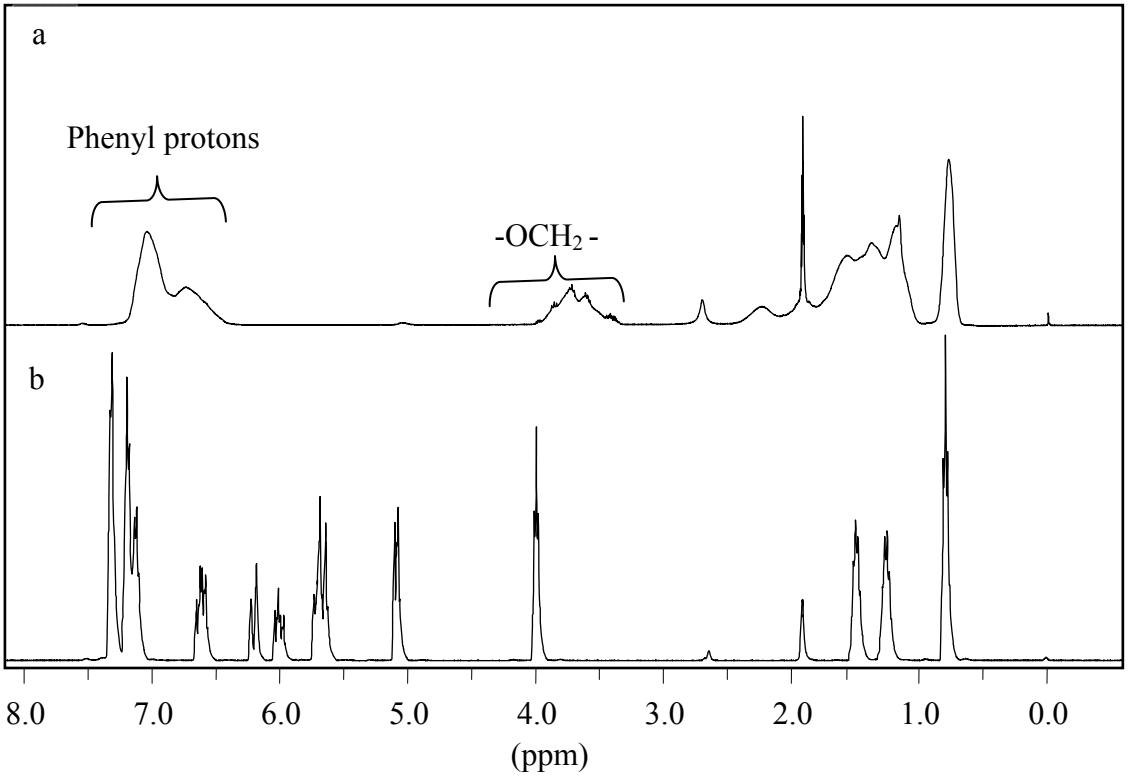

Figure 5.5. ^{1}H NMR spectra of (a) freeze-dried polymer (polL) in acetone-d_6 and (b) a 1:1 (v/v) mixture of **34** and **35** in acetone-d_6

This indicates that all of the monomer is converted to polymer, a fact that is further qualified by a plot of conversion of miniemulsion polymer vs time (Figure 5.2). ^{1}H NMR spectroscopy also showed the composition of the copolymer to be 1:1 (styrene to butyl acrylate) by comparison of the integrated resonance signals due to the phenyl protons for styrene and those of methylene group in butyl acrylate. The five protons on the aromatic ring of styrene absorb at approximately 6.6 - 7.2 ppm, and the two protons of the methylenes closest to the oxygen in the ester portion of butyl acrylate absorb at approximately 3.5 ppm (the $-OCH_2$ group).[140,141] Ligand protons could however not be

detected using NMR spectroscopy because of the low ligand content (2%) in the polymer matrix.

5.6 UV analysis of the miniemulsion polymers

UV analysis of polL and polB was done in THF for freeze dried polymer samples. The UV spectra obtained was overlaid with spectra of ligand **33** for comparison (Figure 5.6).

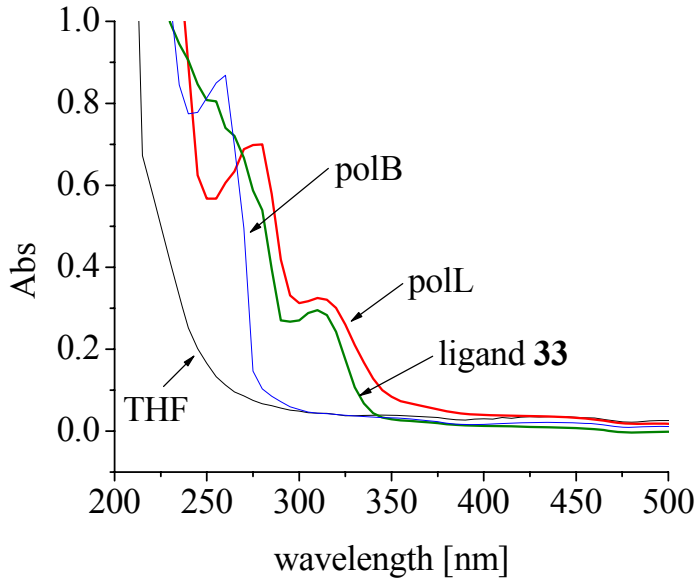

Figure 5.6: UV-Vis spectra of polL, polB and ligand **33** in THF at 30 ^{o}C.

The band around 310 nm observed in **33** and polL but absent in polB was assigned to the n→π* transition of the non-bonding electrons present on the nitrogen of the azomethine group in the Schiff-base.[142] This further confirmed the presence of **33** in polL.

5.7 Particle size distributions

Particle sizes were determined using transmission electron microscopy (TEM) and dynamic light scattering (DLS) techniques. TEM samples for miniemulsion polymers polL and polB were diluted using nanopure water to approximately 1:100 (v/v) prior to taking measurements. DLS analysis was done for samples in both aqueous and methanol solutions. TEM analysis of polL showed monodisperse spherical particles with a mean diameter of ~ 61 nm (Figure 5.7).

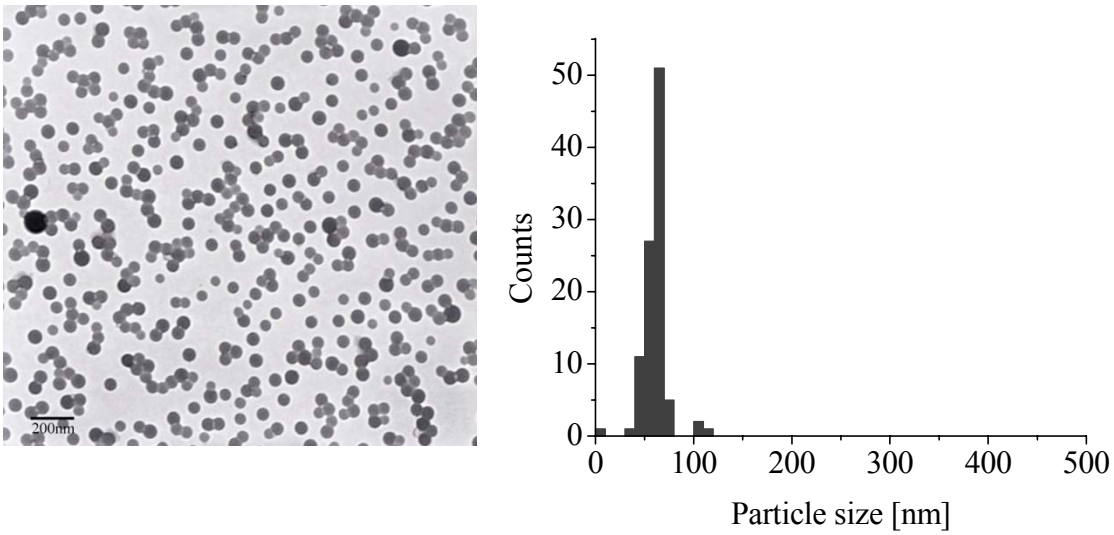

Figure 5.7. TEM image and particle size distribution for PolL taken using 200 mesh copper grids coated with carbon at 40K magnification

Analysis of polL particles in water using DLS showed a slight increase in average particle size to 75.4 nm (Figure 5.8). The difference between particle sizes measured by TEM and DLS is an effective measure of degree to which particles

aggregate in solution.[143] There was therefore no significant aggregation observed for polL in water as the particle sizes measured using TEM and DLS are comparable

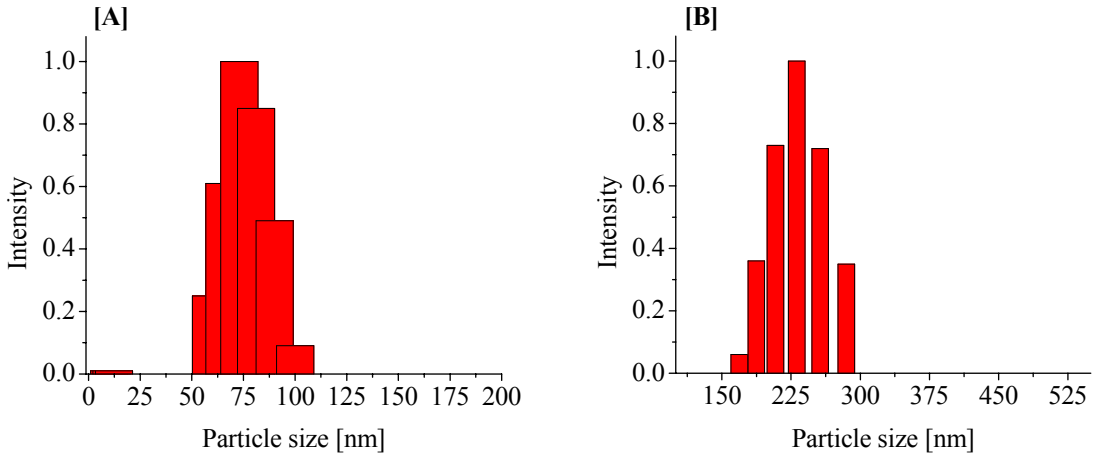

Figure 5.8. Intensity-weighted Nicomp particle size distribution for polL measured using DLS in A) Water and B) Methanol

On the other hand, there was a significant increase in the average particle size when DLS measurements were taken in methanol (233 nm) indicating aggregation of the miniemulsion polymer polL in methanol.

TEM analysis of polB reveals a median diameter of ~60 nm (Figure 5.9) which is comparable to the results obtained for DLS experiment in water and in methanol. This indicates that polB does not aggregate in either water or methanol.

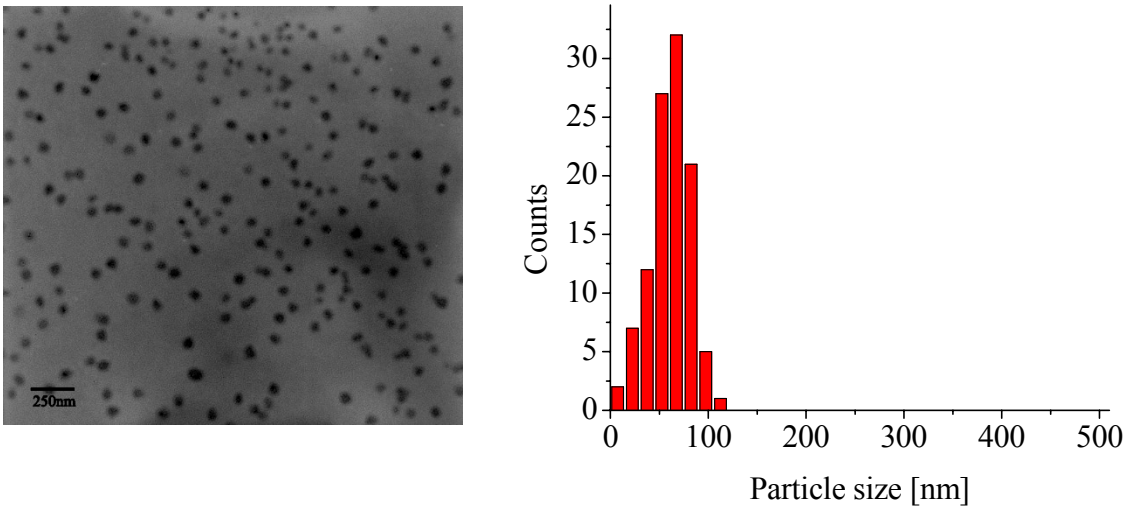

Figure 5.9: TEM image and particle size distribution for polB taken using 200 mesh copper grids coated with carbon at 31.5K magnification

Dynamic light scattering analysis of polB showed comparable particle size distributions in water (66 nm) and in methanol (72 nm) (Figure 5.10).

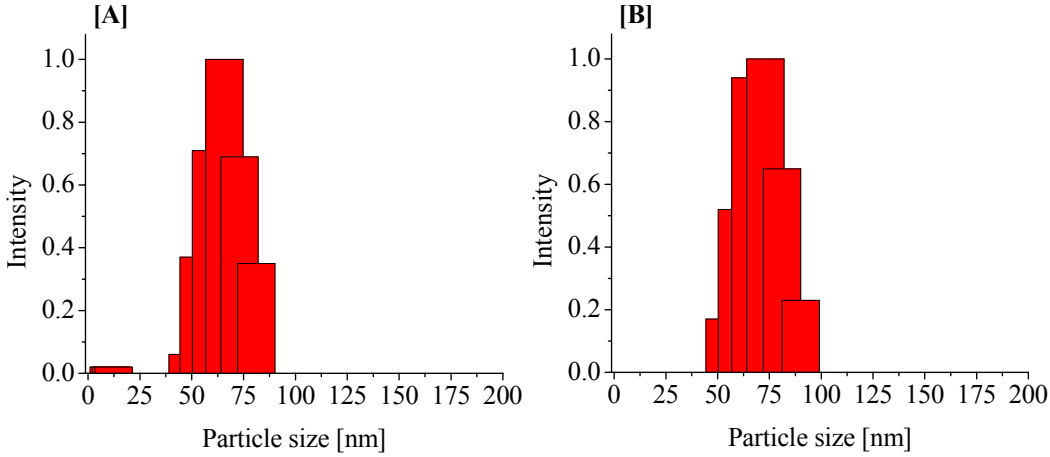

Figure 5.10. Intensity-weighted Nicomp particle size distribution for polB measured using DLS in A) water and B) methanol

5.8 Stability of the polymers in acidic and alkaline media

Stability studies of the miniemulsion polymers in both acidic and alkaline media were important for future application of the microgels as catalysts. Degradation studies of the polymers were therefore performed at different acid and base concentrations. In this regard, sample aliquots of the miniemulsion polymers were treated with either hydrochloric acid or ammonium hydroxide solution for 24 h and subsequently analyzed by IR spectroscopy and gel permeation chromatography.

When the miniemulsion polymer polL was exposed to 0.25 M, 0.5 M and 3 M HCl, the polymer solution formed a precipitate. Upon treatment with 0.05 M HCl and under basic conditions up to 3 M ammonium hydroxide solution, precipitation did not occur. IR spectra of freeze dried polymers did not reveal degradation in either alkaline or acidic conditions.

Gel permeation chromatography (GPC) analysis of the molecular weight distributions for miniemulsion polymers polL and polB showed stability over pH range 1-13 (Table 5.2 and 5.3). Freeze-dried samples of polL and polB were analyzed in THF based on polystyrene standards. The analysis of average molecular weight showed that the polymer matrix was stable over the pH range 1-13 for both polL and polB as there were no significant changes in the molecular weight values (M_n, number average molecular weight; M_w, weight average molecular weigh; M_p, peak molecular weight). Comparing polL and polB, there was a slight increase in the overall molecular weight distributions values for polB than those for polL.

Table 5.2. GPC data for polymer polL obtained at pH 1-13.

pH	Polymer	M_n	M_w	M_p	PDI(M_w/M_n)
--*	polL	47000	62000	76000	1.3
1	polL	44000	57000	75000	1.3
3	polL	48000	62000	77000	1.3
5	polL	47000	60000	77000	1.3
7	polL	55000	68000	79000	1.2
9	polL	40000	61000	77000	1.3
11	polL	44000	55000	76000	1.3
13	polL	44000	56000	76000	1.3

*untreated polymer

Table 5.3. GPC data for polymer polB obtained at pH 1-13.

pH	Polymer	M_n	M_w	M_p	PDI(M_w/M_n)
--*	polB	50000	66000	79000	1.3
1	polB	54000	73000	84000	1.4
3	polB	56000	74000	84000	1.3
5	polB	54000	73000	84000	1.4
7	polB	56000	73000	84000	1.3
9	polB	58000	75000	84000	1.3
11	polB	54000	73000	84000	1.3
13	polB	53000	71000	82000	1.3

*Untreated polymer

5.9 Activation of the polymeric catalyst using copper(II) ions

To activate the catalysts, copper(II) ions were introduced into both polL and polB by dialysis against an aqueous solution of copper(II) acetate and the amount of metal ions loaded quantified using atomic absorption spectrophotometry (AAS). The polymer was then put on dialysis against nanopure water in order to remove excess unbound metal ions. Sample aliquots were taken at regular time intervals during dialysis for AAS analysis.

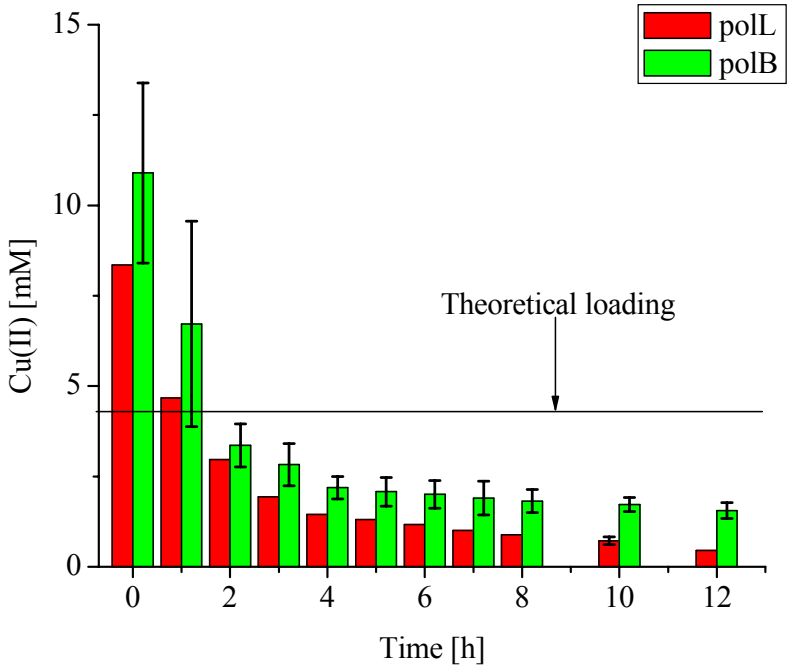

Figure 5.11. A plot of concentration of Cu(II) ions in polL and polB during dialysis of the polymers against nanopure water.

Copper amounts quantified using AAS reveal that a substantial amount of unbound copper(II) ions were effectively removed from both polL and polB in the first three hours of dialysis against water (Figure 5.11). The copper amount then leveled out to around 1.8 ppm for polL and 0.2 ppm for polB after dialysis for 10 h. This translates to 42% of the theoretical (4.28 mM) Cu(II) content retained in polL, while the amount of unbound Cu(II) ions in polB is less than 5%. The ability of polL to bind Cu(II) ions is therefore significantly higher than for polB and is attributed to coordination of Cu(II) ions to the immobilized Schiff-base ligand **33**. Since only 42% of binding sites in polL are bound to copper(II) after washing, it is highly probable that some of the coordination sites are inaccessible to metal ions due to the highly cross linked macromolecular structure of the polymeric matrix.

Since salicylaldehyde based binuclear nickel(II) Schiff-base complexes are known, we investigated the coordination of Ni(II) to the miniemulsion polymers polL and polB.[144] Initial attempts to load excess amount of Ni(II) into the polymer led to precipitation. We therefore loaded a slightly less than the theoeretical value of 4.28 mM which is equivalent to double the stoichiometric amount of ligand in the polymer. The binding of Ni(II) was significantly lower than that of Cu(II) and comparable to control polymer polB (Figure 5.12).

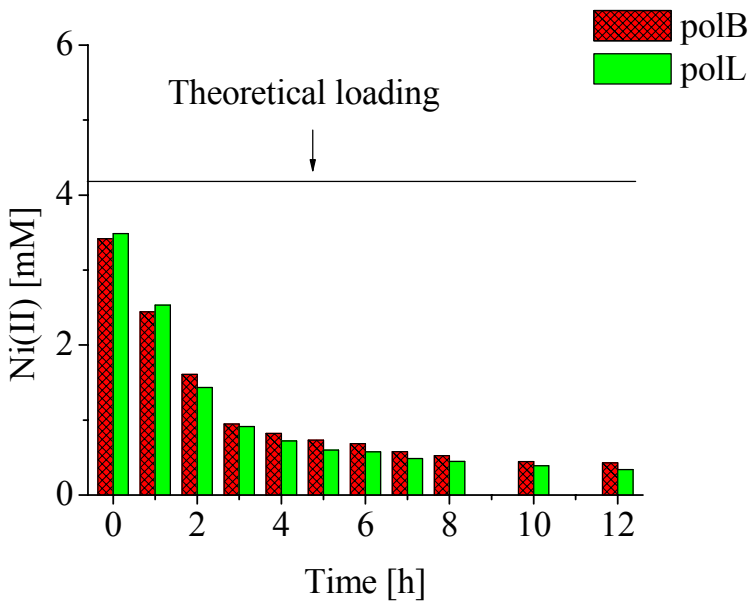

Figure 5.12. A plot of concentration of Ni(II) ions in polL and polB during dialysis of the polymers against nanopure water.

Similar results were obtained during attempts to load Mn(II) ions. The binding of Fe(III) ions was hampered by precipitation of the polymer.

5.10 Conclusion

A pentadentate Schiff-base ligand was immobilized into a poly[styrene-co-butyl acrylate] matrix by miniemulsion polymerization. The polymer particles obtained were shown to bind to Cu(II) ions in water and were stable over a wide pH range (pH 3 – 11). Transmission electron microscopy imaging showed a particle size of ~ 61 nm. Dynamic light scattering experiments in methanol and in water showed that the particle aggregation was solvent dependent.

CHAPTER SIX

EXPERIMENTAL SECTION

This chapter provides the experimental details for Chapters II, III, IV and V.

6.1 Instrumentation

Nuclear Magnetic resonance: ^{1}H and ^{13}C NMR spectra were recorded on a Bruker AV 400 spectrometer (400 MHz for proton and 100 MHz for carbon). Chemical shifts (δ) in ^{1}H NMR were expressed in parts per million and coupling constants (*J*) in Hertz. Chemical shift values were reported relative to the residue signals of the deuterated solvent ($CDCl_3$: δ = 7.24 for ^{1}H and δ = 77.0 for ^{13}C; acetone-d_6, δ = 2.05 for ^{1}H; DMSO-d_6, δ = 2.50 for ^{1}H and δ = 49.0 for ^{13}C)

UV-Vis spectroscopy*:* UV-Vis spectra were recorded on a Varian Cary 50 with WinUV Analysis Suite software, version 3.0, using Suprasil standard (200-2000 nm) of 1 cm thickness and 4.5 mL volume for the determination of species distribution. Disposable 1.5 mL semimicro Brandtech UV cuvettes (220-900 nm) of 10 mm light path with caps were used for oxidation studies

Infrared Spectroscopy: The IR spectra were obtained on a Shimadzu IR Prestige-21 FT-IR spectrophotometer with IR solution software version 1.10. Typically, 16 scans were run at a resolution of 2 cm^{-1} to obtain IR spectra.

High Performance Liquid Chromatography: HPLC separation was performed using a Shimadzu HPLC system with an SPD-10A UV-Vis detector, DGU-14A Shimadzu degasser, SIL-10A Shimadzu auto injector, FRC-10A Shimadzu fraction collector, LC-10A Shimadzu liquid chromatograph pumps A and B. The analytical column was Phenomenex Luna C18, 50 × 3 mm, 3 µm, 100 Å column at 1 mL/min flow rate. The mobile phase for all analysis was composed of 10% B to 100% B linear gradient over 20 min followed by a further 10 min at 100% B, where solvent B was 100% MeOH and solvent A was H_2O + 0.1% acetic acid. Separations were achieved using a semi-preparative Phenomenex Luna C18, 100 × 10 mm, 3 µm, 100 Å column at 2 mL/min flow rate. All compounds were monitored at 254 nm.

pH meter: The pH was measured using a Beckman Φ 250 pH meter equipped with refillable long Futura pH electrode of 0.7 mm thickness. The pH meter was calibrated before each set of readings.

Atomic Absorption Spectroscopy: The AAS data were acquired on a Varian AA240 flame atomic absorption spectrometer using SpectraAA version 5.01 PRO as the software. A copper hollow-cathode lamp was run under the conditions suggested by the manufacturer (current 4.0 mA). The wavelength was 324.8 nm and bandwidth of the slit was 0.5 nm. The flame composition was acetylene (flow rate 2.00 L/min) and air (flow rate 13.50 L/min).

Dynamic Light Scattering: DLS measurements were performed using submicron particle size analyzer (Nicomp PSS 380) with He-Ne laser source of 632.8 nm and the data analyzed using intensity-weighted Nicomp distribution fitting with NICOMP software package version 1.60. DLS samples were diluted 0.1 in 20 mL nanopure water or methanol.

Transmission electron microscopy: TEM measurements were performed using Zeiss EM 10C/10CR transmission electron microscope operated at 60 kV. Samples for transmission electron microscopy were prepared by placing a drop of a diluted (1:100 times) miniemulsion polymer on a 200 mesh copper grid coated with Formvar or carbon and allowing it to air dry for 48 h. No further contrasting was applied. The 200 mesh carbon or formvar coated Cu grids were obtained from Electron Microscopy Sciences.

TEM images was analyzed using the image processing software named ImageJ to obtain particle size distributions. Typically, a TEM image was imported into ImageJ and converted to binary. The particles were segmented by adjusting the threshold and analyzed after setting the circularity of the particles to a range of 0.75 to 1. A total of ~99 particles were obtained after analysis of the TEM image depicted in Figure 5.7 with sizes ranging from 5 to 115 nm.

Gel permeation chromatography: GPC data was obtained on a Shimadzu SEC system with a Phenogel column 10^4 (300 × 7.8 mm, 5 mm) in THF with a flow rate of 1 mL/min and UV-Vis detector at 254 nm. Polystyrene standards of molecular weight 4,000, 10,000, 20,000, 50,000, 70,000 and 150,000 were used for calibration. Molecular weight distribution data was acquired and analyzed using CLASS-VP program version 7 from Shimadzu Scientific Instruments.

Elemental analysis: Samples for elemental analysis were sent to Atlantic Microlab Inc., Atlanta, GA.

6.2 Materials and Reagents

Thin layer chromatography (TLC) was done using silica gel TLC plates from SORBENT Technologies with detection by UV light. Column chromatography was performed using silica gel from Silicycle (40 – 60 μm, 230 – 240 mesh). All melting points were recorded on a Mel-Temp melting point apparatus and the melting points are uncorrected. Nanopure water was obtained from EASY pure II water system from Barnstead (18.2 MΩ/cm).

All Chemicals were reagent grade or better and were used without further purification unless otherwise stated. 3,5-Di-*tert*-butylcatechol (DTBC, **19**) was purchased from Aldrich and recrystallized twice from *n*-pentane under argon before use. HPLC grade methanol (99.93%) was purchased from Aldrich and was used for all UV-Vis experiments. All other reagents were used as received from commercial suppliers.

6.3 Species distribution analysis.

Species distribution analysis was performed using SPECFIT program by applying $M/L/H^+$ complexation and speciation model which solves metal complexation and ligand speciation equilibria using the overall stability constants for the general case:

$$mM + lL + hH \longleftrightarrow [M_mL_lH_h]$$

$$\beta_{mlh} = \frac{[M_m L_l H_h]}{[M]^m [L]^l [H]^h}$$

Where M is a free metal ion, L is a ligand and H is the H^+ ion. The indices *m,l,h* are integers that define the state of complexation or protonation for a given species.

A general speciation model (M/L complexation) was used to solve complexation equilibria at constant pH:

$$mM + lL \longleftrightarrow [M_m L_l]$$

$$\beta_{ml} = \frac{[M_m L_l]}{[M]^m [L]^l}$$

Simultaneous spectroscopic measurements of absorbance vs. wavelength as a function of pH (for M/L/H^+ complexation) or concentration of metal ions (for M/L complexation) were imported as single scan spectra into the SPECFIT program.[97] Sample volumes, amounts of titrant aliquots added, pH, temperature and sample concentrations for each scan were input into a complexation/ pH titration form and the data computed using globalized fitting methodology provided by the SPECFIT program.[97]

All experiments were performed in 4.5 mL UV-Vis cuvettes with solutions thermostatted at 30 ± 0.1 ^oC and maintained at constant ionic strength with 0.1 M $NaClO_4$. For metal / ligand titration experiments at constant pH (Figures 3.5, 3.9 and 3.10), 10 μL aliquots of 0.3 M copper(II) acetate solution were titrated into 2 mL (initial volume) solution of 2 mM (initial concentration) ligand **14c**. After mixing the solutions thoroughly with a pipette, UV-Vis spectra were recorded as a function of the total concentration of copper(II) acetate and the spectral data computed using SPECFIT. Binding constants for the complexation systems were generated (Tables 6.1, 6.2 and 6.3).

Table 6.1. Binding constants for species distribution studies of **14c** and Copper(II) acetate perfomed in MeOH (Figure 3.5)

M	L	Log β	Std. Deviation
1	2	6.209	0.7119
1	1	9.066	0.9753
2	1	10.88	0.9129

Where M is Cu^{2+} and L is ligand **14c**

Table 6.2. Binding constants for species distribution studies of **14c** and Copper(II) acetate perfomed in MeOH/water 80/20 (v/v) (Figure 3.9).

M	L	Log β	Std. Deviation
1	2	5.533	0.5531
1	1	10.32	0.7477
2	1	8.669	0.6571

Where M is Cu^{2+} and L is ligand **14c**

Table 6.3. Binding constants for species distribution studies of **14c** and Copper(II) acetate perfomed in MeOH/water 60/40 (v/v) (Figure 3.10).

M	L	Log β	Std. Deviation
1	2	3.625	0.5586
1	1	7.340	0.7053
2	1	6.908	0.8040

Where M is Cu^{2+} and L is ligand **14c**

In the case of metal / ligand complexation with variable pH (Figures 3.11 and 3.15), a 2 mL aqueous solution containing 1 mM copper(II) chloride, 0.5 mM sodium acetate and 0.5 mM ligand **14c** or **25** was titrated with 10 μL of freshly prepared sodium hydroxide solution and the pH recorded after mixing the solutions. UV-Vis spectra were

then recorded as a function of the pH and the spectroscopic data computed by fitting procedures provided by the program Specfit. The ionic strength of the aqueous solution was maintained constant with 0.1 M $NaClO_4$ at 30 ^oC. The concentration of sodium hydroxide solution titrated was increased gradually from 0.025 M to 1 M to avoid huge pH changes. Binding constants for the complexation systems were generated (Tables 6.4, and 6.5).

Table 6.4 Binding constants for species distribution studies of **14c** and Copper(II) chloride over pH 4-13 (Figure 3.11).

M	L	H	Log β	Std. Deviation
0	1	1	11.88	0.2106
0	1	2	21.96	1.6260
0	1	3	35.58	0.1680
1	1	0	9.651	0.2948
2	1	-3	-9.765	0.3288
2	1	-4	-23.44	0.5356

Where M is Cu^{2+} and L is ligand **14c**

Table 6.5 Binding constants for species distribution studies of **25** and Copper(II) chloride over pH 4-13 (Figure 3.15).

M	L	H	Log β	Std. Deviation
0	1	1	11.44	0.2237
0	1	2	22.94	0.1364
0	1	3	30.59	0.4976
0	1	4	33.99	0.7982
1	1	0	7.606	0.1450
2	1	-1	5.153	0.3866
2	1	-2	-6.082	0.1376

Where M is Cu^{2+} and L is ligand **25**

6.4 Polymer purification

Spectra/Por® Biotech RC dialysis membranes of MW cut-off 15,000 were used to purify the microgels. Prior to dialysis, membranes were cut into appropriate lengths to accommodate 25 mL of the microgel, soaked in nanopure water for 10 min and rinsed. The tubing was closed with Spectra/Por closures, solution poured into the bag with glass funnel and the top of the bag closed with a Spectra/Por closure. Dialysis was done in a 1 L Erlenmeyer flask containing 950 mL of nanopure water for 24 h at ambient temperature while stirring. During this period, water was changed 3 times.

6.5 Spectroscopic study of coordination of acetate to **15c** in methanol

UV-Vis spectra of ligand **14c** and copper(II) chloride (Figure 3.7) were obtained by titration of 20 μL aliquots of 30 mM anhydrous sodium acetate solution into a 2 mL solution of 4 mM copper(II) chloride and 2 mM ligand **14c** in methanol at 30 ^{o}C.

6.6 General procedure for conducting kinetic experiments.

The experiments were done at 30 ^{o}C in three different solvent systems: pure methanol, 80/20 MeOH/H_2O and 60/40 MeOH/H_2O. In a typical experiment, a 2 mM catalyst stock solution was prepared by mixing a solution of 7.9 mg (40 μmol) copper(II) acetate monohydrate and 12.5 mg (20.1 μmol) of ligand **14c** in a 10 mL volumetric flask and adjusting the volume to 10 mL. DTBC stock solution of concentration 0.13 M was prepared by dissolving 222 mg (0.998 mmol) of **18** in 8.0 mL solvent. For the case of methanol, 120-400 μL aliquots of this stock solution were pipetted into cuvettes, 780-500 μL of methanol were added and the mixture thermostated at 30 ^{o}C. 100 μL aliquots of thermostated catalyst stock solution were pipetted into these substrate solutions resulting in substrate solutions concentrations of 15-50 mM and a total catalyst concentration of 0.2 mM. Formation of DTBQ was followed by UV-Vis spectroscopy by observing formation of an absorbance band at 420 nm.[119] Molar absorptivity at 420 nm was determined to be 1670 $M^{-1}cm^{-1}$ by using a commercial sample of **19**.

6.7 Synthesis procedures

2-Hydroxy-4-(4-vinylbenzyloxy)benzaldehyde, 2b. This compound was prepared using a procedure developed by Michael Dittel, *Ph.D. Thesis*, University of Ulm, 2003. A mixture of 2,4-dihydroxybenzaldehyde (2.5 g, 18 mmol), *p*-vinylbenzyl chloride (3.36 g, 22.1 mmol), potassium carbonate (2.5 g, 18 mmol) and potassium iodide (920 mg, 5.50 mmol) in 150 mL acetonitrile was allowed to stir for 24 h at 60 ^{o}C. The mixture was cooled to room temperature and filtered. The filtrate was evaporated and the residue dissolved in 10 mL water containing 1 mL of 6 M hydrochloric acid and extracted using 50 mL ethyl acetate followed by a second extraction with 20 mL ethyl acetate. The combined organic layer was washed consecutively with 15 mL 5% potassium carbonate solution, 15 mL water, and 15 mL 5% citric acid. The organic layer was dried over anhydrous sodium sulfate, filtered and evaporated to form a colorless solid that was recrystallized from ethyl acetate to form colorless crystals in 69% yield (3.2 g, 12 mmol). ^{1}H NMR (400.2 MHz, $CDCl_3$) δ_H 11.46 (s, 1H, OH), 9.69 (s, 1H, CHO), 7.42 (dd, 3H, *J* = 8.3, 4.3, ArH), 7.35 (d, 2H, *J* = 8.1), 6.71 (1H, dd, *J* = 10.86, 17.68, -C*H*=CH_2), 6.59 (1H, dd, *J* = 8.7, 2.4), 6.49 (1H, dd, *J* = 2.27), 5.76 (1H, d, *J* = 17.43 –CH=C$H_a$$H_b$), 5.28 (1H, d, *J* = 10.86, -CH=$CH_a$$H_b$), 5.07 (2H, s, Ar$CH_2$O-); ^{13}C NMR (100.6 MHz, $CDCl_3$) δ_C 194.4, 165.8, 164.4, 137.7, 136.2, 135.3, 135.1, 127.7, 126.5, 115.3, 114.4, 108.9, 101.6, 70.1.

3-(4-Formyl-3-hydroxyphenoxymethyl)benzonitrile, 2c. A mixture of 2,4-dihydroxybenzaldehyde (1.1 g, 8.0 mmol), 3-(bromomethyl)benzonitrile (1.0 g, 22 mmol), potassium carbonate (1.1 g, 8.0 mmol) and potassium iodide (127 mg, 0.765

mmol) in 150 mL acetonitrile was allowed to stir for 24 h at 60 ^{o}C under argon. The mixture was then cooled to room temperature and filtered. The filtrate was evaporated and purified by column chromatography on silica gel using cyclohexane/ethyl acetate 70:30. Product was separated at R_f value of 0.75. A colorless solid was obtained. Yield 85% (1.1 g, 4.34 mmmol). ^{1}H NMR (400 MHz, $CDCl_3$) δ_H 11.45 (s, 1H, OH), 9.72 (s, 1H, CHO), 7.52-7.36 (m, 3H, Ar*H*), 7.32-7.25 (m, 2H), 6.62 (1H, dd, *J* = 8.6, 2.3, Ar*H*), 6.51 (1H, d, *J* = 2.5), 5.19 (2H, s, CH_2). ^{13}C NMR (100.6 MHz, $CDCl_3$) δ_C 194.4, 165.6, 164.4, 135.4, 133.4 132.8, 129.6, 129.4, 128.8, 127.0, 115.5, 108.7, 101.8, 67.5.

4-(2-Chlorobenzyloxy)-2-hydroxybenzaldehyde, 2d. A mixture of 2,4-dihydroxybenzaldehyde (1.0 g, 7.24 mmol), 1-(bromomethyl)-2-chlorobenzene (1.0 g, 4.9 mmol), potassium carbonate (1.0 g, 7.24 mmol) and potassium iodide (122 mg, 0.735 mmol) in 150 mL acetonitrile was allowed to stir for 24 h at 60 ^{o}C under argon. The mixture was cooled to room temperature and filtered. The filtrate was evaporated and purified by column chromatography on silica gel using dichloromethane/methanol 98:2. Product was separated at R_f value of 0.81. A colorless solid was obtained. Yield 51% (650 mg, 2.49 mmol). ^{1}H NMR (400.2 MHz, $CDCl_3$) δ_H 11.45 (s, 1H, OH), 9.71 (s, 1H, CHO), 7.76 (1H, d, *J* = 0.5, Ar*H*), 7.62 (2H, t, *J* = 6.6), 7.54-7.40 (2H, m), 6.59 (1H, dd, *J* = 8.6, 2.3), 6.45 (1H, d, *J* = 2.3, Ar*H*); 5.11 (2H, s, CH_2); ^{13}C NMR (100.6 MHz, $CDCl_3$) δ_C 194.5, 165.0, 164.3, 137.3, 135.4, 131.9, 131.4, 130.6, 129.5, 118.4, 115.5, 112.9, 108.6, 101.5, 68.8.

4-(4-fluorobenzyloxy)-2-hydroxy-benzaldehyde, 2e. A mixture of 2,4-dihydroxybenzaldehyde (2.21 g, 15.9 mmol), 4-fluorobenzaldehyde (2.03 g, 10.6 mmol), potassium carbonate (2.2 g, 15.9 mmol) and potassium iodide (263 mg, 1.58 mmol) in

150 mL acetonitrile was allowed to stir for 24 h at 60 ^{o}C under argon. The mixture was cooled to room temperature and filtered. The filtrate was evaporated and purified by column chromatography on silica gel using cyclohexane/ ethyl acetate 7:3. A colorless solid was obtained. Yield 55% (1.36 g, 5.83 mmol). Found C, 68.31, H, 4.48, $C_{14}H_{11}O_3F$ requires C, 68.29, H, 4.50%; ^{1}H NMR (400.2 MHz, $CDCl_3$) δ_H 11.48 (s, 1H, OH), 9.37 (s, 1H, CHO), 7.54 (d, 1H, *J* = 8.9, Ar*H*), 7.40 (dd, 2H, *J* = 8.5, 5.4, Ar*H*), 7.10 (t, 2H, *J* = 8.6, Ar*H*), 6.61 (dd, 1H, *J* = 8.9, 2.3, Ar*H*), 6.51 (d, 1H, *J* = 2.3, Ar*H*), 5.08 (s, 2H, -C*H*$_2$); ^{13}C NMR (100.6 MHz, $CDCl_3$) δ_C 69.7, 101.6, 108.9, 115.4, 115.6, 115.8, 129.4, 129.5, 131.4, 131.5, 135.4, 161.5, 164.0, 164.5, 165.7, 194.5; IR (thin film) ν_{max}/cm^{-1} 3448 br(OH), 3074 w, 2951, 1637 s (C=O).

2-Methoxyethyl 4-methylbenzenesulfonate, 4a. A solution of tosyl chloride (31.0 g, 158 mmol) in dichloromethane (20 mL) was added dropwise over 2 h to an ice-cooled solution of 2-methoxyethanol (12.0 g, 158 mmol) and pyridine (12.5 g, 158 mmol) in dichloromethane (100 mL) and the resultant mixture allowed to stir overnight while warming to room temperature. The reaction mixture was washed with distilled water (20 mL), and the aqueous layer extracted using dichloromethane (3 x 50 mL). The combined organic fractions were dried over anhydrous sodium sulfate and concentrated under reduced pressure to give a crude product that was purified by distillation at reduced pressure. Yield 26% (9.6 g, 41 mmol). ^{1}H NMR (400 MHz, $CDCl_3$) δ_H 7.76 (2H, d, *J* = 8.3, ArH), 7.34 (2H, d, *J* = 8.1, ArH), 4.14 (2H, t, *J* = 4.7, -OC*H*$_2$CH$_2$OCH$_3$), 3.56 (2H, t, *J* = 2.3, -OCH$_2$C*H*$_2$OCH$_3$), 3.28 (3H, s, -OCH$_3$), 2.43 (3H, s, ArCH$_3$); ^{13}C NMR (100 MHz, $CDCl_3$) δ_C 144.9, 132.9, 129.8, 127.9, 69.8, 69.2, 58.9, 21.6. The product is

identical in properties to the one described by Heathcote, R.; Howell, J. A. S.; Jennings, N.; Cartlidge, D.; Cobden, L.; Coles, S.; Hursthouse, M. *Dalton Trans.* **2007**, 1309-1315.

Toluene-4-sulfonic acid 2-(2-methoxyethoxy)ethyl ester, 4b. The synthesis was conducted in analogy to a procedure described by Kazemi, F.; Massah, A. R.; Javaherian, M. *Tetrahedron* **2007**, *63*, 5083-5087. A mixture of potassium carbonate (10.01 g, 72 mmol), 2-(2-methoxyethoxy)ethanol (2.4 g, 20 mmol) and tosyl chloride (5.7 g, 30.0 mmol) was put into a mortar and ground for 5 min. Potassium hydroxide (5.6 g, 85 mmol) was added and ground for another 2 min. A few drops of *t*-BuOH were added to the mixture and ground for another 1 min. (to aid the removal of TsCl). The reaction product was extracted twice by addition of diethyl ether (50 mL), stirring of the resulting slurry, and filtering. Evaporation of combined diethyl ether extracts afforded a colorless oil that was pure by NMR analysis. Yield 62% (3.42 g, 1.52 mmol) ^{1}H NMR (400 MHz, $CDCl_3$) δ_H 7.79 (2H, d, J = 8.3, Ar-H), 7.34 (2H, d, J = 8.1, ArH), 4.16 (2H, t, J = 4.9, Ar-$SO_3C\mathit{H}_2CH_2$), 3.69 (2H, t, J = 4.9, Ar-$SO_3CH_2C\mathit{H}_2$), 3.59-3.55 (2H, m, OCH_2), 3.50 - 3.45 (2H, m, OCH_2), 3.34 (3H, s, OCH_3), 2.44 (3H, s, aryl-CH_3); ^{13}C NMR (100 MHz, $CDCl_3$) δ_C 144.9, 133.1, 129.9, 128.2, 71.9, 70.8, 69.4, 68.9, 59.2, 21.8. The product is identical in properties to the one described by Kohmoto, S.; Mori, E.; Kishikawa, K. *J. Am. Chem. Soc.* **2007**, *129*, 13364-13365.

Toluene-4-sulfonic acid 2-[2-(2-methoxyethoxy)ethoxy]ethyl ester, 4c. A solution of tosyl chloride (3.62 g, 22.1 mmol) in 10 mL dichloromethane was added dropwise over 2 h to an ice-cooled solution of 2-[2-(2-methoxyethoxy)ethoxy]ethanol (3.7 g, 22 mmol) and triethylamine (6.2 mL, 22 mmol) in 30 mL dichloromethane and the mixture allowed to stir overnight while warming to room temperature. The reaction

mixture was washed with distilled water (20 mL), and the aqueous layer extracted using dichloromethane (3 × 50 mL). The combined organic fractions were dried over anhydrous sodium sulfate, filtered, and concentrated under reduced pressure. Column chromatography using cyclohexane/ethyl acetate (1:1 v/v) gave a pale yellow oil in 71% yield, (5.01 g, 15.7 mmol). ^{1}H NMR (400 MHz, $CDCl_3$) δ_H 7.77 (d, 2H, *J* = 7.6, ArH), 7.32 (d, 2H, *J* = 8.1, ArH), 4.13 (t, 2H, *J* = 4.7, OCH_2), 3.66 (t, 2H, J = 4.17, OCH_2), 3.53–3.61 (m, 6H, OCH_2), 3.48–3.52 (m, 2H, OCH_2), 3.34 (s, 3H, OCH_3), 2.42 (s, 3H, $ArCH_3$); ^{13}C NMR (100 MHz, $CDCl_3$) δ_C 144.9, 133.0, 129.9, 128.0, 72.0, 70.8, 70.6, 70.5, 69.4, 68.7, 59.1, 21.7.

Cyclohexylmethyl tosylate, 4d. Tosyl chloride (7.4 g, 45 mmol) was added in small portions to an ice cold solution of cyclohexyl methanol (5.0 g, 44 mmol) and pyridine (3.8 mL, 47 mmol) in 25 mL dichloromethane. The resulting mixture was stirred overnight while warming to ambient temperature. The organic layer was washed successively with 1M HCl, 5% $NaHCO_3$, and water, dried (anhyd. $NaSO_4$,) and evaporated. The tosylate was dried on the vacuum line at 70 ^{o}C for 12 h to get 8.31 g (31.0 mmol) of colorless oil in 70% yield. ^{1}H NMR (250 MHz, $CDCl_3$): δ_H 7.75 (2H, d, *J* = 8.4, ArH), 7.31 (2H, d, *J* = 8.7, ArH), 3.77 (2H, d, *J* = 6.3, -OCH_2 - H), 2.42 (3H, s, CH_3), 1.65 (6H, m), 1.31 – 1.00 (3H, m), 0.98 – 0.72 (2H, m); ^{13}C NMR (62 MHz, $CDCl_3$): δ_C 144.5, 133.1, 129.7, 127.8, 75.3, 37.1, 29.0, 26.0, 25.3, 21.6. This compound is identical in properties to the one described by Oh, H. K.; Song, S. J.; Jo, D.-S.; Lee, I. *J. Phys. Org. Chem.* **1997**, *10*, 91-96.

Allyl 4-methylbenzenesulfonate 4e. A solution of tosyl chloride (3.68 g, 22.9 mmol) in 50 mL CH_2Cl_2 was added dropwise to an ice cold solution of allyl alcohol

(1.3 g, 23 mmol) and pyridine (1.8 g, 23. mmol) in 25 mL dichloromethane. The resulting mixture was stirred overnight while warming to ambient temperature. Water (20 mL) was added and the layers separated. The organic layer was dried using anhydrous sodium sulfate, filtered, and evaporated to obtain a crude product that was purified using column chromatography over silica gel using 9:1 cyclohexane/ethyl acetate to obtain colorless oil in 52% yield (2.52g, 11.8 mmol). ^{1}H NMR (400 MHz, $CDCl_3$) δ_H 7.77 (2H, d, J = 8.3, ArH), 7.32 (2H, dd, J = 8.2, 0.3, ArH), 5.79 (1H, m), 5.22 (1H, ddd, J = 10.2, 1.8, 0.8, CH=CH_2), 4.50 (2H, dt, J = 6.1, 1.3, -OCH_2), 2.42 (3H, s, -ArCH_3); ^{13}C NMR (100 MHz, $CDCl_3$) δ_C 144.8, 133.1, 130.2, 129.8, 127.8, 120.2, 70.3, 21.6.

Decyl 4-methylbenzenesulfonate, 4f. A solution of tosyl chloride (3.6 g, 19 mmol) in dichloromethane (50 mL) was added dropwise over 2 h to an ice-cooled solution of 1-decanol (2.0 g, 13 mmol) and pyridine (2.1 mL, 25 mmol) in dichloromethane (50 mL) and the resulting mixture stirred overnight while warming to room temperature. The reaction mixture was successively washed with l0 mL of 1 M HCl, 5% $NaHCO_3$ and H_2O. The organic layer was dried over anhydrous sodium sulfate, filtered, and evaporated to obtain crude product that was purified by column chromatography using 98:2 (v/v) petroleum ether/ether over silica gel to obtain colorless oil. Yield, 80% (3.18 g, 10.2 mmol). ^{1}H NMR (400 MHz, $CDCl_3$) δ_H 7.75 (2H, d, J = 8.3, ArH), 7.31 (2H, d, J = 7.9, ArH), 3.98 (2H, t, J = 6.5, CH_2O), 2.42 (3H, s, aryl-CH_3), 1.59 (2H, m, C$H_2$$CH_2$O), 1.18 (14H, br s, -$(CH_2)_7$-), 0.84 (3H, t, J = 6.9, -CH_3); ^{13}C NMR (100 MHz, $CDCl_3$) δ_C 144.6, 133.1, 129.7, 127.8, 70.7, 31.8, 29.4, 29.3, 29.2, 28.8, 28.7, 25.2, 22.6, 21.5, 14.0. This compound is identical in properties to the one described by

Kabalka, G. W.; Varma, M.; Varma, R. S.; Srivastava, P. C.; Knapp, F. F., Jr. *J. Org. Chem.* **1986**, *51*, 2386-2388, and was therefore not characterized further.

2-(2-Chloroethoxy)ethyl 4-methylbenzenesulfonate, 4g. The synthesis was conducted in analogy to a procedure described by Kazemi, F.; Massah, A. R.; Javaherian, M. *Tetrahedron* **2007**, *63*, 5083-5087. A mixture of potassium carbonate (5.0 g, 36 mmol), 2-(2-chloroethoxy)ethanol (1.25 g, 10.0 mmol) and tosyl chloride (2.86 g, 15.0 mmol) was put into a mortar and ground for 5 min. Potassium hydroxide (2.81 g, 42.6 mmol) was then added and ground for another 2 min. A few drops of *t*-BuOH were added to the mixture and ground for another 1 min. (to aid the removal of TsCl). The reaction product was extracted by addition of diethyl ether (50 mL), stirring of the resulting slurry, filtration, and evaporation of diethyl ether evaporated to obtain colorless oil that was pure by NMR analysis. Yield 75% (2.09 g, 7.51 mmol); ^{1}H NMR (400 MHz, $CDCl_3$) δ_H 7.78 (2H, d, J = 8.3, Ar*H*), 7.32 (2H, d, J = 8.3, ArH), 4.15 (2H, t, J = 4.8, Ar-$SO_3CH_2CH_2$), 3.71 – 3.63 (4H, m, $OCH_2CH_2OCH_2CH_2Cl$), 3.52 (2H, t, J = 5.4, OCH_2CH_2Cl), 2.42 (3H, s, CH_3); ^{13}C NMR (100 MHz, $CDCl_3$) δ_C 144.9, 132.9, 129.8, 127.9, 71.4, 69.1, 68.7, 42.5, 21.6. The product is identical in properties to that described by Benco, John S.; Nienaber, Hubert A.; Dennen, Katherine; McGimpsey, W. Grant. *J. Photochem. Photobiol., A* **2002**, *152* (1-3), 33-40, and was therefore not further characterized.

2-Hydroxy-4-(2-methoxyethoxy)benzaldehyde, 5a. A mixture of 3.0 g (22 mmol) 2,4-dihydroxybenzaldehyde, 4.0 g (18 mmol) toluene-4-sulfonic acid 2-methoxyethyl ester, 3.0 g (22 mmol), potassium carbonate in 150 mL acetonitrile was stirred for 48 h at 60 ^{o}C. The mixture was cooled, filtered, and the solvent evaporated to

obtain a dark brown oil. The oil was purified using silica gel column chromatography 98:2 (v/v) dichloromethane/methanol and the product collected at R_f value of 0.87. Product was a crystalline colorless solid (750 mg, 21%); m.p 63-64 ^oC; Found: C, 61.27%; H, 6.16%. $C_{10}H_{12}O_4$ requires C, 61.22%, H, 6.16%; ^1H NMR (400 MHz, $CDCl_3$) δ_H 11.50 (1H, s, OH), 9.74 (1H, s, CHO), 7.43 (1H, d, *J* = 8.6, Ar*H*), 6.58 (1H, dd, *J* = 8.7, 2.4, Ar*H*), 6.44 (1H, d, *J* = 2.3, Ar*H*) 4.19 (2H, t, *J* = 4.7, ArOCH_2-), 3.79 (2H, t, *J* = 4.7, CH_2), 3.48 (3H, s, -CH_3). ^{13}C NMR (100 MHz, $CDCl_3$) δ_C 194.5, 166.0, 164.4, 135.3, 115.3, 108.9, 101.2, 71.9, 70.6, 67.8, 59.3; IR: ν_{max} (thin film)/cm^{-1} 2929, 2890w (CH), 1627s (C=O), 1225m, 1173s (C-O-C); HRMS (+TOF MS) m/z found: 197.0811; calcd. for $C_{10}H_{12}O_4+H^+$ ($M+H^+$) 197.0814.

2-Hydroxy-4-(2-(2-methoxyethoxy)ethoxy)benzaldehyde, 5b. A mixture of 1.41 g (10.2 mmol) 2,4-dihydroxybenzaldehyde, 1.8 g (7.11 mmol) 2-(2-methoxyethoxy)ethyl-4-methylbenzenesulfonate, and 1.41 g (10.2 mmol) potassium carbonate was stirred in 150 mL acetonitrile at 70 ºC for 48 h. The reaction mixture was cooled to room temperature, filtered over a short silica gel column and eluted using dichloromethane. A brown oil (0.60 g) was obtained that was purified by column chromatography over SiO_2 with 1:1 cyclohexane/ethyl acetate to yield 0.60 g (2.5 mmol, 37 %) colorless oil; IR (thin film) ν_{max}/cm^{-1} 3247br (OH), 3063w (=CH), 2868s (C–H asy-str), 1646s (C=O), 1109s (C–O); ^1H NMR (400 MHz, $CDCl_3$) δ_H 11.46 (1H, s, OH), 9.71 (1H, s, CHO), 7.42 (1H, *J* = 8.6, Ar*H*), 6.56 (1H, dd, *J* = 8.7, 2.4, Ar*H*), 6.43 (1H, d, *J* = 2.3, Ar*H*) 4.19 (2H, t, *J* = 4.9, ArOCH_2-), 3.87 (2H, t, *J* = 4.9, CH_2), 3.72 (2H, m), 3.58 (2H, m) 3.39 (3H, s, -CH_3). ^{13}C NMR (100 MHz, $CDCl_3$) δ_C 194.6, 166.2, 164.6,

135.4, 115.4, 108.9, 101.5, 72.1, 71.0, 69.5, 68.0, 59.3 HRMS calcd for $(C_{12}H_{16}O_5 + Li)^+$ 247.1158; found 247.1160.

2-Hydroxy-4-(2-(2-(2-methoxyethoxy)ethoxy)ethoxy)benzaldehyde, 5c. A mixture of 2.1 g (15 mmol) 2,4-dihydroxybenzaldehyde, 3.2 g (10 mmol) toluene-4-sulfonic acid 2-[2-(2-methoxyethoxy)ethoxy]ethyl ester and 2.0 g (15 mmol) potassium carbonate was stirred in 150 mL acetonitrile at 60 ^oC for 48 h. The reaction mixture was cooled to room temperature, filtered, and the solvent evaporated to obtain a brownish solid. The crude product was purified by column chromatography over SiO_2 with 1:1 ethyl acetate/ cyclohexane. Yield: 900 mg (3.17 mmol 32%) yellow oil; Found: C, 58.85%; H, 7.24%. $C_{14}H_{20}O_6$ requires C, 59.14%, H, 7.09%; ^1H NMR (400 MHz, $CDCl_3$) δ_H 11.46 (1H, s, OH), 9.71 (1H, s, CHO), 7.43 (1H, d, Ar*H*), 6.56 (1H, dd, *J* = 8.7, 2.2 ArH), 6.43 (1H, d, Ar*H*) 4.17 (2H, t, *J* = 4.9, ArOCH_2-), 3.87 (2H, t, *J* = 4.9), 3.73 (2H, m), 3.67 (4H, m), 3.55 (3H, s, -CH_3); ^{13}C NMR (400 MHz, $CDCl_3$) δ_C 194.4, 166.0, 164.4, 135.3, 115.2, 108.8, 101.3, 71.9, 70.9, 70.6, 70.5, 69.3, 59.0.

2,4-Bis(cyclohexylmethoxy)benzaldehyde, 5d′. A mixture of 741 mg (5.3 mmol) 2,4-dihydroxybenzaldehyde, 1.0 g (3.75 mmol) cyclohexyl tosylate, and 889 mg (6.5 mmol) potassium carbonate was stirred in 60 mL acetonitrile at 70 ^oC for 48 h. The reaction mixture was cooled to room temperature, filtered over a small silica gel column and eluted using dichloromethane then dichloromethane/methanol 90:10 to obtain 790 mg of crude yellow oil. 43.2 mg of the crude oil was purified by semi-preparative HPLC to obtain a colorless oil. Yield 16% (9.8 mg, 0.03 mmol). ^1H NMR (400 MHz, $CDCl_3$) δ_H 10.32 (s, 1H, CHO), 7.76 (1H, d, *J* = 8.6, ArH), 6.48 (1H, dd, *J* = 8.6, 1.5, Ar*H*), 6.38 (1H, d, *J* = 8.6, 2.2, Ar*H*), 3.79 (4H, q, *J* = 5.9, ArOCH_2-), 1.92 – 1.62 (14H,

m, CH_2, CH), 1.41 – 1.10 (m, 8H, C*H*$_2$); ^{13}C NMR (100.6 MHz, $CDCl_3$) δ_C 188.4, 165.9, 163.5, 130.1, 118.9, 106.2, 98.9, 73.8, 37.6, 29.8, 29.7, 26.4, 25.7, 25.7; HRMS calcd for $(C_{21}H_{30}O_3 + H)^+$ 331.2273; found 331.2268.

4-Cyclohexylmethoxysalicylaldehyde, 5d. colorless solid; m.p 55-57 ^oC; Found C 71.77, H 7.60%; $C_{14}H_{18}O_3$ requires C 71.77, H 7.74%; ^{1}H NMR (400 MHz, $CDCl_3$) δ_H 11.46 (1H, s, ArO*H*), 9.67 (1H, s, ArC*H*O), 7.39 (1H, d, *J* = 8.7, Ar*H*), 6.50 (1H, dd, *J* = 8.7, 2.1, Ar*H*), 6.38 (1H, d, *J* = 2.4, Ar*H*), 3.77 (2H, d, *J* = 6.0, -OCH_2-), 1.72 (m, 6H, C_6H_{11}), 1.14 (5H, m, -C_6H_{11}); ^{13}C NMR (100.6 MHz, $CDCl_3$) δ_C 194.3, 166.6, 164.5, 135.2, 115.0, 108.8, 101.1, 73.9, 37.4, 29.7, 25.7; IR ν_{max} (KBr)/cm^{-1} 3136w (arom. CH), 2922, 2852s, 1636 (C=O), 122s (C-O-C); HRMS (-TOF MS) *m/z* found: 233.1186; calcd for $C_{14}H_{17}O_3$ $(M-H^+)^-$ 233.1178.

4-Allyloxy-2-hydroxybenzaldehyde, 5e. A mixture of 2,4-dihydroxybenzaldehyde (1.5 g, 11 mmol), allyl tosylate (1.5 g, 7.1 mmol), and potassium carbonate (1.2 g, 11 mmol) was stirred in 150 mL acetonitrile at 60 ^oC for 12 h. The reaction mixture was cooled to room temperature, filtered, and the solvent evaporated to obtain a brown solid. The crude product was dissolved in 10 mL distilled water and extracted with chloroform (2 × 50 mL). The combined organic layers were dried over anhydrous sodium sulfate and evaporated to obtain 1.10 g of a crude product that was purified by column chromatography over SiO_2 with 9:1 cyclohexane/ ethyl acetate to obtain a colorless oil in 48% yield (0.61 g, 3.4 mmol). Found: C 67.13, H 5.65%; $C_{10}H_{10}O_3$ requires C 67.41, H 5.66%; ^{1}H NMR (400.2 MHz, $CDCl_3$) δ_H 11.44 (s, 1H, Ar-O*H*), 9.68 (1H, s, Ar-C*H*O), 7.40 (1H, d, *J* = 8.6, Ar-*H*), 6.53 (1H, dd, *J* = 8.6, 2.27, Ar-*H*), 6.41 (1H, d, *J* = 2.3, Ar-*H*), 6.00 (m, 1H, -C*H*=CH_2), 5.40 (1H, ddd, *J* =

17.2, 2.9, 1.6, -CH=CH_2), 5.31 (1H, ddd, J = 10.5, 2.7, 1.4, -CH=CH_2), 4.56 (2H, dt, J = 5.3, 1.5, -CH_2-); ^{13}C NMR (100.6 MHz, $CDCl_3$) δ_C 194.6, 166.0, 164.6, 135.5, 132.2, 118.7, 115.4, 109.0, 101.6, 69.3; ν_{max} (thin film)/cm^{-1}: 3259w (OH), 3084w (arom. C-H), 2840, 2748w (CHO), 1628s (C=O), 1577m (C=C), 1222s (C-O-C)

4-(Decyloxy)-2-hydroxybenzaldehyde, 5f. A mixture of 331 mg (2.4 mmol) 2, 4-dihydroxybenzaldehyde, 625 mg (2.0 mmol) decyl tosylate, and 397 mg (2.88 mmol) potassium carbonate was stirred in 50 mL acetonitrile at 70 ºC for 48 h. The reaction mixture was then cooled to room temperature, filtered over celite and evaporated to obtain crude dark oil. This was filtered again over a small silica gel column and eluted using dichloromethane then dichloromethane/methanol 90:10 to obtain 430 mg of crude yellow oil. 86 mg of the crude oil was purified by semi-preparative HPLC to obtain product in 37% yield (41.3 mg, 0.15 mmol); ^{1}H NMR (400 MHz, $CDCl_3$) δ_H 11.48 (s, 1H, OH), 9.67 (s, 1H, CHO), 7.37 (1H, d, J = 8.6, ArH), 6.50 (1H, dd, J = 8.6, 2.3, ArH), 6.38 (1H, d, 2.3, ArH) 3.97 (2H, t, J = 6.6, ArOCH_2-), 1.77 (2H, m, ArOCH_2CH_2-), 1.15 – 1.50 (14H, m, CH_2), 0.86 (3H, t, J = 6.8, CH_3); ^{13}C NMR (100 MHz, $CDCl_3$) δ_C 194.5, 166.7, 164.7, 135.4, 115.2, 108.9, 101.2, 68.8, 32.1, 29.7, 29.5, 29.1, 26.1, 22.9, 14.3. This compound is identical in properties to the one described by Barbera, J.; Gimenez, R.; Gimeno, N.; Marcos, M.; Del, M.; Pina, C.; Serrano, J. L. *Liq. Cryst.* **2003**, *30*, 651-661.

4-(2-(2-Chloroethoxy)ethoxy)-2-hydroxybenzaldehyde, 5g. A mixture of 0.6 g (4.4 mmol) 2,4-dihydroxybenzaldehyde, 1 g (3.6 mmol) 2-(2-chloroethoxy)ethyl 4-methylbenzenesulfonate, and 0.72 g (5.2 mmol) potassium carbonate was stirred in 100 mL acetonitrile at 70 ºC for 48 h. The reaction mixture was allowed to cool to room

temperature, filtered over celite and evaporated. A dark brown oil was obtained that was purified by column chromatography over SiO_2 with 7:3 cyclohexane/ethyl acetate to yield 0.44 g (1.8 mmol, 50%) colorless oil; Found: C, 54.19; H, 5.41. $C_{11}H_{13}ClO_4$ requires: C, 54.00; H, 5.36; IR (thin film) ν_{max}/cm^{-1} 3088br (OH), 2942s (C–H), 1651s (C=O), 1121s (C–O); ^{1}H NMR (400 MHz, $CDCl_3$) δ_H 11.44 (1H, s, OH), 9.69 (1H, s, CHO), 7.41 (1H, d, *J* = 8.6, Ar*H*), 6.54 (1H, dd, *J* = 8.7, 2.4, Ar*H*), 6.40 (1H, d, *J* = 2.4, Ar*H*) 4.16 (2H, t, *J* = 4.81, $ArOCH_2$-), 3.87 (2H, t, *J* = 4.6, CH_2Cl), 3.80 (2H, m), 3.63 (2H, m). ^{13}C NMR (100 MHz, $CDCl_3$) δ_C 194.6, 166.0, 164.6, 135.5, 115.5, 108.9, 101.5, 71.8, 69.5, 68.5, 68.0, 42.9; HRMS calcd for $(C_{11}H_{13}ClO_4 + Li)^+$ 251.0662; found 251.0665.

2,3-Bis(allyloxy)benzaldehyde, 7. A mixture of 1.50 g (10.6 mmol) 2, 3-dihydroxybenzaldehyde, 1.5 g (7.1 mmol) allyl tosylate, and 1.21 g (10.8 mmol) potassium carbonate was stirred in 150 mL acetonitrile at 60 ^oC for 12 h. The reaction mixture was then cooled to room temperature, filtered and the solvent evaporated to obtain a crude brown solid. The crude product was purified by column chromatography over SiO_2 with 9:1 cyclohexane/ ethyl acetate to yield 31% (480 mg, 2.21 mmol) colorless oil. ^{1}H NMR (400 MHz, $CDCl_3$) δ_H 10.42 (s, 1H, CHO), 7.39 (dd, 7,58, 2.02, 1H, ArH), 7.09 (m, 2H, ArH), 6.04 (m, 2H, CH_2=C*H*-), 5.49 – 5.16 (m, 4H, CH_2), 4.67 (dt, *J* = 6.1, 1.3, 2H, $ArOCH_2$), 4.59 (dt, *J* = 5.3, 1.5, 2H, $ArOCH_2$); ^{13}C NMR (100.6 MHz, $CDCl_3$) δ_C 190.4, 151.9, 151.5, 133.1, 133.6, 130.2, 124.0, 119.7, 119.4, 118.9, 117.9, 75.1, 69.8

2,3-Bis(2-(2-chloroethoxy)ethoxy)benzaldehyde, 8. A mixture of 600 mg (4.4 mmol) 2, 3-dihydroxybenzaldehyde, 1.0 g (3.6 mmol) 2-(2-chloroethoxy)ethyl 4-

methylbenzenesulfonate, and 720 mg (5.2 mmol) potassium carbonate was stirred in 50 mL acetonitrile at 70 ^{o}C for 48 h. The reaction mixture was cooled to room temperature, filtered, and evaporated to obtain crude yellow oil. This was filtered again over a small silica gel column and eluted using cyclohexane/ethyl acetate 1:1 to obtain 1.18 g of yellow oil. The crude product was purified using silica gel column chromatography and eluted using CH_2Cl_2/MeOH 99:1 (v/v). The spot at R_f value 0.72 was collected and evaporated to obtain an oil, 250 mg (0.71 mmol) in 20% yield. ^{1}H NMR (400 MHz, $CDCl_3$), δ_H 10.48 (s, 1H, CHO), 7.41 (dd, 1H, *J* = 7.6, 1.8, Ar*H*), 7.16-7.05 (m, 2H, Ar*H*), 4.38 (2H, t, *J* = 4.4, ArOC*H*$_2$-), 4.18 (2H, t, *J* = 4.6, ArOC*H*$_2$-), 3.89 (2H, t, *J* = 4.6, C*H*$_2$Cl), 3.83 – 3.76 (4H, m, -C*H*$_2$), 3.73 (t, *J* = 5.9, 2H, C*H*$_2$), 3.66 – 3.57 (m, 4H, -CH_2); ^{13}C NMR (100.6 MHz, $CDCl_3$) δ_C 190.8, 151.9, 151.6, 130.2, 124.0, 119.7, 119.6, 73.0, 71.4, 71.2, 70.3, 69.6, 68.5, 42.9, 42.7; HRMS calcd for $(C_{15}H_{20}Cl_2O_5 + Li)^+$ 357.0848; found 357.0852.

1,3-Bis[2-hydroxy-4-(2-methoxyethoxy)benzylideneamino]propan-2-ol, 14a. To a solution of 2-hydroxy-4-(2-methoxyethoxy)benzaldehyde (910 mg, 4.5 mmol) in 150 mL of ethanol/methanol (1:1 v/v) was added a solution of 1,3-diamino-2-propanol (210 mg, 2.3 mmol) in 10 mL of ethanol. This solution was allowed to stir for 48 h at ambient temperature. The resulting solution was evaporated to give a yellow crude product that was recrystallized using MeOH/EtOH (1:1 v/v) mixture to give a yellow powder. Yield 79% (810 mg, 1.8 mmol): Melting point, 120-121 ºC; ^{1}H NMR ($CDCl_3$, 400.2 MHz) δ_H 8.16 (2H, s, –CH=N–), 7.06 (2H, d, *J* = 8.3, ArH), 6.37 (4H, m, ArH), 4.15 (1H, m,–CHOH–), 4.06 (4H, t, *J* = 4.7, ArOCH$_2$–), 3.70 (4H, m,–CH$_2$–), 3.59 (2H, m,–CH$_2$–); ^{13}C NMR ($CDCl_3$, 100.6 MHz) δ_C 166.1, 165.1, 163.2, 132.9, 112.2,

107.0, 101.8, 70.7, 70.2, 67.2, 61.3, 59.2; IR ν_{max} (KBr)/cm^{-1} 3356 (br, OH), 3075w (=CH arom) 2880s (C–H), 1636v (C=N), 1118s (C–O). Positive ion ESI MS, calcd for $(C_{23}H_{30}N_2O_7 + H)^+$ 446.21, found 446.16.

1,3-Bis[2-hydroxy-4-[2-(2-methoxyethoxy)ethoxy]benzylideneamino]propan-2-ol, 14b. To a solution of 2-hydroxy-4-(2- (2-methoxyethoxy)ethoxy)benzaldehyde, 1.28 g (5.33 mmol), in 100 mL of ethanol\ methanol (1:1, v/v) was added a solution of 1,3-diamino-2-hydroxypropane (240 mg, 2.67 mmol) in 20 mL of 95% ethanol. This was allowed to stir for 24 h at ambient temperature. The solution was evaporated to give a crude product, which was dissolved in 20 mL of water and extracted using chloroform (3 x 50 mL). The combined organic layer was dried over anhydrous sodium sulfate, filtered, and evaporated to form a yellow solid that was purified by recrystallization using diethylether. Yield 69% (0.98 g, 1.8 mmol) ^{1}H NMR (400 MHz, $CDCl_3$) δ_H 8.16 (1H, s, -CH=N-), 7.05 (2H, d, J = 9.1, ArH), 6.36 (m, 4H, ArH), 4.14 (1H, m, -C*H*OH), 4.10 (4H, t, J = 4.9, ArOCH_2-), 3.82 (4H, t, J = 4.7, ArOCH_2OCH_2-), 3.73 (2H, m, -CH_2-), 3.68 (4H, t, J = 4.7, -CH_2), 3.59 (m, 2H), 3.54 (4H, t, J = 4.7, -CH_2-,), 3.36 (6H, s, -OCH_3); ^{13}C NMR (100 MHz, $CDCl_3$) δ_C 166.6, 165.7, 163.1, 132.9, 112.2, 107.0, 101.9, 71.9, 70.7, 70.3, 69.5, 67.4, 61.5, 59.0.

1,3-Bis[2-hydroxy-4-[2-(2-methoxyethoxy)ethoxy]ethoxybenzylideneamino]propan-2-ol, 14c. To a solution of 2-hydroxy-4-(2-(2-(2-methoxyethoxy)ethoxy)ethoxy)benzaldehyde, 1 g (3.5 mmol), in 150 mL of ethanol\methanol (1:1, v/v) was added a solution of 1,3-diamino-2-hydroxypropane (158 mg, 1.75 mmol) in 10 mL of 95% ethanol. This was allowed to stir for 48 h at ambient temperature. The solution was evaporated to give a crude product, which was dissolved

in 20 mL of water and extracted using chloroform (2 x 100 mL). The combined organic layer was dried over anhydrous sodium sulfate, filtered, and evaporated to form a yellow solid that was used without further purification. Yield 90% (1.03 g, 1.58 mmol) Found: C, 59.09, H, 7.35, N, 4.42; $C_{31}H_{46}N_2O_{11}.1/2H_2O$ requires C, 58.92, H, 7.44, N, 4.42. ^{1}H NMR (400 MHz, $CDCl_3$) δ_H 8.14 (2H s -CH=N-), 7.04 (2H, d, *J* = 8.8, Ar*H*), 6.36 (2H, d, *J* = 2.5, Ar*H*), 6.33 (2H, s, Ar*H*), 4.14 (1H, m, -C*H*OH-), 4.09 (4H, t, *J* = 4.7, $ArOCH_2$-), 3.82 (t, 4H, *J* = 4.8, $ArOCH_2CH_2$-) 3.74 (6H, dd, *J* = 3.3, 5.8,-CH_2 -), 3.71-3.56 (10H, m, -CH_2 -), 3.55-3.50 (4H, m, -CH_2 -), 3.35(6H, s, OCH_3); ^{13}C NMR (100 MHz, $CDCl_3$) δ_C 166.4, 165.9, 163.3, 133.1, 112.2, 107.0, 101.9, 71.9, 70.8, 70.6, 70.5, 70.2, 69.5, 67.5, 61.2, 59.0; IR: ν_{max} (KBr)/cm^{-1} 3573br (OH), 3073w (=CH arom), 2871s (C-H), 1622v (C=N), 1115s (C-O); positive ion ESI MS, calculated for $(C_{31}H_{46}N_2O_{11} + H)^+$ 622.31, found 622.81.

1,3-Bis(2-hydroxy-4-[2-(methoxyethoxy)]benzylideneamino)propan-2-ol Dicopper complex, 15a. Solution of copper(II) acetate (100 mg, 0.500 mmol) in 10 mL DMF was added dropwise to a solution of ligand **14a** (110 mg, 0.251 mmol) in 30 mL DMF. Triethyl-amine (76 mg, 0.75 mmol) was added and the resultant mixture allowed to stir at 60 ºC for 24 h. The mixture was concentrated under vacuum and allowed to evaporate slowly. A green solid formed that was recrystallized from ethanol to obtain dark green crystals. Yield 44% (70 mg, 0.11 mmol). Found: C, 47.63; H, 4.80; N, 4.40. $C_{25}H_{31}Cu_2N_2O_9$ requires: C, 47.62, H, 4.95, N, 4.44. IR: ν_{max} (KBr)/cm^{-1} 3455br (OH), 2905s (C–H), 1630v (C=N), 1128s (C–O).

1,3-Bis[{2-hydroxy-4-[2-(2-methoxyethoxy)ethoxy]ethoxybenzylideneamino]propan-2-ol}ato (*m*-acetato) dicopper (II) complex, 15c. 125 mg (0.4 mmol) of

the ligand was dissolved in 50 mL ethanol. To this solution was added dropwise 80 mg (0.44 mmol) of copper (II) acetate dissolved in methanol. The resulting solution was heated at 60 ^{o}C for 24 h and the solvent was evaporated to obtain a green solid. The crude product was purified using a Sephadex (LH 20-100) column to remove excess acetate and eluted with methanol to obtain a green solid product. Yield 12% (20 mg, 0.023 mmol); Found C, 48.29; H, 5.77; N, 3.58; $C_{33}H_{46}Cu_2N_2O_{13}\cdot H_2O$ requires C, 48.11; H, 5.87; N, 3.40; ν_{max} (KBr)/cm^{-1} 3466br (OH), 2894s (C-H), 1629v (C=N), 1122s (C-O); HRMS cald for $(C_{33}H_{46}Cu_2N_2O_{13} + K)^+$ 843.1429, found 843.1126.

1,4-Diphthaloylamino-2-butanol, 22. This compound was synthesized in analogy to a procedure developed by Murase, I.; Ueno, S.; Kida, S. *Inorg. Chim. Acta* **1984**, *87*, 155-157. A mixture of 1,4-dibromo-2-butanol (12 g, 52 mmol) and potassium phthalimide (20.0 g, 107 mmol) in 70 mL dry DMF was warmed to 80 ^{o}C and allowed to stir for 24 h under argon gas. The mixture was allowed to cool to room temperature to form a precipitate that was filtered and washed with water. The solid phthalimide was air dried and recrystallized from DMF to form white crystals. Yield 69% (12.48 g, 34.25 mmol); m.p 248-249 ^{o}C. Found: C, 65.56; H, 4.48; N, 7.85. $C_{20}H_{16}N_2O_5$ requires C, 65.92; H, 4.43; N, 7.79.

1,4-Diaminobutan-2-ol dihydrochloride, 23. This compound was synthesized in analogy to a procedure developed by Murase, I.; Ueno, S.; Kida, S. *Inorg. Chim. Acta* **1984**, *87*, 155-157. 1,4-Diphthaloylamino-2-butanol (10.2 g, 28.0 mmol) was refluxed in acetic acid (50 mL) and concentrated hydrochloric acid (30 mL) for 40 h. During this period, 10 mL aliquots of hydrochloric acid were added in 10 h time intervals. Upon cooling the solution, a white precipitate was formed that was filtered and

the filtrate distilled to dryness under vacuum. The solid obtained was dissolved in 30 mL water and filtered to remove insoluble impurity. The filtrate was again distilled under reduced pressure to obtain a white solid that was treated with 100 mL ethanol overnight to obtain white crystalline solid after filtration. This solid was recrystallized from methanol, filtered and dried over oil pump for 12 h at 100 ^{o}C to form white crystals. Yield, 60% (3.0 g, 17 mmol); m.p 229-231 ^{o}C.

N,N'-bis(2-pyridylmethyl)-1,4-diaminobutan-2-ol, 25. To a solution of 1,4-diaminobutan-2-ol dihydrochloride (0.51 g, 2.8 mmol) in 20 mL methanol was added 10 mL methanol solution of sodium hydroxide (230 mg, 5.6 mmol) and the solution stirred for 30 minutes at ambient temperature. The resultant solution was filtered to remove precipitated NaCl. A solution of 2-pyridine carboxaldehyde (0.60 g, 5.6 mmol) in 10 mL methanol was added dropwise to the filtrate and the resultant yellow solution stirred overnight at ambient temperature. Sodium borohydride (158 mg, 5.64 mmol) was added in small portions, after which the solution was refluxed for 1 h. It was cooled to ambient temperature and evaporated to dryness by rotary evaporation. The crude product was dissolved in 20 mL of nanopure water and extracted using dichloromethane (2 x 50 mL). The combined organic layer was dried using anhydrous sodium sulfate, filtered and evaporated to obtain an oil that was purified using a Sephadex LH-20-100 column eluted with methanol. Yield: 40% (320 mg, 1.12 mmol), yellow oil. IR (thin film): ν_{max}/cm^{-1} 3303br (OH), 3063w (N–H), 2927s (C–H asy-str), 2830s (C–H sym-str), 729s (N–H wag); ^{1}H NMR (400.2 MHz, $CDCl_3$) δ_H 8.54 (m, 2H, H ortho to pyridine N), 7.75–7.55 (m, 2H, ArH), 7.35–7.25 (m, 2H, ArH), 7.22–7.06 (m, 2H, ArH), 4.04–3.83 (m, 5H, $ArOCH_2$, C*H*OH), 3.40–3.05 (2H, NH), 3.04–2.76 (m, 2H, CH_2CH_2NH), 2.75–2.58 (m,

2H, CH_2NH), 1.77–1.52 (m, 2H, C*H*$_2$CH$_2$NH); ^{13}C NMR (100.6 MHz, $CDCl_3$) δ_C 160.1, 159.3, 149.4, 149.3, 136.7, 136.6, 122.5, 122.3, 122.2, 122.0, 71.3, 55.7, 55.2, 55.0, 33.7; HRMS calcd for $(C_{16}H_{22}N_4O + H)^+$ 287.1872; found 287.1874.

N,N'-bis(2-pyridylmethyl)-1,4-diaminobutan-2-ol dicopper complex, 26 Copper(II) acetate monohydrate (1.4 g, 7.0 mmol) was dissolved in 10 mL nanopure water and mixed with a solution of sodium perchlorate (2.8 g, 23 mmol) in 5 mL water. The resultant solution was diluted with 140 mL methanol. Ligand (716 mg, 2.52 mmol) dissolved in 20 mL ethanol was added slowly to the copper solution to form a deep blue solution immediately. This solution was concentrated to a volume of 30 mL by using rotary evaporator and allowed to stand at ambient temperature for 4 days, when blue crystals formed. mp > 260 ^oC Found: C, 31.52; H, 3.70; N, 8.09. $C_{18}H_{26}Cl_2Cu_2N_4O_{12}$ requires C, 31.36; H, 3.95; N, 8.13. IR: ν_{max} (KBr)/cm^{-1} 3443br (OH) 3247w (N-H), 2930w (C-H), 1564s (N-H def), 1095s (C–O). ***Caution: Perchlorate salts are potentially explosive and should therefore be handled with appropriate care.***

1,4-Bis[{2-hydroxy-4-[2-(2-methoxyethoxy)ethoxy]ethoxy}benzylidene amino] butan-2-ol, 29c. 1,4 Diamino-2-butanol dihydrochloride (174 mg, 0.98 mmol) was dissolved in 20 mL methanol. To this solution was added sodium hydroxide (78.4 mg, 1.96 mmol) and allowed to stir for 30 min. The mixture was filtered to remove sodium chloride. To the filtrate was added a solution of 2-hydroxy-4-{2-[2-methoxyethoxy)ethoxy}benzaldehyde, 560 mg (1.96 mmol), in 100 mL of methanol to form a yellow solution that was allowed to stir overnight. A yellow precipitate was formed, filtered, and recrystallized using DMF. Yield 89% (560 mg, 0.88 mmol); Found C, 60.46; H, 7.69; N, 4.51; $C_{32}H_{48}N_2O_{11}$ requires C, 60.36; H, 7.60; N, 4.40; ^{1}H NMR

(400 MHz, $CDCl_3$) δ_H 13.77 (2H, s, OH), 8.38 (1H, s -CH=N-), 8.31 (1H, s -CH=N-), 7.23 (2H, d, 8.59, Ar*H*), 6.36 (2H, m, Ar*H*), 6.30 (2H, dd, *J* = 5.6, 2.0, Ar*H*), 4.70 (1H, m, -C*H*OH-), 4.11 (4H, t, *J* = 4.4, ArOCH_2-), 3.80 (1H, s, OH), 3.75 (t, 4H, *J* = 4.6, ArOCH_2CH_2-), 3.54 (16H, m, -CH_2 -), 3.45 (4H, t, *J* = 5.2, -CH_2 -), 3.27 (6H, s, OCH_3), 1.79 (2H, m, CH_2-).

1,4-Bis[{2-hydroxy-4-[2-(methoxyethoxy)]}-benzylideneamino]butan-2-ol, 29a. 1,4-Diamino-2-butanol dihydrochloride (163 mg, 0.92 mmol) was dissolved in 20 mL methanol. To this solution was added sodium hydroxide (74 mg, 1.85 mmol) and allowed to stir for 30 min. The mixture was filtered to remove sodium chloride. To the filtrate was added a solution of 2-hydroxy-4-(2-methoxyethoxy)benzaldehyde, 360 mg (1.8 mmol), in 100 mL of methanol to form a yellow solution that was allowed to stir overnight. A yellow precipitate was formed, filtered, and recrystallized using DMF. Yield 68% (290 mg, 0.63 mmol); Found C, 62.39; H, 6.79; N, 6.14; $C_{24}H_{32}N_2O_7$ requires C, 62.59; H, 7.00; N, 6.08; ^{1}H NMR (400 MHz, $CDCl_3$) δ_H 13.73 (2H, s, OH), 8.38 (1H, s -CH=N-), 8.32 (1H, s -CH=N-), 7.23 (2H, d, *J* = 8.3, ArH), 6.36 (2H, m, ArH), 6.30 (2H, dd, *J* = 5.7, 2.4, ArH), 4.70 (1H, m, -C*H*OH-), 4.11 (4H, t, *J* = 4.8, ArOCH_2-), 3.80 (1H, s, OH), 3.66 (8H, m, -CH_2 -), 3.45 (4H, t, *J* = 5.2, -CH_2 -), 3.32 (6H, s, OCH_3), 1.78 (2H, m, CH_2-).

1,3 Bis[2 hydroxy 4 [4-vinylbenzyloxy]benzylideneamino]propan-2-ol, 33. To a solution of 2-hydroxy-4-(4-vinylbenzyloxy)benzaldehyde (620 mg, 2.4 mmol) in 150 mL ethanol/methanol 1:1 (v:v) mixture was added a solution of 1,3-diaminopropanol (110 mg, 1.2 mmol) in 10 mL ethanol. The mixture turned yellow immediately and was allowed to stir for 48 h at ambient temperature. The solvent was then evaporated using a

rotavap to obtain a yellow solid. The solid was recrystallized using ethanol/methanol 1:1 (v/v) to obtain the desired product. Yield 82% (550 mg, 098 mmol); ^{1}H NMR (400.2 MHz, DMSO-d_6) δ_H 8.14 (s, 2H, C*H*=N), 7.38 (8H, dd, *J* = 8.2, 21.1, Ar*H*), 7.05 (d, 2H, 8.59, Ar*H*), 6.69 (2H, dd, *J* = 17.7, 10.9 –C*H*=CH_2), 6.42 (4H, m), 5.74 (2H, d, *J* = 17.7, -CH=CH_2-), 5.24 (2H, d, *J* = 10.9, -CH=CH_2 -), 5.02 (4H, s, ArCH_2), 4.14 (1H, m, C*H*OH), 3.73 (2 H, dd, *J* = 4.04, 12.6), 3.59 (2H, dd, *J* = 6.4, 12.8); ^{13}C NMR (100.6 MHz, DMSO-d_6) δ_C 167.0, 166.3, 162.9, 137.2, 136.9, 136.8, 133.8, 128.4, 126.7, 114.0, 112.6, 106.8, 102.6, 69.8, 69.4, 60.9

REFERENCES

(1) Collinson, S. R.; Fenton, D. E. *Coord. Chem. Rev.* **1996**, *148*, 19-40.

(2) Cozzi, P. G. *Chem. Soc. Rev.* **2004**, *33*, 410-421.

(3) Ma, H.; Chen, S.; Niu, L.; Zhao, S.; Li, S.; Li, D. *J. Appl. Electrochem.* **2002**, *32*, 65-72.

(4) Sasi, S.; Kurup, M. R. P.; Suresh, E. *J. Chem. Crystallogr.* **2007**, *37*, 31-36.

(5) Jain, S.; Reiser, O. *ChemSusChem* **2008**, *1*, 534-541.

(6) Ispir, E.; Serin, S. *J. Therm. Anal. Calorim.* **2008**, *94*, 281-288.

(7) Naeimi, H.; Moradian, M. *Polyhedron* **2008**, *27*, 3639-3645.

(8) Zhou, X.-G.; Yu, X.-Q.; Huang, J.-S.; Che, C.-M.; Li, S.-G.; Li, L.-S. *Chem. Commun.* **1999**, 1789-1790.

(9) Gupta, K. C.; Sutar, A. K. *J. Mol. Catal. A: Chem.* **2007**, *272*, 64-74.

(10) Tidwell, T. T. *Angew. Chem., Int. Ed.* **2008**, *47*, 1016-1020.

(11) Rideout, D. C.; Breslow, R. *J. Am. Chem. Soc.* **1980**, *102*, 7816-7817.

(12) Lindstroem, U. M. *Chem. Rev.* **2002**, *102*, 2751-2771.

(13) Brunelet, T.; Jouitteau, C.; Gelbard, G. *J. Org. Chem.* **1986**, *51*, 4016-4022.

(14) Blackburn, L.; Taylor, R. J. K. *Org. Lett.* **2001**, *3*, 1637-1639.

(15) Corey, E. J.; Suggs, J. W. *Tetrahedron Lett.* **1975**, 2647-265

(16) Firouzabadi, H.; Tamami, B.; Goudarzian, N.; Hatam, M.; Lakouraj, M. M. *Synth. Commun.* **1991**, *21*, 2077-2088.

(17) Khodaie, M. M.; Salehi, P.; Goodarzi, M. *Synth. Commun.* **2001**, *31*, 1253-1256.

(18) Paxton, R. J.; Taylor, R. J. K. *Synlett* **2007**, 633-637.

(19) Shaabani, A.; Mirzaei, P.; Naderi, S.; Lee, D. G. *Tetrahedron* **2004**, *60*, 11415-11420.

(20) Shirini, F.; Tajik, H.; Jalili, F. *Synth. Commun.* **2001**, *31*, 2885-2889.

(21) Yamada, Y. M. A.; Tabata, H.; Ichinohe, M.; Takahashi, H.; Ikegami, S. *Tetrahedron* **2004**, *60*, 4087-4096.

(22) Li, C.-J.; Chen, L. *Chem. Soc. Rev.* **2006**, *35*, 68-82.

(23) Uozumi, Y.; Nakao, R. *Angew. Chem., Int. Ed.* **2003**, *42*, 194-197.

(24) Ansari Imtiaz, A.; Gree, R. *Org. Lett.* **2002**, *4*, 1507-1509.

(25) Choudary, B. M.; Kantam, M. L.; Rahman, A.; Reddy, C. V.; Rao, K. K. *Angew. Chem., Int. Ed.* **2001**, *40*, 763-766.

(26) Dijksman, A.; Marino-Gonzalez, A.; Mairata i Payeras, A.; Arends, I. W. C. E.; Sheldon, R. A. *J. Am. Chem. Soc.* **2001**, *123*, 6826-6833.

(27) Ebitani, K.; Fujie, Y.; Kaneda, K. *Langmuir* **1999**, *15*, 3557-3562.

(28) Iwahama, T.; Yoshino, Y.; Keitoku, T.; Sakaguchi, S.; Ishii, Y. *J. Org. Chem.* **2000**, *65*, 6502-6507.

(29) Maeda, Y.; Kakiuchi, N.; Matsumura, S.; Nishimura, T.; Kawamura, T.; Uemura, S. *J. Org. Chem.* **2002**, *67*, 6718-6724.

(30) Marko, I. E.; Gautier, A.; Chelle-Regnaut, I.; Giles, P. R.; Tsukazaki, M.; Urch, C. J.; Brown, S. M. *J. Org. Chem.* **1998**, *63*, 7576-7577.

(31) Marko, I. E.; Giles, P. R.; Tsukazaki, M.; Brown, S. M.; Urch, C. J. *Science.* **1996**, *274*, 2044-2046.

(32) Marko, I. E.; Giles, P. R.; Tsukazaki, M.; Chelle-Regnaut, I.; Urch, C. J.; Brown, S. M. *J. Am. Chem. Soc.* **1997**, *119*, 12661-12662.

(33) Haber, J.; Matachowski, L.; Pamin, K.; Poltowicz, J. *Catal. Today* **2004**, *91-92*, 195-198.

(34) Maeda, Y.; Kakiuchi, N.; Matsumura, S.; Nishimura, T.; Kawamura, T.; Uemura, S. *J. Org. Chem.* **2002**, *67*, 6718-6724.

(35) Astruc, D.; Lu, F.; Aranzaes, J. R. *Angew. Chem., Int. Ed.* **2005**, *44*, 7852-7872.

(36) Biffis, A.; Cunial, S.; Spontoni, P.; Prati, L. *J. Catal.* **2007**, *251*, 1-6.

(37) Liu, R.; Liang, X.; Dong, C.; Hu, X. *J. Am. Chem. Soc.* **2004**, *126*, 4112-4113.

(38) Komiya, N.; Nakae, T.; Sato, H.; Naota, T. *Chem Commun.,* **2006**, 4829-4831.

(39) Striegler, S. *Tetrahedron* **2006**, *62*, 9109-9114.

(40) Mukherjee, A. K. *Anal. Chim. Acta* **1955**, *13*, 268-272.

(41) Bhattacharjee, S.; Anderson, J. A. *Chem. Commun.* **2004**, 554-555.

(42) Bhattacharjee, S.; Dines, T. J.; Anderson, J. A. *J. Catal.* **2004**, *225*, 398-407.

(43) Correia, I.; Pessoa, J. C.; Duarte, M. T.; Da Piedade, M. F. M.; Jackush, T.; Kiss, T.; Castro, M. M. C. A.; Geraldes, C. F. G. C.; Avecilla, F. *Eur. J. Inorg. Chem.* **2005**, 732-744.

(44) Bahramian, B.; Mirkhani, V.; Moghadam, M.; Tangestaninejad, S. *Catal. Commun.* **2006**, *7*, 289-296.

(45) Witt, K. A.; Davis T. P.; *Aaps J* **2006**, *8*, E76-88.

(46) Ugelstad, J.; El-Aasser, M. S.; Vanderhoff, J. W. *J. Polym. Sci., Polym. Lett. Ed.* **1973**, *11*, 503-513.

(47) Lefay, C.; Save, M.; Charleux, B.; Magnet, S. *Aust. J. Chem.* **2006**, *59*, 544-548.

(48) Wang, H.; Ge, X.; Song, L.; Liu, H. *Colloid Polym. Sci.* **2007**, *285*, 1093-1100.

(49) Landfester, K.; Bechthold, N.; Foerster, S.; Antonietti, M. *Macromol. Rapid Commun.* **1999**, *20*, 81-84.

(50) Yildiz, U.; Landfester, K. *Polymer* **2008**, *49*, 4930-4934.

(51) Gooch, J. W.; Dong, H.; Schork, F. J. *J. Appl. Polym. Sci.* **2000**, *76*, 105-114.

(52) Cai, N.; Xu, Y.; Jia, G.; Yuan, C. *Polym. Bull.* **2007**, *59*, 491-498.

(53) Huang, X.; Sudol, E. D.; Dimonie, V. L.; Anderson, C. D.; El-Aasser, M. S. *Macromolecules* **2006**, *39*, 6944-6950.

(54) Jia, G.; Cai, N.; Xu, Y.; Liu, C.; Tan, X. *Eur. Polym. J.* **2007**, *43*, 4453-4459.

(55) Luo, Y.; Liu, B.; Wang, Z.; Gao, J.; Li, B. *J. Polym. Sci., Part A: Polym. Chem.* **2007**, *45*, 2304-2315.

(56) Mouran, D.; Reimers, J.; Schork, F. J. *J. Polym. Sci., Part A: Polym. Chem.* **1996**, *34*, 1073-1081.

(57) Ni, K.-F.; Shan, G.-R.; Weng, Z.-X. *Macromolecules* **2006**, *39*, 2529-2535.

(58) Qi, G.; Jones C. W.; Schork, F. J. *Biomacromolecules* **2006**, *7*, 2927-2930.

(59) Rodriguez, V. S.; El-Aasser, M. S.; Asua, J. M.; Silebi, C. A. *J. Polym. Sci., Part A: Polym. Chem.* **1989**, *27*, 3659-3671.

(60) Qi, G.; Jones, C. W.; Schork, F. J. *Biomacromolecules* **2006**, *7*, 2927-2930.

(61) Kim, N.; Sudol, E. D.; Dimonie, V. L.; El-Aasser, M. S. *Macromolecules* **2004**, *37*, 2427-2433.

(62) Bradley, M. A.; Prescott, S. W.; Schoonbrood, H. A. S.; Landfester, K.; Grieser, F. *Macromolecules* **2005**, *38*, 6346-6351.

(63) Graillat, C.; Guyot, A. *Macromolecules* **2003**, *36*, 6371-6377.

(64) Oh, J. K.; Yang, J.; Rademacher, J.; Farwaha, R.; Winnik, M. A. *Macromolecules* **2004**, *37*, 5752-5761.

(65) Asua, J. M. *Prog. Polym. Sci.* **2002**, *27*, 1283-1346.

(66) Landfester, K.; Ramirez, L. P. *J. Phys.: Condens. Matter* **2003**, *15*, S1345-S1361.

(67) Brintzinger, H. H.; Fischer, D.; Muelhaupt, R.; Rieger, B.; Waymouth, R. M. *Angew. Chem., Int. Ed. Engl.* **1995**, *34*, 1143-1170.

(68) Erdem, B.; Sudol, E. D.; Dimonie, V. L.; El-Aasser, M. S. *J. Polym. Sci., Part A: Polym. Chem.* **2000**, *38*, 4441-4450.

(69) Ghurmallah, H.; Al-Ghamdi, E.; Sudol, D.; Dimonie, V. L.; El-Aasser, M. S. *J. Appl. Polym. Sci.* **2006**, *101*, 3479-3486.

(70) Liu, Z.; Pei, L.; Ji, H.; Yao, X. *Chin. J. Chem. Eng.* **2008**, *16*, 384-388.

(71) Naundorf, C.; Matsui, S.; Saito, J.; Fujita, T.; Klapper, M.; Muellen, K. *J. Polym. Sci., Part A: Polym. Chem.* **2006**, *44*, 3103-3113.

(72) Jang, Y.-J.; Nenov, N.; Klapper, M.; Muellen, K. *Polym. Bull.* **2003**, *50*, 343-350.

(73) Bauers, F. M.; Mecking, S. *Angew. Chem., Int. Ed.* **2001**, *40*, 3020-3022.

(74) Liu, L.; Breslow, R. *Bioorg. Med. Chem.* **2004**, *12*, 3277-3287.

(75) Klibanov, A. M. *Nature* **2001**, *409*, 241-246.

(76) Schmitke, J. L.; Wescott, C. R.; Klibanov, A. M. *J. Am. Chem. Soc.* **1996**, *118*, 3360-3365.

(77) Wang, Q.; Yang, Z.; Wang, L.; Ma, M.; Xu, B. *Chem. Commun.* **2007**, 1032-1034.

(78) Chantarasiri, N.; Tuntulani, T.; Chanma, N. *Eur. Polym. J.* **2000**, *36*, 889-894.

(79) Dou, W.; Wang, Y.-W.; Yao, J.-N.; Liu, W.-S.; Wang, D.-Q. *Anal. Sci.: X-Ray Struct. Anal. Online* **2006**, *22*, 277-278.

(80) Bagai, R.; Abboud, K. A.; Christou, G. *Dalton Trans.* **2006**, 3306-3312.

(81) Sanchez, M.; Keizer, T. S.; Parkin, S.; Hopfl, H.; Atwood, D. A. *J. Organomet. Chem.* **2002**, *654*, 36-43.

(82) Sarkar, S.; Dey, K.; Biswas, S.; Bhaumik, B. *J. Coord. Chem.* **2007**, *60*, 1143-1156.

(83) Weng, C.-H.; Cheng, S.-C.; Wei, H.-M.; Wei, H.-H.; Lee, C.-J. *Inorg. Chim. Acta* **2006**, *359*, 2029-2040.

(84) Duan, X. F.; Zeng, J.; Zhang, Z. B.; Zi, G. F. *J. Org. Chem.* **2007**, *72*, 10283-10286.

(85) Maslak, V.; Yan, Z.; Xia, S.; Gallucci, J.; Hadad, C. M.; Badjic, J. D. *J. Am. Chem. Soc.* **2006**, *128*, 5887-5894.

(86) Liepa, A. J. *Aust. J. Chem.* **1984**, *37*, 2545-2558.

(87) Gichinga, M. G.; Striegler, S. *Tetrahedron* **2009**, *65*, 4917-4922.

(88) Bibeau, C. T.; Hubbard, B. K.; Abelt, C. J. *Chem. Commun.* **1997**, 437-438.

(89) Chaplin, D. J.; Edvardsen, K.; Pinney, K. G.; Prezioso, J. A.; Wood, M.; Patent number WO 2004078126, March 01, 2001.

(90) Kilenyi, S. N.; Mahaux, J. M.; Van Durme, E. *J. Org. Chem* **1991**, *56*, 2591-2594.

(91) Rolff, M.; Tuczek, F. *Angew. Chem., Int. Ed.* **2008**, *47*, 2344-2347.

(92) Fabien, M.; Thomas, F.; Hamman, S; Philouze, C.; Saint-Aman, E.; Pierre, J.-L. *Eur. J. Inorg. Chem* **2006**, 3684-3696.

(93) Whittaker, J. W. *Chem Rev* **2003**, *103*, 2347-2363.

(94) Ilhan, S.; Temel, H.; Yilmaz, I.; Sekerci, M. *Polyhedron* **2007**, *26*, 2795-2802.

(95) Jana, S.; Dutta, B.; Bera, R.; Koner, S. *Langmuir* **2007**, *23*, 2492-2496.

(96) Farrugia, L. J. *J. Appl. Crystallogr.* **1997**, *30*, 565.

(97) Binstead, R. A.; Jung, B.; Zuberbuhler, A. D. *SPECFIT*, 3.0 ed.; Spectrum Software Associates: Marlborough, MA, 2000.

(98) Tas, E.; Aslanoglu, M.; Guler, M.; Ulusoy, M. *J. Coord. Chem.* **2004**, *57*, 583-589.

(99) Striegler, S.; Dittel, M. *J. Am. Chem. Soc.* **2003**, *125*, 11518-11524.

(100) Jarho, E. M.; Venaelaeinen, J. I.; Juntunen, J.; Yli-Kokko, A. L.; Vepsaelaeinen, J.; Christiaans, J. A. M.; Forsberg, M. M.; Jaervinen, T.; Maennistoe, P. T.; Wallen, E. A. A. *Bioorg. Med. Chem. Lett.* **2006**, *16*, 5590-5593.

(101) Murase, I.; Ueno, S.; Kida, S. *Inorg. Chim. Acta* **1984**, *87*, 155-157.

(102) Striegler, S.; Gichinga, M. G. *Chem. Commun.* **2008**, 5930-5932.

(103) Gajda, T.; Jancso, A.; Mikkola, S.; Loennberg, H.; Sirges, H. *J. Chem. Soc., Dalton Trans.* **2002**, 1757-1763.

(104) Gajda, T.; Kramer, R.; Jancso, A. *Eur. J. Inorg. Chem* **2000**, 1635-1644.

(105) Decker, H.; Dillinger, R.; Tuczek, F. *Angew. Chem., Int. Ed.* **2000**, *39*, 1591-1595.

(106) Kitajima, N.; Moro-oka, Y. *Chem. Rev* **1994**, *94*, 737-757.

(107) Ryan, S.; Adams, H.; Fenton, D. E.; Becker, M.; Schindler, S. *Inorg. Chem.* **1998**, *37*, 2134-2140.

(108) Solomon, E. I.; Sundaram, U. M.; Machonkin, T. E. *Chem. Rev.* **1996**, *96*, 2563-2605.

(109) Neves, A.; Rossi, L. M.; Bortoluzzi, A. J.; Szpoganicz, B.; Wiezbicki, C.; Schwingel, E.; Haase, W.; Ostrovsky, S. *Inorg. Chem.* **2002**, *41*, 1788-1794.

(110) Thirumavalavan, M.; Akilan, P.; Kandaswamy, M.; Chinnakali, K.; Kumar, G. S.; Fun, H. K. *Inorg. Chem.* **2003**, *42*, 3308-3317.

(111) Karlin, K. D.; Tyeklar, Z.; *Bioinorganic Chemistry of Copper*; Chapman & Hall: New York, 1993.

(112) Merkel, M.; Moeller, N.; Piacenza, M.; Grimme, S.; Rompel, A.; Krebs, B. *Chem. Eur. J.* **2005**, *11*, 1201-1209.

(113) Selmeczi, K.; Reglier, M.; Giorgi, M.; Speier, G. *Coord. Chem. Rev.* **2003**, *245*, 191-201.

(114) Monzani, E.; Casella, L.; Zoppellaro, G.; Gullotti, M.; Pagliarin, R.; Bonomo, R. P.; Tabbi, G.; Nardin, G.; Randaccio, L. *Inorg. Chim. Acta* **1998**, *282*, 180-192.

(115) Mimmi, M. C.; Gullotti, M.; Santagostini, L.; Saladino, A.; Casella, L.; Monzani, E.; Pagliarin, R. *J. Mol. Catal. A: Chem.* **2003**, *204-205*, 381-389.

(116) Monzani, E.; Battaini, G.; Perotti, A.; Casella, L.; Gullotti, M.; Santagostini, L.; Nardin, G.; Randaccio, L.; Geremia, S.; Zanello, P.; Opromolla, G. *Inorg. Chem.* **1999**, *38*, 5359-5369.

(117) Klabunde, T.; Eicken, C.; Sacchettini, J. C.; Krebs, B. *Nat. Struct. Biol.* **1998**, *5*, 1084-1090.

(118) Neves, A.; Rossi, L. M.; Bortoluzzi, A. J.; Szpoganicz, B.; Wiezbicki, C.; Schwingel, E.; Haase, W.; Ostrovsky, S. *Inorg. Chem.* **2002**, *41*, 1788-1794.

(119) Gichinga, M. G.; Striegler, S. *J. Am. Chem. Soc.* **2008**, *130*, 5150-5156.

(120) Seacat, A. M.; Kuppusamy, P.; Zweier, J. L.; Yager, J. D. *Arch. Biochem. Biophys.* **1997**, *347*, 45-52.

(121) Kormann, C.; Bahnemann, D. W.; Hoffmann, M. R. *Environ. Sci. Technol.* **1988**, *22*, 798-806.

(122) Masteri-Farahani, M.; Farzaneh, F.; Ghandi, M. *Catal. Commun.* **2006**, *8*, 6-10.

(123) Cameron, P. A.; Gibson, V. C.; Redshaw, C.; Segal, J. A.; Bruce, M. D.; White, A. J. P.; Williams, D. J. *Chem. Commun.* **1999**, 1883-1884.

(124) Comas-Vives, A.; Gonzalez-Arellano, C.; Corma, A.; Iglesias, M.; Sanchez, F.; Ujaque, G. *J. Am. Chem. Soc.* **2006**, *128*, 4756-4765.

(125) Jiang, W.; Xu, B.; Zhong, J.; Li, J.; Liu, F. *J. Chem. Sci.* **2008**, *120*, 411-417.

(126) Sinnott, M. L. *Chem. Rev* **1990**, *90*, 1171-1202.

(127) Ortega-Caballero, F.; Rousseau, C.; Christensen, B.; Petersen, T. E.; Bols, M. *J. Am. Chem. Soc.* **2005**, *127*, 3238-3239.

(128) Bjerre, J.; Nielsen, E. H.; Bols, M. *Eur. J. Org. Chem.* **2008**, 745-752.

(129) Rousseau, C.; Nielsen, N.; Bols, M. *Tetrahedron Lett.* **2004**, *45*, 8709-8711.

(130) Bjerre, J.; Fenger, T. H.; Marinescu, L. G.; Bols, M. *Eur. J. Org. Chem.* **2007**, 704-710.

(131) Baty, J.; Sinnott, M. L. *Chem. Commun.* **2004**, 866-867.

(132) Clark, C. R.; Hay, R. W.; Dea, I. C. M. *J. Chem. Soc. Chem. Commun.* **1970**, 794-795.

(133) Ortega-Caballero, F.; Bols, M. *Can. J. Chem.* **2006**, *84*, 650-658.

(134) Luisi, P. L. *Naturwissenschaften* **1979**, *66*, 498-504.

(135) Efendiev, A. *Macromol. Symp.* **2006**, *235*, 89-97.

(136) Schunicht, C.; Biffis, A.; Wulff, G. *Tetrahedron* **2000**, *56*, 1693-1699.

(137) Spanka, C.; Clapham, B.; Janda, K. D. *J. Org. Chem.* **2002**, *67*, 3045-3050.

(138) Striegler, S.; Gichinga, M. G.; Dittel, M. *Org. Lett.* **2008**, *10*, 241-244.

(139) Zetterlund, P. B.; Kagawa, Y.; Okubo, M. *Chem. Rev.* **2008**, *108*, 3747-3794.

(140) Biffis, A.; Graham, N. B.; Siedlaczek, G.; Stalberg, S.; Wulff, G. *Macromol. Chem. Phys.* **2001**, *202*, 163-171.

(141) Hua, H.; Dube, M. A. *J. Polym. Sci., Part A: Polym. Chem.* **2001**, *39*, 1860-1876.

(142) Kawasaki, T.; Kamata, T.; Ushijima, H.; Kanakubo, M.; Murata, S.; Mizukami, F.; Fujii, Y.; Usui, Y. *J. Chem. Soc., Perkin Trans. 2* **1999**, 193-198.

(143) Sen, T.; Magdassi, S.; Nizri, G.; Bruce, I. J. *Micro Nano Lett.* **2006**, *1*, 39-42.

(144) Mazurek, W.; Bond, A. M.; O'Connor, M. J.; Wedd, A. G. *Inorg. Chem.* **1986**, *25*, 906-915.

APPENDIX 1

CRYSTAL STRUCTURE DATA FOR COMPOUND **15A**

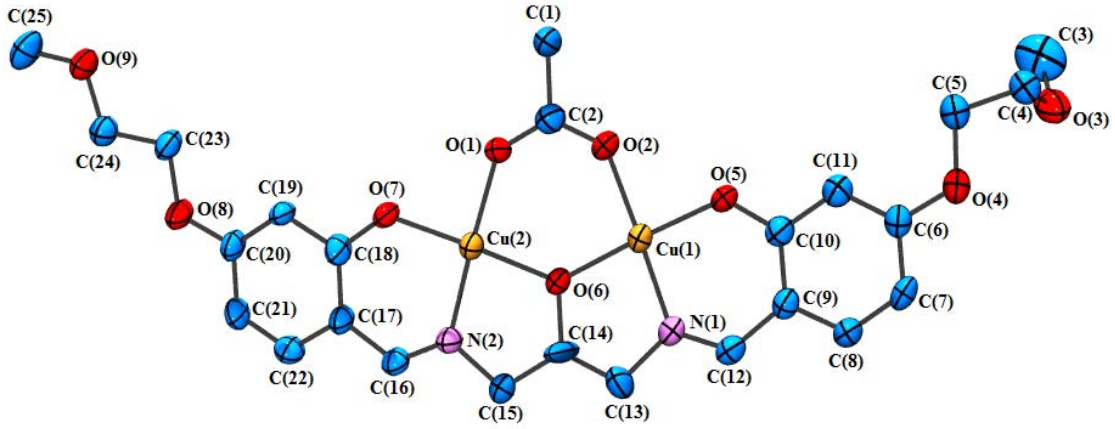

```
data_p-1

_audit_creation_method           SHELXL-97
_chemical_name_systematic
_chemical_name_common            ?
_chemical_melting_point          ?
_chemical_formula_moiety         'C25 H30 Cu2 N2 O9'
_chemical_formula_sum            'C25 H30 Cu2 N2 O9'
_chemical_formula_weight         629.59

loop_
 _atom_type_symbol
 _atom_type_description
 _atom_type_scat_dispersion_real
 _atom_type_scat_dispersion_imag
 _atom_type_scat_source
 'C'  'C'   0.0033   0.0016
 'International Tables Vol C Tables 4.2.6.8 and 6.1.1.4'
 'H'  'H'   0.0000   0.0000
 'International Tables Vol C Tables 4.2.6.8 and 6.1.1.4'
 'N'  'N'   0.0061   0.0033
 'International Tables Vol C Tables 4.2.6.8 and 6.1.1.4'
 'O'  'O'   0.0106   0.0060
 'International Tables Vol C Tables 4.2.6.8 and 6.1.1.4'
 'Cu'  'Cu'   0.3201   1.2651
 'International Tables Vol C Tables 4.2.6.8 and 6.1.1.4'

_symmetry_cell_setting           'Triclinic'
_symmetry_space_group_name_H-M    'P -1'
_symmetry_space_group_name_Hall   '-P 1'
```

```
loop_
 _symmetry_equiv_pos_as_xyz
 'x, y, z'
 '-x, -y, -z'

_cell_length_a                    6.381(2)
_cell_length_b                    10.723(4)
_cell_length_c                    19.732(7)
_cell_angle_alpha                 94.606(7)
_cell_angle_beta                  91.898(7)
_cell_angle_gamma                 107.159(7)
_cell_volume                      1283.5(8)
_cell_formula_units_Z             2
_cell_measurement_temperature     193(2)
_cell_measurement_reflns_used     3677
_cell_measurement_theta_min       2.00
_cell_measurement_theta_max       28.31

_exptl_crystal_description        'rectangular'
_exptl_crystal_colour             'green'
_exptl_crystal_size_max           0.128
_exptl_crystal_size_mid           0.076
_exptl_crystal_size_min           0.024
_exptl_crystal_density_meas       'nm'
_exptl_crystal_density_diffrn     1.629
_exptl_crystal_density_method     'not measured'
_exptl_crystal_F_000              648
_exptl_absorpt_coefficient_mu     1.714
_exptl_absorpt_correction_type    'numerical'
_exptl_absorpt_correction_T_min   0.855
```

```
_exptl_absorpt_correction_T_max   0.960
_exptl_absorpt_process_details    'SHELXPREP'

_exptl_special_details
;
 ?
;

_diffrn_ambient_temperature       193(2)
_diffrn_radiation_wavelength      0.71073
_diffrn_radiation_type            MoK\a
_diffrn_radiation_source          'fine-focus sealed tube'
_diffrn_radiation_monochromator   'graphite'
_diffrn_measurement_device_type   'Bruker APEX'
_diffrn_measurement_method        '0.3 wide /w exposures'
_diffrn_detector_area_resol_mean  ?
_diffrn_standards_number          'na'
_diffrn_standards_interval_count  'na'
_diffrn_standards_interval_time   'na'
_diffrn_standards_decay_%         0
_diffrn_reflns_number             13126
_diffrn_reflns_av_R_equivalents   0.0618
_diffrn_reflns_av_sigmaI/netI     0.1178
_diffrn_reflns_limit_h_min        -8
_diffrn_reflns_limit_h_max        8
_diffrn_reflns_limit_k_min        -14
_diffrn_reflns_limit_k_max        14
_diffrn_reflns_limit_l_min        -26
_diffrn_reflns_limit_l_max        25
_diffrn_reflns_theta_min          2.00
```

```
_diffrn_reflns_theta_max          28.31
_reflns_number_total              6310
_reflns_number_gt                 3677
_reflns_threshold_expression      >2sigma(I)

_computing_data_collection        'SMART'
_computing_cell_refinement        'SMART, SAINT'
_computing_data_reduction         'SAINT'
_computing_structure_solution     'SHELXS-97 (Sheldrick, 1990)'
_computing_structure_refinement   'SHELXL-97 (Sheldrick, 1997)'
_computing_molecular_graphics     'SHELXP-97 (Sheldrick, 1990)'
_computing_publication_material   'SHELXS-97 (Sheldrick, 2000)'

_refine_special_details
;
 Refinement of F^2^ against ALL reflections.  The weighted R-factor wR and
 goodness of fit S are based on F^2^, conventional R-factors R are based
 on F, with F set to zero for negative F^2^. The threshold expression of
 F^2^ > 2sigma(F^2^) is used only for calculating R-factors(gt) etc. and is
 not relevant to the choice of reflections for refinement.  R-factors based
 on F^2^ are statistically about twice as large as those based on F, and R-
 factors based on ALL data will be even larger.
;

_refine_ls_structure_factor_coef  Fsqd
_refine_ls_matrix_type            full
_refine_ls_weighting_scheme       calc
_refine_ls_weighting_details
 'calc w=1/[\s^2^(Fo^2^)+(0.0482P)^2^+0.0000P] where P=(Fo^2^+2Fc^2^)/3'
_atom_sites_solution_primary      direct
```

```
_atom_sites_solution_secondary    difmap
_atom_sites_solution_hydrogens    geom
_refine_ls_hydrogen_treatment     constr
_refine_ls_extinction_method      none
_refine_ls_extinction_coef        ?
_refine_ls_number_reflns          6310
_refine_ls_number_parameters      343
_refine_ls_number_restraints      0
_refine_ls_R_factor_all           0.0984
_refine_ls_R_factor_gt            0.0523
_refine_ls_wR_factor_ref          0.1151
_refine_ls_wR_factor_gt           0.1056
_refine_ls_goodness_of_fit_ref    0.883
_refine_ls_restrained_S_all       0.883
_refine_ls_shift/su_max           0.002
_refine_ls_shift/su_mean          0.000

loop_
 _atom_site_label
 _atom_site_type_symbol
 _atom_site_fract_x
 _atom_site_fract_y
 _atom_site_fract_z
 _atom_site_U_iso_or_equiv
 _atom_site_adp_type
 _atom_site_occupancy
 _atom_site_symmetry_multiplicity
 _atom_site_calc_flag
 _atom_site_refinement_flags
 _atom_site_disorder_assembly
```

_atom_site_disorder_group

Cu1 Cu -1.26031(8) -0.43434(5) 1.18264(2) 0.02544(14) Uani 1 1 d . . .

Cu2 Cu -1.60318(8) -0.56665(4) 1.31067(2) 0.02451(14) Uani 1 1 d . . .

N1 N -1.0752(5) -0.5437(3) 1.16338(16) 0.0257(8) Uani 1 1 d . . .

N2 N -1.5802(5) -0.7395(3) 1.32005(16) 0.0234(7) Uani 1 1 d . . .

O1 O -1.6568(4) -0.4044(2) 1.28963(14) 0.0295(7) Uani 1 1 d . . .

O2 O -1.4248(5) -0.3161(3) 1.21088(15) 0.0359(8) Uani 1 1 d . . .

O3 O -0.7472(5) -0.0199(3) 0.81960(15) 0.0393(8) Uani 1 1 d . . .

O4 O -0.6699(5) -0.1348(3) 0.94406(14) 0.0363(7) Uani 1 1 d . . .

O5 O -1.1376(5) -0.3183(3) 1.11681(14) 0.0338(7) Uani 1 1 d . . .

O6 O -1.4002(4) -0.5646(2) 1.24070(14) 0.0277(7) Uani 1 1 d . . .

O7 O -1.8181(4) -0.5817(2) 1.37591(14) 0.0259(6) Uani 1 1 d . . .

O8 O -2.4170(4) -0.7939(2) 1.50466(14) 0.0317(7) Uani 1 1 d . . .

O9 O -2.7099(5) -0.6016(3) 1.59554(14) 0.0331(7) Uani 1 1 d . . .

C1 C -1.6586(8) -0.2003(4) 1.2550(2) 0.0454(13) Uani 1 1 d . . .

H1A H -1.7704 -0.2105 1.2887 0.068 Uiso 1 1 calc R . .

H1B H -1.7241 -0.1944 1.2102 0.068 Uiso 1 1 calc R . .

H1C H -1.5377 -0.1201 1.2681 0.068 Uiso 1 1 calc R . .

C2 C -1.5724(7) -0.3161(4) 1.2519(2) 0.0294(10) Uani 1 1 d . . .

C3 C -0.9412(9) 0.0012(5) 0.7951(3) 0.0592(15) Uani 1 1 d . . .

H3A H -0.9894 -0.0494 0.7508 0.089 Uiso 1 1 calc R . .

H3B H -0.9143 0.0947 0.7899 0.089 Uiso 1 1 calc R . .

H3C H -1.0557 -0.0269 0.8273 0.089 Uiso 1 1 calc R . .

C4 C -0.6688(7) 0.0484(4) 0.8841(2) 0.0320(10) Uani 1 1 d . . .

H4A H -0.7056 0.1320 0.8876 0.038 Uiso 1 1 calc R . .

H4B H -0.5068 0.0694 0.8883 0.038 Uiso 1 1 calc R . .

C5 C -0.7662(7) -0.0300(4) 0.9417(2) 0.0329(10) Uani 1 1 d . . .

H5A H -0.7332 0.0264 0.9853 0.040 Uiso 1 1 calc R . .

H5B H -0.9277 -0.0656 0.9337 0.040 Uiso 1 1 calc R . .

C6 C -0.7423(7) -0.2245(4) 0.9900(2) 0.0292(10) Uani 1 1 d . . .

C7 C -0.6260(7) -0.3169(4) 0.9929(2) 0.0318(10) Uani 1 1 d . . .

H7A H -0.5082 -0.3146 0.9643 0.038 Uiso 1 1 calc R . .

C8 C -0.6861(7) -0.4102(4) 1.0378(2) 0.0348(11) Uani 1 1 d . . .

H8A H -0.6069 -0.4723 1.0403 0.042 Uiso 1 1 calc R . .

C9 C -0.8601(6) -0.4175(4) 1.0800(2) 0.0261(9) Uani 1 1 d . . .

C10 C -0.9755(7) -0.3230(4) 1.0781(2) 0.0278(10) Uani 1 1 d . . .

C11 C -0.9128(7) -0.2268(4) 1.0316(2) 0.0303(10) Uani 1 1 d . . .

H11A H -0.9887 -0.1632 1.0289 0.036 Uiso 1 1 calc R . .

C12 C -0.9159(7) -0.5232(4) 1.1230(2) 0.0290(10) Uani 1 1 d . . .

H12A H -0.8297 -0.5820 1.1216 0.035 Uiso 1 1 calc R . .

C13 C -1.1238(7) -0.6572(4) 1.2030(2) 0.0349(11) Uani 1 1 d . . .

H13A H -1.1395 -0.7374 1.1723 0.042 Uiso 1 1 calc R . .

H13B H -1.0002 -0.6470 1.2367 0.042 Uiso 1 1 calc R . .

C14 C -1.3191(12) -0.6705(6) 1.2372(4) 0.121(4) Uani 1 1 d . . .

H14A H -1.4187 -0.7187 1.1972 0.145 Uiso 1 1 calc R . .

C15 C -1.4036(7) -0.7687(4) 1.2824(2) 0.0290(10) Uani 1 1 d . . .

H15A H -1.2841 -0.7722 1.3148 0.035 Uiso 1 1 calc R . .

H15B H -1.4608 -0.8555 1.2559 0.035 Uiso 1 1 calc R . .

C16 C -1.7113(6) -0.8281(4) 1.35224(19) 0.0233(9) Uani 1 1 d . . .

H16A H -1.6873 -0.9116 1.3505 0.028 Uiso 1 1 calc R . .

C17 C -1.8897(6) -0.8112(4) 1.3903(2) 0.0244(9) Uani 1 1 d . . .

C18 C -1.9316(6) -0.6893(4) 1.4021(2) 0.0252(9) Uani 1 1 d . . .

C19 C -2.1086(6) -0.6819(4) 1.4418(2) 0.0231(9) Uani 1 1 d . . .

H19A H -2.1365 -0.6001 1.4510 0.028 Uiso 1 1 calc R . .

C20 C -2.2410(6) -0.7920(4) 1.4673(2) 0.0246(9) Uani 1 1 d . . .

C21 C -2.2049(7) -0.9139(4) 1.4539(2) 0.0297(10) Uani 1 1 d . . .

H21A H -2.3006 -0.9901 1.4700 0.036 Uiso 1 1 calc R . .

C22 C -2.0307(7) -0.9219(4) 1.4174(2) 0.0289(10) Uani 1 1 d . . .

H22A H -2.0031 -1.0042 1.4099 0.035 Uiso 1 1 calc R . .

C23 C -2.4626(7) -0.6731(4) 1.5243(2) 0.0282(10) Uani 1 1 d . . .

H23A H -2.5003 -0.6331 1.4839 0.034 Uiso 1 1 calc R . .

H23B H -2.3352 -0.6098 1.5505 0.034 Uiso 1 1 calc R . .

C24 C -2.6558(7) -0.7139(4) 1.5678(2) 0.0290(10) Uani 1 1 d . . .

H24A H -2.7835 -0.7735 1.5400 0.035 Uiso 1 1 calc R . .

H24B H -2.6195 -0.7618 1.6052 0.035 Uiso 1 1 calc R . .

C25 C -2.9064(7) -0.6424(4) 1.6311(2) 0.0378(11) Uani 1 1 d . . .

H25A H -2.9443 -0.5652 1.6501 0.057 Uiso 1 1 calc R . .

H25B H -2.8833 -0.6937 1.6680 0.057 Uiso 1 1 calc R . .

H25C H -3.0265 -0.6965 1.5995 0.057 Uiso 1 1 calc R . .

loop_

_atom_site_aniso_label

_atom_site_aniso_U_11

_atom_site_aniso_U_22

_atom_site_aniso_U_33

_atom_site_aniso_U_23

_atom_site_aniso_U_13

_atom_site_aniso_U_12

Cu1 0.0273(3) 0.0247(3) 0.0282(3) 0.0068(2) 0.0118(2) 0.0114(2)

Cu2 0.0251(3) 0.0209(3) 0.0300(3) 0.0061(2) 0.0124(2) 0.0086(2)

N1 0.029(2) 0.0274(18) 0.0250(19) 0.0047(15) 0.0092(16) 0.0136(15)

N2 0.0241(19) 0.0182(16) 0.0296(19) 0.0039(14) 0.0085(15) 0.0076(14)

O1 0.0317(17) 0.0247(15) 0.0402(18) 0.0137(13) 0.0177(14) 0.0161(13)

O2 0.0418(19) 0.0346(17) 0.0425(19) 0.0142(14) 0.0239(15) 0.0237(14)

O3 0.055(2) 0.0310(16) 0.0341(19) 0.0028(14) 0.0056(16) 0.0164(15)

O4 0.0405(19) 0.0394(17) 0.0363(18) 0.0148(14) 0.0188(15) 0.0185(15)

O5 0.0386(18) 0.0351(16) 0.0400(18) 0.0158(14) 0.0221(15) 0.0247(14)

O6 0.0305(16) 0.0250(15) 0.0337(16) 0.0086(12) 0.0167(13) 0.0144(13)

O7 0.0264(15) 0.0176(13) 0.0357(16) 0.0035(12) 0.0154(13) 0.0081(12)

O8 0.0330(17) 0.0203(14) 0.0428(18) 0.0044(13) 0.0211(14) 0.0070(13)

O9 0.0313(17) 0.0315(16) 0.0417(18) 0.0087(14) 0.0185(14) 0.0142(13)

C1 0.055(3) 0.039(3) 0.059(3) 0.026(2) 0.037(3) 0.030(2)

C2 0.027(2) 0.028(2) 0.037(3) 0.0061(19) 0.008(2) 0.0121(19)

C3 0.066(4) 0.051(3) 0.057(4) -0.001(3) -0.013(3) 0.014(3)

C4 0.034(3) 0.030(2) 0.034(3) 0.008(2) 0.007(2) 0.011(2)

C5 0.037(3) 0.032(2) 0.033(3) 0.0093(19) 0.011(2) 0.012(2)

C6 0.032(2) 0.028(2) 0.029(2) 0.0063(18) 0.0108(19) 0.0098(19)

C7 0.030(2) 0.037(2) 0.034(2) 0.006(2) 0.016(2) 0.016(2)

C8 0.040(3) 0.032(2) 0.042(3) 0.013(2) 0.020(2) 0.021(2)

C9 0.025(2) 0.027(2) 0.029(2) 0.0034(18) 0.0088(18) 0.0091(18)

C10 0.028(2) 0.025(2) 0.032(2) 0.0027(18) 0.0077(19) 0.0091(18)

C11 0.030(2) 0.033(2) 0.031(2) 0.0065(19) 0.0067(19) 0.013(2)

C12 0.029(2) 0.028(2) 0.035(3) 0.0047(19) 0.010(2) 0.0140(19)

C13 0.033(3) 0.035(2) 0.044(3) 0.021(2) 0.015(2) 0.015(2)

C14 0.153(7) 0.075(4) 0.203(8) 0.104(5) 0.158(7) 0.098(5)

C15 0.028(2) 0.031(2) 0.034(2) 0.0103(19) 0.0138(19) 0.0143(19)

C16 0.025(2) 0.0189(19) 0.025(2) -0.0013(16) 0.0042(17) 0.0065(17)

C17 0.024(2) 0.019(2) 0.029(2) 0.0023(17) 0.0106(18) 0.0046(17)

C18 0.024(2) 0.019(2) 0.030(2) 0.0010(17) 0.0075(18) 0.0013(17)

C19 0.024(2) 0.0162(19) 0.031(2) 0.0023(16) 0.0106(18) 0.0082(16)

C20 0.021(2) 0.024(2) 0.028(2) 0.0020(17) 0.0096(18) 0.0045(17)

C21 0.034(3) 0.020(2) 0.034(2) 0.0073(18) 0.015(2) 0.0037(18)

C22 0.033(2) 0.017(2) 0.037(3) 0.0030(18) 0.009(2) 0.0065(18)

C23 0.029(2) 0.023(2) 0.033(2) 0.0003(18) 0.0138(19) 0.0074(18)

C24 0.028(2) 0.025(2) 0.034(2) 0.0047(18) 0.0102(19) 0.0086(18)

C25 0.026(2) 0.050(3) 0.041(3) 0.001(2) 0.011(2) 0.016(2)

_geom_special_details

;

All esds (except the esd in the dihedral angle between two l.s. planes)

are estimated using the full covariance matrix. The cell esds are taken
into account individually in the estimation of esds in distances, angles
and torsion angles; correlations between esds in cell parameters are only
used when they are defined by crystal symmetry. An approximate (isotropic)
treatment of cell esds is used for estimating esds involving l.s. planes.
;

loop_
_geom_bond_atom_site_label_1
_geom_bond_atom_site_label_2
_geom_bond_distance
_geom_bond_site_symmetry_2
_geom_bond_publ_flag
Cu1 O5 1.897(3) . ?
Cu1 O6 1.910(3) . ?
Cu1 N1 1.921(3) . ?
Cu1 O2 1.931(3) . ?
Cu2 O7 1.893(2) . ?
Cu2 O6 1.921(2) . ?
Cu2 N2 1.925(3) . ?
Cu2 O1 1.942(3) . ?
N1 C12 1.291(5) . ?
N1 C13 1.461(5) . ?
N2 C16 1.292(4) . ?
N2 C15 1.465(4) . ?
O1 C2 1.258(5) . ?
O2 C2 1.261(4) . ?
O3 C3 1.401(6) . ?
O3 C4 1.413(5) . ?
O4 C6 1.365(4) . ?

O4 C5 1.435(5) . ?

O5 C10 1.316(4) . ?

O6 C14 1.378(5) . ?

O7 C18 1.323(4) . ?

O8 C20 1.359(4) . ?

O8 C23 1.436(4) . ?

O9 C24 1.422(4) . ?

O9 C25 1.428(5) . ?

C1 C2 1.497(5) . ?

C1 H1A 0.9800 . ?

C1 H1B 0.9800 . ?

C1 H1C 0.9800 . ?

C3 H3A 0.9800 . ?

C3 H3B 0.9800 . ?

C3 H3C 0.9800 . ?

C4 C5 1.509(5) . ?

C4 H4A 0.9900 . ?

C4 H4B 0.9900 . ?

C5 H5A 0.9900 . ?

C5 H5B 0.9900 . ?

C6 C11 1.380(5) . ?

C6 C7 1.406(5) . ?

C7 C8 1.368(5) . ?

C7 H7A 0.9500 . ?

C8 C9 1.398(5) . ?

C8 H8A 0.9500 . ?

C9 C10 1.419(5) . ?

C9 C12 1.438(5) . ?

C10 C11 1.414(5) . ?

C11 H11A 0.9500 . ?

C12 H12A 0.9500 . ?

C13 C14 1.412(6) . ?

C13 H13A 0.9900 . ?

C13 H13B 0.9900 . ?

C14 C15 1.429(6) . ?

C14 H14A 1.0000 . ?

C15 H15A 0.9900 . ?

C15 H15B 0.9900 . ?

C16 C17 1.432(5) . ?

C16 H16A 0.9500 . ?

C17 C18 1.412(5) . ?

C17 C22 1.417(5) . ?

C18 C19 1.414(5) . ?

C19 C20 1.377(5) . ?

C19 H19A 0.9500 . ?

C20 C21 1.399(5) . ?

C21 C22 1.364(5) . ?

C21 H21A 0.9500 . ?

C22 H22A 0.9500 . ?

C23 C24 1.503(5) . ?

C23 H23A 0.9900 . ?

C23 H23B 0.9900 . ?

C24 H24A 0.9900 . ?

C24 H24B 0.9900 . ?

C25 H25A 0.9800 . ?

C25 H25B 0.9800 . ?

C25 H25C 0.9800 . ?

loop_

_geom_angle_atom_site_label_1

_geom_angle_atom_site_label_2
_geom_angle_atom_site_label_3
_geom_angle
_geom_angle_site_symmetry_1
_geom_angle_site_symmetry_3
_geom_angle_publ_flag
O5 Cu1 O6 173.68(13) . . ?
O5 Cu1 N1 93.56(12) . . ?
O6 Cu1 N1 84.77(12) . . ?
O5 Cu1 O2 87.79(11) . . ?
O6 Cu1 O2 94.54(11) . . ?
N1 Cu1 O2 173.61(14) . . ?
O7 Cu2 O6 175.31(12) . . ?
O7 Cu2 N2 93.30(12) . . ?
O6 Cu2 N2 83.90(12) . . ?
O7 Cu2 O1 87.64(11) . . ?
O6 Cu2 O1 94.58(11) . . ?
N2 Cu2 O1 171.43(13) . . ?
C12 N1 C13 120.1(3) . . ?
C12 N1 Cu1 127.1(3) . . ?
C13 N1 Cu1 112.7(2) . . ?
C16 N2 C15 120.6(3) . . ?
C16 N2 Cu2 125.7(3) . . ?
C15 N2 Cu2 113.6(2) . . ?
C2 O1 Cu2 135.0(3) . . ?
C2 O2 Cu1 136.1(3) . . ?
C3 O3 C4 112.9(3) . . ?
C6 O4 C5 118.3(3) . . ?
C10 O5 Cu1 127.1(3) . . ?
C14 O6 Cu1 113.1(2) . . ?

C14 O6 Cu2 113.9(3) . . ?

Cu1 O6 Cu2 132.45(14) . . ?

C18 O7 Cu2 127.5(2) . . ?

C20 O8 C23 119.4(3) . . ?

C24 O9 C25 109.3(3) . . ?

C2 C1 H1A 109.5 . . ?

C2 C1 H1B 109.5 . . ?

H1A C1 H1B 109.5 . . ?

C2 C1 H1C 109.5 . . ?

H1A C1 H1C 109.5 . . ?

H1B C1 H1C 109.5 . . ?

O1 C2 O2 126.6(4) . . ?

O1 C2 C1 116.7(3) . . ?

O2 C2 C1 116.7(3) . . ?

O3 C3 H3A 109.5 . . ?

O3 C3 H3B 109.5 . . ?

H3A C3 H3B 109.5 . . ?

O3 C3 H3C 109.5 . . ?

H3A C3 H3C 109.5 . . ?

H3B C3 H3C 109.5 . . ?

O3 C4 C5 112.2(4) . . ?

O3 C4 H4A 109.2 . . ?

C5 C4 H4A 109.2 . . ?

O3 C4 H4B 109.2 . . ?

C5 C4 H4B 109.2 . . ?

H4A C4 H4B 107.9 . . ?

O4 C5 C4 107.4(3) . . ?

O4 C5 H5A 110.2 . . ?

C4 C5 H5A 110.2 . . ?

O4 C5 H5B 110.2 . . ?

C4 C5 H5B 110.2 . . ?

H5A C5 H5B 108.5 . . ?

O4 C6 C11 124.6(4) . . ?

O4 C6 C7 114.4(3) . . ?

C11 C6 C7 121.1(4) . . ?

C8 C7 C6 118.5(4) . . ?

C8 C7 H7A 120.7 . . ?

C6 C7 H7A 120.7 . . ?

C7 C8 C9 122.3(4) . . ?

C7 C8 H8A 118.9 . . ?

C9 C8 H8A 118.9 . . ?

C8 C9 C10 119.3(4) . . ?

C8 C9 C12 117.7(4) . . ?

C10 C9 C12 123.0(3) . . ?

O5 C10 C11 117.4(4) . . ?

O5 C10 C9 124.5(4) . . ?

C11 C10 C9 118.1(3) . . ?

C6 C11 C10 120.6(4) . . ?

C6 C11 H11A 119.7 . . ?

C10 C11 H11A 119.7 . . ?

N1 C12 C9 124.4(4) . . ?

N1 C12 H12A 117.8 . . ?

C9 C12 H12A 117.8 . . ?

C14 C13 N1 111.1(4) . . ?

C14 C13 H13A 109.4 . . ?

N1 C13 H13A 109.4 . . ?

C14 C13 H13B 109.4 . . ?

N1 C13 H13B 109.4 . . ?

H13A C13 H13B 108.0 . . ?

O6 C14 C13 116.9(4) . . ?

O6 C14 C15 117.0(4) . . ?

C13 C14 C15 124.0(4) . . ?

O6 C14 H14A 94.8 . . ?

C13 C14 H14A 94.8 . . ?

C15 C14 H14A 94.8 . . ?

C14 C15 N2 110.3(3) . . ?

C14 C15 H15A 109.6 . . ?

N2 C15 H15A 109.6 . . ?

C14 C15 H15B 109.6 . . ?

N2 C15 H15B 109.6 . . ?

H15A C15 H15B 108.1 . . ?

N2 C16 C17 125.6(4) . . ?

N2 C16 H16A 117.2 . . ?

C17 C16 H16A 117.2 . . ?

C18 C17 C22 118.6(3) . . ?

C18 C17 C16 123.0(3) . . ?

C22 C17 C16 118.4(3) . . ?

O7 C18 C17 123.4(3) . . ?

O7 C18 C19 117.7(3) . . ?

C17 C18 C19 118.8(3) . . ?

C20 C19 C18 120.6(3) . . ?

C20 C19 H19A 119.7 . . ?

C18 C19 H19A 119.7 . . ?

O8 C20 C19 124.4(3) . . ?

O8 C20 C21 114.8(3) . . ?

C19 C20 C21 120.8(3) . . ?

C22 C21 C20 119.2(3) . . ?

C22 C21 H21A 120.4 . . ?

C20 C21 H21A 120.4 . . ?

C21 C22 C17 121.9(4) . . ?

C21 C22 H22A 119.1 . . ?

C17 C22 H22A 119.1 . . ?

O8 C23 C24 103.6(3) . . ?

O8 C23 H23A 111.0 . . ?

C24 C23 H23A 111.0 . . ?

O8 C23 H23B 111.0 . . ?

C24 C23 H23B 111.0 . . ?

H23A C23 H23B 109.0 . . ?

O9 C24 C23 110.0(3) . . ?

O9 C24 H24A 109.7 . . ?

C23 C24 H24A 109.7 . . ?

O9 C24 H24B 109.7 . . ?

C23 C24 H24B 109.7 . . ?

H24A C24 H24B 108.2 . . ?

O9 C25 H25A 109.5 . . ?

O9 C25 H25B 109.5 . . ?

H25A C25 H25B 109.5 . . ?

O9 C25 H25C 109.5 . . ?

H25A C25 H25C 109.5 . . ?

H25B C25 H25C 109.5 . . ?

loop_

_geom_torsion_atom_site_label_1

_geom_torsion_atom_site_label_2

_geom_torsion_atom_site_label_3

_geom_torsion_atom_site_label_4

_geom_torsion

_geom_torsion_site_symmetry_1

_geom_torsion_site_symmetry_2

_geom_torsion_site_symmetry_3

_geom_torsion_site_symmetry_4

_geom_torsion_publ_flag

O5 Cu1 N1 C12 5.8(4) . . . . ?

O6 Cu1 N1 C12 179.7(4) . . . . ?

O2 Cu1 N1 C12 -96.2(11) . . . . ?

O5 Cu1 N1 C13 -177.1(3) . . . . ?

O6 Cu1 N1 C13 -3.2(3) . . . . ?

O2 Cu1 N1 C13 80.8(12) . . . . ?

O7 Cu2 N2 C16 10.9(3) . . . . ?

O6 Cu2 N2 C16 -165.3(4) . . . . ?

O1 Cu2 N2 C16 -85.1(9) . . . . ?

O7 Cu2 N2 C15 -173.2(3) . . . . ?

O6 Cu2 N2 C15 10.6(3) . . . . ?

O1 Cu2 N2 C15 90.7(8) . . . . ?

O7 Cu2 O1 C2 174.9(4) . . . . ?

O6 Cu2 O1 C2 -9.2(4) . . . . ?

N2 Cu2 O1 C2 -88.6(9) . . . . ?

O5 Cu1 O2 C2 174.1(4) . . . . ?

O6 Cu1 O2 C2 0.0(4) . . . . ?

N1 Cu1 O2 C2 -83.5(12) . . . . ?

O6 Cu1 O5 C10 -77.0(11) . . . . ?

N1 Cu1 O5 C10 -2.6(4) . . . . ?

O2 Cu1 O5 C10 171.2(4) . . . . ?

O5 Cu1 O6 C14 70.6(12) . . . . ?

N1 Cu1 O6 C14 -4.3(5) . . . . ?

O2 Cu1 O6 C14 -178.0(5) . . . . ?

O5 Cu1 O6 Cu2 -118.6(10) . . . . ?

N1 Cu1 O6 Cu2 166.5(2) . . . . ?

O2 Cu1 O6 Cu2 -7.2(2) . . . . ?

O7 Cu2 O6 C14 -61.3(16) . . . . ?

N2 Cu2 O6 C14 -7.7(5) . . . . ?

O1 Cu2 O6 C14 -179.2(5) . . . . ?

O7 Cu2 O6 Cu1 128.0(13) . . . . ?

N2 Cu2 O6 Cu1 -178.5(2) . . . . ?

O1 Cu2 O6 Cu1 10.0(2) . . . . ?

O6 Cu2 O7 C18 40.4(16) . . . . ?

N2 Cu2 O7 C18 -12.8(3) . . . . ?

O1 Cu2 O7 C18 158.7(3) . . . . ?

Cu2 O1 C2 O2 5.2(7) . . . . ?

Cu2 O1 C2 C1 -175.9(3) . . . . ?

Cu1 O2 C2 O1 1.0(8) . . . . ?

Cu1 O2 C2 C1 -177.9(3) . . . . ?

C3 O3 C4 C5 88.2(4) . . . . ?

C6 O4 C5 C4 -176.2(4) . . . . ?

O3 C4 C5 O4 71.5(4) . . . . ?

C5 O4 C6 C11 4.5(6) . . . . ?

C5 O4 C6 C7 -174.7(4) . . . . ?

O4 C6 C7 C8 179.6(4) . . . . ?

C11 C6 C7 C8 0.3(7) . . . . ?

C6 C7 C8 C9 0.7(7) . . . . ?

C7 C8 C9 C10 -1.8(7) . . . . ?

C7 C8 C9 C12 177.2(4) . . . . ?

Cu1 O5 C10 C11 179.1(3) . . . . ?

Cu1 O5 C10 C9 -1.0(6) . . . . ?

C8 C9 C10 O5 -178.1(4) . . . . ?

C12 C9 C10 O5 3.0(7) . . . . ?

C8 C9 C10 C11 1.8(6) . . . . ?

C12 C9 C10 C11 -177.1(4) . . . . ?

O4 C6 C11 C10 -179.5(4) . . . . ?

C7 C6 C11 C10 -0.3(7) . . . . ?

O5 C10 C11 C6 179.1(4) . . . . ?

C9 C10 C11 C6 -0.8(6) . . . . ?

C13 N1 C12 C9 177.6(4) . . . . ?

Cu1 N1 C12 C9 -5.6(6) . . . . ?

C8 C9 C12 N1 -178.4(4) . . . . ?

C10 C9 C12 N1 0.5(7) . . . . ?

C12 N1 C13 C14 -172.8(6) . . . . ?

Cu1 N1 C13 C14 9.9(6) . . . . ?

Cu1 O6 C14 C13 11.6(9) . . . . ?

Cu2 O6 C14 C13 -161.0(5) . . . . ?

Cu1 O6 C14 C15 175.9(5) . . . . ?

Cu2 O6 C14 C15 3.3(9) . . . . ?

N1 C13 C14 O6 -14.0(9) . . . . ?

N1 C13 C14 C15 -177.0(7) . . . . ?

O6 C14 C15 N2 5.2(9) . . . . ?

C13 C14 C15 N2 168.2(7) . . . . ?

C16 N2 C15 C14 164.8(5) . . . . ?

Cu2 N2 C15 C14 -11.3(6) . . . . ?

C15 N2 C16 C17 -179.6(4) . . . . ?

Cu2 N2 C16 C17 -4.0(6) . . . . ?

N2 C16 C17 C18 -5.7(7) . . . . ?

N2 C16 C17 C22 174.2(4) . . . . ?

Cu2 O7 C18 C17 7.6(6) . . . . ?

Cu2 O7 C18 C19 -170.0(3) . . . . ?

C22 C17 C18 O7 -176.0(4) . . . . ?

C16 C17 C18 O7 3.9(6) . . . . ?

C22 C17 C18 C19 1.6(6) . . . . ?

C16 C17 C18 C19 -178.4(4) . . . . ?

O7 C18 C19 C20 176.3(4) . . . . ?

C17 C18 C19 C20 -1.5(6) . . . . ?

C23 O8 C20 C19 -5.1(6) . . . . ?

C23 O8 C20 C21 176.9(4) . . . . ?

C18 C19 C20 O8 -178.6(4) . . . . ?

C18 C19 C20 C21 -0.7(6) . . . . ?

O8 C20 C21 C22 -179.3(4) . . . . ?

C19 C20 C21 C22 2.7(6) . . . . ?

C20 C21 C22 C17 -2.5(7) . . . . ?

C18 C17 C22 C21 0.3(6) . . . . ?

C16 C17 C22 C21 -179.6(4) . . . . ?

C20 O8 C23 C24 -176.4(4) . . . . ?

C25 O9 C24 C23 174.3(4) . . . . ?

O8 C23 C24 O9 175.6(3) . . . . ?

_diffrn_measured_fraction_theta_max 0.985

_diffrn_reflns_theta_full 28.31

_diffrn_measured_fraction_theta_full 0.985

_refine_diff_density_max 0.809

_refine_diff_density_min -0.688

_refine_diff_density_rms 0.098

APPENDIX 2

CRYSTAL STRUCTURE DATA FOR COMPOUND **26**

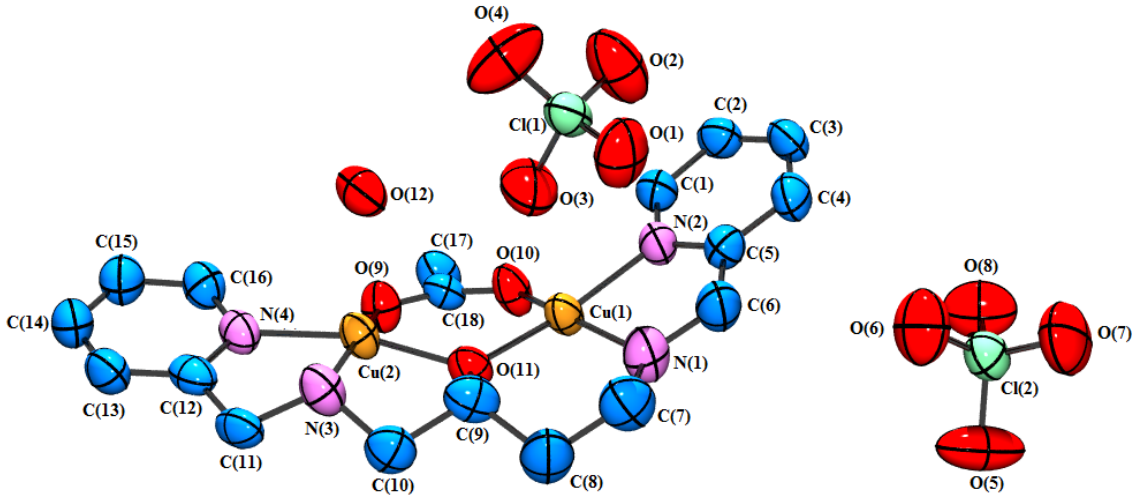

```
data_save

_audit_creation_method           SHELXL-97
_chemical_name_systematic
;
 ?
;
_chemical_name_common            ?
_chemical_melting_point          ?
_chemical_formula_moiety         'C18 H24 Cl Cu2 N4 O8, Cl O4'
_chemical_formula_sum            'C18 H24 Cl2 Cu2 N4 O12'
_chemical_formula_weight         686.41

loop_
 _atom_type_symbol
 _atom_type_description
 _atom_type_scat_dispersion_real
 _atom_type_scat_dispersion_imag
 _atom_type_scat_source
 'C'  'C'   0.0033   0.0016
 'International Tables Vol C Tables 4.2.6.8 and 6.1.1.4'
 'H'  'H'   0.0000   0.0000
 'International Tables Vol C Tables 4.2.6.8 and 6.1.1.4'
 'N'  'N'   0.0061   0.0033
 'International Tables Vol C Tables 4.2.6.8 and 6.1.1.4'
 'O'  'O'   0.0106   0.0060
 'International Tables Vol C Tables 4.2.6.8 and 6.1.1.4'
 'Cl'  'Cl'   0.1484   0.1585
 'International Tables Vol C Tables 4.2.6.8 and 6.1.1.4'
 'Cu'  'Cu'   0.3201   1.2651
```

'International Tables Vol C Tables 4.2.6.8 and 6.1.1.4'

```
_symmetry_cell_setting          'Monoclinic'
_symmetry_space_group_name_H-M    'P 21/n'
_symmetry_space_group_name_Hall   '-P 2yn'
loop_
 _symmetry_equiv_pos_as_xyz
 'x, y, z'
 '-x+1/2, y+1/2, -z+1/2'
 '-x, -y, -z'
 'x-1/2, -y-1/2, z-1/2'

_cell_length_a                  15.0763(17)
_cell_length_b                  12.2502(14)
_cell_length_c                  15.3221(18)
_cell_angle_alpha                90.00
_cell_angle_beta                 116.020(2)
_cell_angle_gamma                90.00
_cell_volume                    2543.0(5)
_cell_formula_units_Z            4
_cell_measurement_temperature     153(2)
_cell_measurement_reflns_used     4539
_cell_measurement_theta_min       2.23
_cell_measurement_theta_max       28.34

_exptl_crystal_description        'Platelet'
_exptl_crystal_colour            'Blue'
_exptl_crystal_size_max           0.304
_exptl_crystal_size_mid           0.250
_exptl_crystal_size_min           0.168
```

```
_exptl_crystal_density_meas       'nm'
_exptl_crystal_density_diffrn     1.793
_exptl_crystal_density_method     'not measured'
_exptl_crystal_F_000              1392
_exptl_absorpt_coefficient_mu     1.951
_exptl_absorpt_correction_type    'numerical'
_exptl_absorpt_correction_T_min   0.5671
_exptl_absorpt_correction_T_max   0.7155
_exptl_absorpt_process_details    'SHELXPREP'

_exptl_special_details
;
 ?
;

_diffrn_ambient_temperature       153(2)
_diffrn_radiation_wavelength      0.71073
_diffrn_radiation_type            MoK\a
_diffrn_radiation_source          'fine-focus sealed tube'
_diffrn_radiation_monochromator   'graphite'
_diffrn_measurement_device_type   'Bruker APEX'
_diffrn_measurement_method        '0.3 wide /w exposures'
_diffrn_detector_area_resol_mean  ?
_diffrn_standards_number          'na'
_diffrn_standards_interval_count  'na'
_diffrn_standards_interval_time   'na'
_diffrn_standards_decay_%         0
_diffrn_reflns_number             24008
_diffrn_reflns_av_R_equivalents   0.0453
_diffrn_reflns_av_sigmaI/netI     0.0486
```

```
_diffrn_reflns_limit_h_min       -20
_diffrn_reflns_limit_h_max        20
_diffrn_reflns_limit_k_min       -16
_diffrn_reflns_limit_k_max        16
_diffrn_reflns_limit_l_min       -20
_diffrn_reflns_limit_l_max        20
_diffrn_reflns_theta_min         2.23
_diffrn_reflns_theta_max         28.34
_reflns_number_total             6303
_reflns_number_gt                4539
_reflns_threshold_expression     >2sigma(I)

_computing_data_collection       'SMART'
_computing_cell_refinement       'SMART, SAINT'
_computing_data_reduction        'SAINT'
_computing_structure_solution    'SHELXS-97 (Sheldrick, 1990)'
_computing_structure_refinement  'SHELXL-97 (Sheldrick, 1997)'
_computing_molecular_graphics    'SHELXP-97 (Sheldrick, 1990)'
_computing_publication_material  'SHELXS-97 (Sheldrick, 2000)'

_refine_special_details
;
 Refinement of F^2^ against ALL reflections.  The weighted R-factor wR and
 goodness of fit S are based on F^2^, conventional R-factors R are based
 on F, with F set to zero for negative F^2^. The threshold expression of
 F^2^ > 2sigma(F^2^) is used only for calculating R-factors(gt) etc. and is
 not relevant to the choice of reflections for refinement.  R-factors based
 on F^2^ are statistically about twice as large as those based on F, and R-
 factors based on ALL data will be even larger.
;
```

```
_refine_ls_structure_factor_coef  Fsqd
_refine_ls_matrix_type            full
_refine_ls_weighting_scheme       calc
_refine_ls_weighting_details
 'calc w=1/[\s^2^(Fo^2^)+(0.1193P)^2^+3.1883P] where P=(Fo^2^+2Fc^2^)/3'
_atom_sites_solution_primary      direct
_atom_sites_solution_secondary    difmap
_atom_sites_solution_hydrogens    geom
_refine_ls_hydrogen_treatment     constr
_refine_ls_extinction_method      SHELXL
_refine_ls_extinction_coef        0
_refine_ls_number_reflns          6303
_refine_ls_number_parameters      343
_refine_ls_number_restraints      0
_refine_ls_R_factor_all           0.0818
_refine_ls_R_factor_gt            0.0584
_refine_ls_wR_factor_ref          0.1830
_refine_ls_wR_factor_gt           0.1637
_refine_ls_goodness_of_fit_ref    0.970
_refine_ls_restrained_S_all       0.970
_refine_ls_shift/su_max           0.000
_refine_ls_shift/su_mean          0.000

loop_
 _atom_site_label
 _atom_site_type_symbol
 _atom_site_fract_x
 _atom_site_fract_y
 _atom_site_fract_z
```

_atom_site_U_iso_or_equiv
_atom_site_adp_type
_atom_site_occupancy
_atom_site_symmetry_multiplicity
_atom_site_calc_flag
_atom_site_refinement_flags
_atom_site_disorder_assembly
_atom_site_disorder_group
Cl2 Cl -0.08792(9) 0.47279(9) 0.33548(8) 0.0376(3) Uani 1 1 d . . .
O8 O -0.0154(3) 0.4069(3) 0.4089(3) 0.0626(12) Uani 1 1 d . . .
O7 O -0.1593(4) 0.5148(5) 0.3646(4) 0.0765(15) Uani 1 1 d . . .
O6 O -0.0408(3) 0.5660(4) 0.3173(4) 0.0667(12) Uani 1 1 d . . .
O5 O -0.1367(4) 0.4094(4) 0.2497(3) 0.0766(15) Uani 1 1 d . . .
Cu1 Cu 0.32331(4) 0.51714(5) 0.23731(4) 0.03108(17) Uani 1 1 d . . .
Cu2 Cu 0.46043(4) 0.59669(4) 0.12270(4) 0.03145(17) Uani 1 1 d . . .
N2 N 0.3169(3) 0.4786(3) 0.3618(3) 0.0318(8) Uani 1 1 d . . .
N4 N 0.5674(3) 0.6214(3) 0.0809(3) 0.0330(8) Uani 1 1 d . . .
N3 N 0.3911(3) 0.7053(3) 0.0188(3) 0.0396(9) Uani 1 1 d . . .
H3AA H 0.4015 0.7736 0.0482 0.048 Uiso 1 1 calc R . .
N1 N 0.1865(3) 0.5676(4) 0.2016(3) 0.0426(10) Uani 1 1 d . . .
H1B H 0.1548 0.5024 0.1743 0.051 Uiso 1 1 calc R . .
C18 C 0.5110(3) 0.4141(3) 0.2573(3) 0.0289(8) Uani 1 1 d . . .
C12 C 0.5399(4) 0.6820(4) 0.0002(3) 0.0365(10) Uani 1 1 d . . .
C4 C 0.2213(4) 0.5027(4) 0.4494(4) 0.0386(10) Uani 1 1 d . . .
H4A H 0.1617 0.5258 0.4506 0.046 Uiso 1 1 calc R . .
C2 C 0.3818(4) 0.4230(4) 0.5265(3) 0.0378(10) Uani 1 1 d . . .
H2A H 0.4348 0.3923 0.5817 0.045 Uiso 1 1 calc R . .
C5 C 0.2340(3) 0.5135(4) 0.3666(3) 0.0340(9) Uani 1 1 d . . .
C10 C 0.2860(4) 0.6808(4) -0.0182(3) 0.0408(11) Uani 1 1 d . . .
H10B H 0.2687 0.6159 -0.0610 0.049 Uiso 1 1 calc R . .

H10A H 0.2460 0.7434 -0.0560 0.049 Uiso 1 1 calc R . .

C3 C 0.2974(4) 0.4574(4) 0.5320(3) 0.0380(10) Uani 1 1 d . . .

H3A H 0.2910 0.4504 0.5907 0.046 Uiso 1 1 calc R . .

C17 C 0.5801(3) 0.3216(4) 0.3056(3) 0.0377(10) Uani 1 1 d . . .

H17C H 0.6327 0.3207 0.2844 0.057 Uiso 1 1 calc R . .

H17B H 0.5437 0.2525 0.2878 0.057 Uiso 1 1 calc R . .

H17A H 0.6090 0.3311 0.3762 0.057 Uiso 1 1 calc R . .

C16 C 0.6625(4) 0.5932(4) 0.1311(4) 0.0369(10) Uani 1 1 d . . .

H16A H 0.6815 0.5518 0.1890 0.044 Uiso 1 1 calc R . .

C1 C 0.3883(3) 0.4339(4) 0.4395(3) 0.0337(9) Uani 1 1 d . . .

H1A H 0.4459 0.4083 0.4355 0.040 Uiso 1 1 calc R . .

C15 C 0.7334(4) 0.6220(4) 0.1020(4) 0.0428(11) Uani 1 1 d . . .

H15A H 0.8001 0.5998 0.1380 0.051 Uiso 1 1 calc R . .

C13 C 0.6076(4) 0.7152(4) -0.0327(4) 0.0436(12) Uani 1 1 d . . .

H13A H 0.5872 0.7584 -0.0897 0.052 Uiso 1 1 calc R . .

C9 C 0.2663(3) 0.6590(4) 0.0693(3) 0.0400(11) Uani 1 1 d . . .

H9A H 0.2792 0.7278 0.1082 0.048 Uiso 1 1 calc R . .

C14 C 0.7048(4) 0.6848(5) 0.0181(4) 0.0477(13) Uani 1 1 d . . .

H14A H 0.7521 0.7063 -0.0039 0.057 Uiso 1 1 calc R . .

C11 C 0.4322(4) 0.7084(4) -0.0508(3) 0.0381(10) Uani 1 1 d . . .

H11A H 0.4228 0.7819 -0.0804 0.046 Uiso 1 1 calc R . .

H11B H 0.3980 0.6547 -0.1032 0.046 Uiso 1 1 calc R . .

C6 C 0.1613(4) 0.5703(5) 0.2777(4) 0.0435(11) Uani 1 1 d . . .

H6A H 0.0958 0.5357 0.2569 0.052 Uiso 1 1 calc R . .

H6B H 0.1557 0.6473 0.2941 0.052 Uiso 1 1 calc R . .

C7 C 0.1298(4) 0.6371(5) 0.1197(4) 0.0504(13) Uani 1 1 d . . .

H7A H 0.1378 0.7141 0.1415 0.061 Uiso 1 1 calc R . .

H7B H 0.0590 0.6181 0.0940 0.061 Uiso 1 1 calc R . .

C8 C 0.1618(4) 0.6257(6) 0.0398(4) 0.0526(14) Uani 1 1 d . . .

H8A H 0.1535 0.5487 0.0182 0.063 Uiso 1 1 calc R . .

H8B H 0.1181 0.6709 -0.0162 0.063 Uiso 1 1 calc R . .

O11 O 0.3351(2) 0.5773(3) 0.1280(2) 0.0327(7) Uani 1 1 d . . .

O10 O 0.4396(2) 0.4261(3) 0.2779(2) 0.0386(8) Uani 1 1 d . . .

O9 O 0.5297(2) 0.4729(3) 0.2006(2) 0.0355(7) Uani 1 1 d . . .

O12 O 0.5325(3) 0.7161(3) 0.2508(3) 0.0471(9) Uani 1 1 d . . .

Cl1 Cl 0.37342(8) 0.78216(10) 0.37738(8) 0.0376(3) Uani 1 1 d . . .

O4 O 0.4380(3) 0.8699(4) 0.3905(4) 0.0758(14) Uani 1 1 d . . .

O1 O 0.2728(3) 0.8168(4) 0.3373(3) 0.0603(11) Uani 1 1 d . . .

O3 O 0.3829(4) 0.7047(4) 0.3106(3) 0.0701(13) Uani 1 1 d . . .

O2 O 0.3997(3) 0.7263(4) 0.4680(3) 0.0737(14) Uani 1 1 d . . .

loop_

_atom_site_aniso_label

_atom_site_aniso_U_11

_atom_site_aniso_U_22

_atom_site_aniso_U_33

_atom_site_aniso_U_23

_atom_site_aniso_U_13

_atom_site_aniso_U_12

Cl2 0.0386(6) 0.0402(6) 0.0348(6) 0.0018(5) 0.0168(5) 0.0053(5)

O8 0.070(3) 0.047(2) 0.050(2) 0.0110(18) 0.007(2) 0.0141(19)

O7 0.057(3) 0.111(4) 0.076(3) -0.008(3) 0.041(3) 0.012(3)

O6 0.073(3) 0.057(3) 0.080(3) 0.014(2) 0.043(3) 0.000(2)

O5 0.077(3) 0.066(3) 0.049(3) -0.024(2) -0.007(2) 0.019(2)

Cu1 0.0271(3) 0.0420(3) 0.0232(3) 0.0029(2) 0.0101(2) 0.0052(2)

Cu2 0.0359(3) 0.0342(3) 0.0263(3) 0.0065(2) 0.0154(2) 0.0067(2)

N2 0.0303(18) 0.038(2) 0.0286(18) 0.0011(15) 0.0143(15) 0.0007(15)

N4 0.042(2) 0.0295(18) 0.0299(19) 0.0009(15) 0.0183(17) -0.0023(16)

N3 0.045(2) 0.044(2) 0.032(2) 0.0054(17) 0.0184(18) 0.0050(18)

N1 0.037(2) 0.048(2) 0.043(2) 0.0091(19) 0.0184(19) 0.0105(18)

C18 0.032(2) 0.031(2) 0.0207(18) -0.0012(16) 0.0088(16) 0.0027(16)

C12 0.050(3) 0.030(2) 0.027(2) -0.0051(18) 0.0154(19) -0.006(2)

C4 0.040(3) 0.041(3) 0.042(3) -0.005(2) 0.025(2) -0.002(2)

C2 0.039(2) 0.044(3) 0.026(2) 0.0009(19) 0.0100(19) -0.005(2)

C5 0.030(2) 0.037(2) 0.034(2) -0.0023(18) 0.0134(19) -0.0014(18)

C10 0.038(2) 0.046(3) 0.031(2) 0.007(2) 0.0082(19) 0.003(2)

C3 0.048(3) 0.043(3) 0.028(2) -0.0037(19) 0.021(2) -0.006(2)

C17 0.037(2) 0.043(3) 0.032(2) 0.008(2) 0.0148(19) 0.013(2)

C16 0.041(3) 0.035(2) 0.036(2) 0.0024(19) 0.019(2) 0.0018(19)

C1 0.033(2) 0.038(2) 0.030(2) -0.0001(18) 0.0130(18) -0.0007(18)

C15 0.043(3) 0.044(3) 0.044(3) -0.002(2) 0.022(2) -0.003(2)

C13 0.054(3) 0.049(3) 0.029(2) -0.001(2) 0.019(2) -0.011(2)

C9 0.037(2) 0.042(3) 0.031(2) 0.004(2) 0.0066(19) 0.013(2)

C14 0.053(3) 0.057(3) 0.041(3) -0.007(2) 0.027(2) -0.018(3)

C11 0.050(3) 0.038(2) 0.021(2) 0.0019(18) 0.0103(19) -0.009(2)

C6 0.033(2) 0.060(3) 0.035(2) 0.005(2) 0.013(2) 0.000(2)

C7 0.036(3) 0.066(4) 0.041(3) 0.006(3) 0.009(2) 0.012(2)

C8 0.037(3) 0.075(4) 0.037(3) 0.011(3) 0.008(2) 0.002(3)

O11 0.0309(15) 0.0401(17) 0.0221(14) 0.0063(12) 0.0070(12) 0.0067(13)

O10 0.0348(17) 0.055(2) 0.0292(16) 0.0126(14) 0.0170(14) 0.0154(15)

O9 0.0362(17) 0.0358(17) 0.0373(17) 0.0105(14) 0.0187(14) 0.0079(13)

O12 0.062(2) 0.046(2) 0.0372(19) -0.0031(15) 0.0253(18) -0.0020(17)

Cl1 0.0357(5) 0.0463(6) 0.0277(5) -0.0036(4) 0.0110(4) 0.0030(5)

O4 0.043(2) 0.057(3) 0.098(4) 0.005(3) 0.004(2) -0.003(2)

O1 0.037(2) 0.079(3) 0.061(3) 0.017(2) 0.0186(18) 0.0100(19)

O3 0.093(3) 0.063(3) 0.073(3) -0.034(2) 0.054(3) -0.027(2)

O2 0.074(3) 0.105(4) 0.043(2) 0.024(2) 0.027(2) 0.030(3)

_geom_special_details

```
 All esds (except the esd in the dihedral angle between two l.s. planes)
 are estimated using the full covariance matrix.  The cell esds are taken
 into account individually in the estimation of esds in distances, angles
 and torsion angles; correlations between esds in cell parameters are only
 used when they are defined by crystal symmetry.  An approximate (isotropic)
 treatment of cell esds is used for estimating esds involving l.s. planes.
;

loop_
 _geom_bond_atom_site_label_1
 _geom_bond_atom_site_label_2
 _geom_bond_distance
 _geom_bond_site_symmetry_2
 _geom_bond_publ_flag
Cl2 O5 1.423(4) . ?
Cl2 O8 1.426(4) . ?
Cl2 O7 1.429(4) . ?
Cl2 O6 1.435(4) . ?
Cu1 O11 1.908(3) . ?
Cu1 O10 1.935(3) . ?
Cu1 N1 1.987(4) . ?
Cu1 N2 2.008(4) . ?
Cu2 O9 1.929(3) . ?
Cu2 O11 1.941(3) . ?
Cu2 N3 1.985(4) . ?
Cu2 N4 2.002(4) . ?
Cu2 O12 2.303(4) . ?
N2 C1 1.324(6) . ?
N2 C5 1.353(6) . ?
N4 C12 1.342(6) . ?
```

N4 C16 1.342(6) . ?

N3 C11 1.450(6) . ?

N3 C10 1.460(6) . ?

N3 H3AA 0.9300 . ?

N1 C6 1.376(6) . ?

N1 C7 1.446(7) . ?

N1 H1B 0.9300 . ?

C18 O9 1.252(5) . ?

C18 O10 1.257(5) . ?

C18 C17 1.497(6) . ?

C12 C13 1.382(7) . ?

C12 C11 1.496(7) . ?

C4 C5 1.370(7) . ?

C4 C3 1.397(7) . ?

C4 H4A 0.9500 . ?

C2 C3 1.377(7) . ?

C2 C1 1.386(6) . ?

C2 H2A 0.9500 . ?

C5 C6 1.493(7) . ?

C10 C9 1.520(7) . ?

C10 H10B 0.9900 . ?

C10 H10A 0.9900 . ?

C3 H3A 0.9500 . ?

C17 H17C 0.9800 . ?

C17 H17B 0.9800 . ?

C17 H17A 0.9800 . ?

C16 C15 1.373(7) . ?

C16 H16A 0.9500 . ?

C1 H1A 0.9500 . ?

C15 C14 1.394(8) . ?

C15 H15A 0.9500 . ?
C13 C14 1.375(8) . ?
C13 H13A 0.9500 . ?
C9 O11 1.439(5) . ?
C9 C8 1.492(7) . ?
C9 H9A 1.0000 . ?
C14 H14A 0.9500 . ?
C11 H11A 0.9900 . ?
C11 H11B 0.9900 . ?
C6 H6A 0.9900 . ?
C6 H6B 0.9900 . ?
C7 C8 1.505(8) . ?
C7 H7A 0.9900 . ?
C7 H7B 0.9900 . ?
C8 H8A 0.9900 . ?
C8 H8B 0.9900 . ?
Cl1 O4 1.405(5) . ?
Cl1 O1 1.428(4) . ?
Cl1 O2 1.439(4) . ?
Cl1 O3 1.448(4) . ?

loop_
_geom_angle_atom_site_label_1
_geom_angle_atom_site_label_2
_geom_angle_atom_site_label_3
_geom_angle
_geom_angle_site_symmetry_1
_geom_angle_site_symmetry_3
_geom_angle_publ_flag
O5 Cl2 O8 109.0(3) . . ?

O5 Cl2 O7 109.3(3) . . ?

O8 Cl2 O7 112.3(3) . . ?

O5 Cl2 O6 110.8(3) . . ?

O8 Cl2 O6 109.3(3) . . ?

O7 Cl2 O6 106.2(3) . . ?

O11 Cu1 O10 94.86(13) . . ?

O11 Cu1 N1 97.12(15) . . ?

O10 Cu1 N1 162.20(17) . . ?

O11 Cu1 N2 170.53(15) . . ?

O10 Cu1 N2 88.47(14) . . ?

N1 Cu1 N2 81.81(17) . . ?

O9 Cu2 O11 98.65(13) . . ?

O9 Cu2 N3 167.21(16) . . ?

O11 Cu2 N3 86.31(15) . . ?

O9 Cu2 N4 91.37(14) . . ?

O11 Cu2 N4 165.29(14) . . ?

N3 Cu2 N4 81.75(16) . . ?

O9 Cu2 O12 92.70(14) . . ?

O11 Cu2 O12 98.39(13) . . ?

N3 Cu2 O12 98.25(16) . . ?

N4 Cu2 O12 91.82(14) . . ?

C1 N2 C5 119.2(4) . . ?

C1 N2 Cu1 126.4(3) . . ?

C5 N2 Cu1 114.1(3) . . ?

C12 N4 C16 119.4(4) . . ?

C12 N4 Cu2 114.4(3) . . ?

C16 N4 Cu2 125.8(3) . . ?

C11 N3 C10 117.4(4) . . ?

C11 N3 Cu2 111.2(3) . . ?

C10 N3 Cu2 105.9(3) . . ?

C11 N3 H3AA 107.3 . . ?

C10 N3 H3AA 107.3 . . ?

Cu2 N3 H3AA 107.3 . . ?

C6 N1 C7 116.4(4) . . ?

C6 N1 Cu1 114.4(3) . . ?

C7 N1 Cu1 124.6(3) . . ?

C6 N1 H1B 97.1 . . ?

C7 N1 H1B 97.1 . . ?

Cu1 N1 H1B 97.1 . . ?

O9 C18 O10 125.9(4) . . ?

O9 C18 C17 117.3(4) . . ?

O10 C18 C17 116.8(4) . . ?

N4 C12 C13 121.3(5) . . ?

N4 C12 C11 115.2(4) . . ?

C13 C12 C11 123.5(4) . . ?

C5 C4 C3 119.0(4) . . ?

C5 C4 H4A 120.5 . . ?

C3 C4 H4A 120.5 . . ?

C3 C2 C1 119.1(4) . . ?

C3 C2 H2A 120.5 . . ?

C1 C2 H2A 120.5 . . ?

N2 C5 C4 121.8(4) . . ?

N2 C5 C6 115.1(4) . . ?

C4 C5 C6 123.0(4) . . ?

N3 C10 C9 107.0(4) . . ?

N3 C10 H10B 110.3 . . ?

C9 C10 H10B 110.3 . . ?

N3 C10 H10A 110.3 . . ?

C9 C10 H10A 110.3 . . ?

H10B C10 H10A 108.6 . . ?

C2 C3 C4 118.6(4) . . ?

C2 C3 H3A 120.7 . . ?

C4 C3 H3A 120.7 . . ?

C18 C17 H17C 109.5 . . ?

C18 C17 H17B 109.5 . . ?

H17C C17 H17B 109.5 . . ?

C18 C17 H17A 109.5 . . ?

H17C C17 H17A 109.5 . . ?

H17B C17 H17A 109.5 . . ?

N4 C16 C15 122.4(5) . . ?

N4 C16 H16A 118.8 . . ?

C15 C16 H16A 118.8 . . ?

N2 C1 C2 122.2(4) . . ?

N2 C1 H1A 118.9 . . ?

C2 C1 H1A 118.9 . . ?

C16 C15 C14 118.1(5) . . ?

C16 C15 H15A 120.9 . . ?

C14 C15 H15A 120.9 . . ?

C14 C13 C12 119.2(5) . . ?

C14 C13 H13A 120.4 . . ?

C12 C13 H13A 120.4 . . ?

O11 C9 C8 112.1(4) . . ?

O11 C9 C10 107.9(4) . . ?

C8 C9 C10 111.7(4) . . ?

O11 C9 H9A 108.4 . . ?

C8 C9 H9A 108.4 . . ?

C10 C9 H9A 108.4 . . ?

C13 C14 C15 119.5(5) . . ?

C13 C14 H14A 120.2 . . ?

C15 C14 H14A 120.2 . . ?

N3 C11 C12 109.1(4) . . ?

N3 C11 H11A 109.9 . . ?

C12 C11 H11A 109.9 . . ?

N3 C11 H11B 109.9 . . ?

C12 C11 H11B 109.9 . . ?

H11A C11 H11B 108.3 . . ?

N1 C6 C5 113.4(4) . . ?

N1 C6 H6A 108.9 . . ?

C5 C6 H6A 108.9 . . ?

N1 C6 H6B 108.9 . . ?

C5 C6 H6B 108.9 . . ?

H6A C6 H6B 107.7 . . ?

N1 C7 C8 111.9(4) . . ?

N1 C7 H7A 109.2 . . ?

C8 C7 H7A 109.2 . . ?

N1 C7 H7B 109.2 . . ?

C8 C7 H7B 109.2 . . ?

H7A C7 H7B 107.9 . . ?

C9 C8 C7 113.6(5) . . ?

C9 C8 H8A 108.9 . . ?

C7 C8 H8A 108.9 . . ?

C9 C8 H8B 108.9 . . ?

C7 C8 H8B 108.9 . . ?

H8A C8 H8B 107.7 . . ?

C9 O11 Cu1 119.8(3) . . ?

C9 O11 Cu2 109.7(3) . . ?

Cu1 O11 Cu2 123.46(15) . . ?

C18 O10 Cu1 137.8(3) . . ?

C18 O9 Cu2 131.0(3) . . ?

O4 Cl1 O1 111.9(3) . . ?

O4 Cl1 O2 110.3(3) . . ?

O1 Cl1 O2 110.3(3) . . ?

O4 Cl1 O3 108.9(3) . . ?

O1 Cl1 O3 107.9(3) . . ?

O2 Cl1 O3 107.5(3) . . ?

_diffrn_measured_fraction_theta_max 0.993

_diffrn_reflns_theta_full 28.34

_diffrn_measured_fraction_theta_full 0.993

_refine_diff_density_max 1.485

_refine_diff_density_min -1.043

_refine_diff_density_rms 0.137

APPENDIX 3

MOLAR ABSORPTIVITY OF DTBQ AT 420 NM IN METHANOL

A PLOT OF ABSORBANCE VS CONCENTRATION OF DTBQ (**20**) AT 420 NM IN MEOH AT 30 ^{o}C.

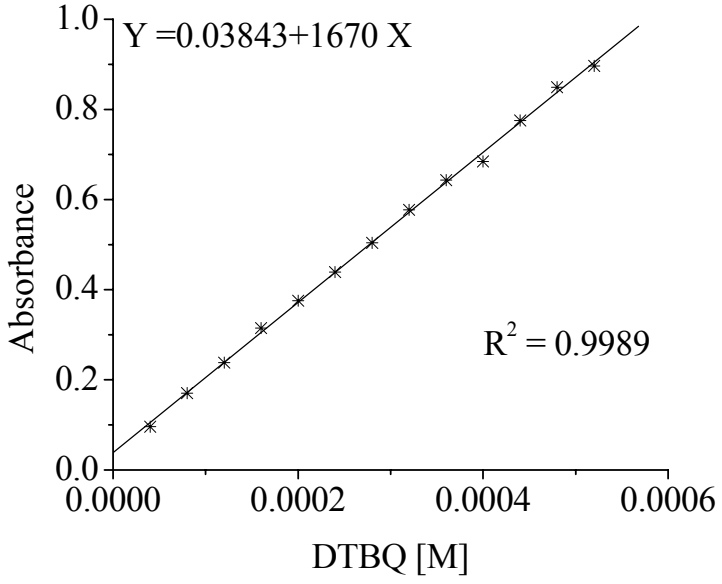

Molar absorpivity (ε) = 1670 $M^{-1}cm^{-1}$

APPENDIX 4

A PLOT OF ABSORBANCE VS TIME FOR THE OXIDATION OF DTBC IN METHANOL

A PLOT OF ABSORBANCE VS TIME FOR THE OXIDATION OF DTBC

(15 mM) USING **15C** (0.2 mM) IN METHANOL AT 30 ^{o}C.

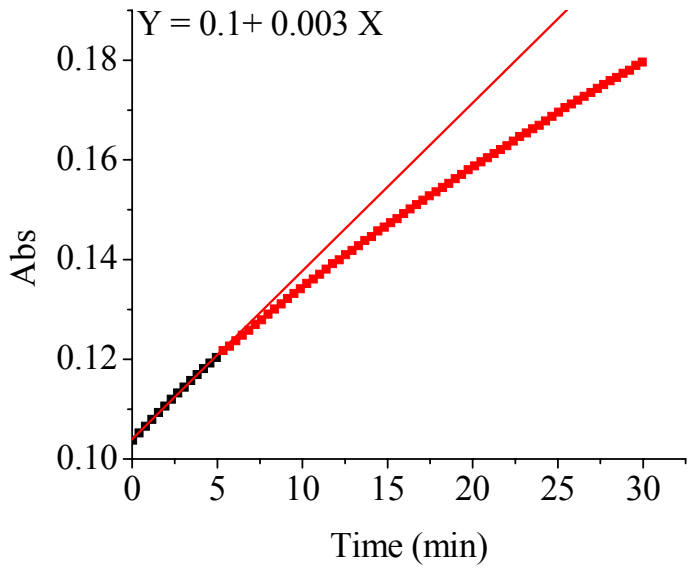

APPENDIX 5

MOLAR ABSORPTIVITY OF FOR 4-NITROPHENOL AT 30 ^{o}C IN 50 mM CAPS BUFFER AT pH 10.5

A PLOT OF ABSORBANCE VS CONCENTRATION OF 4-NITROPHENOL AT 410 NM IN CAPS BUFFER AT pH 10.5.

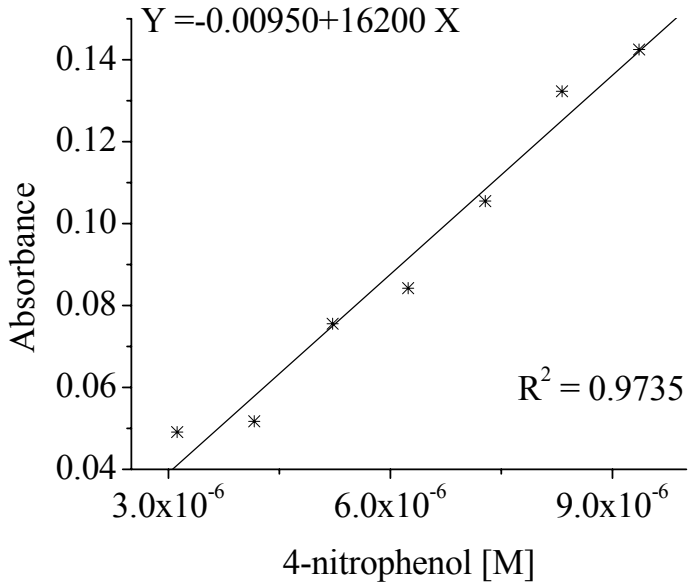

Molar absorpivity (ε) = 16200 $M^{-1}cm^{-1}$

APPENDIX 6

KINETIC PROFILES FOR THE NON-CATALYTIC HYDROLYSIS OF 4-NITROPHENYL-α-D-GALACTOPYRANOSIDE IN CAPS BUFFER AT pH 10.5. AND BORATE BUFFER AT pH 9.00

A PLOT OF RATE VS CONCENTRATION FOR NON-CATALYTIC HYDROLYSIS OF 4-NITROPHENYL-α-D-GALACTOPYRANOSIDE IN CAPS BUFFER AT pH 10.5.

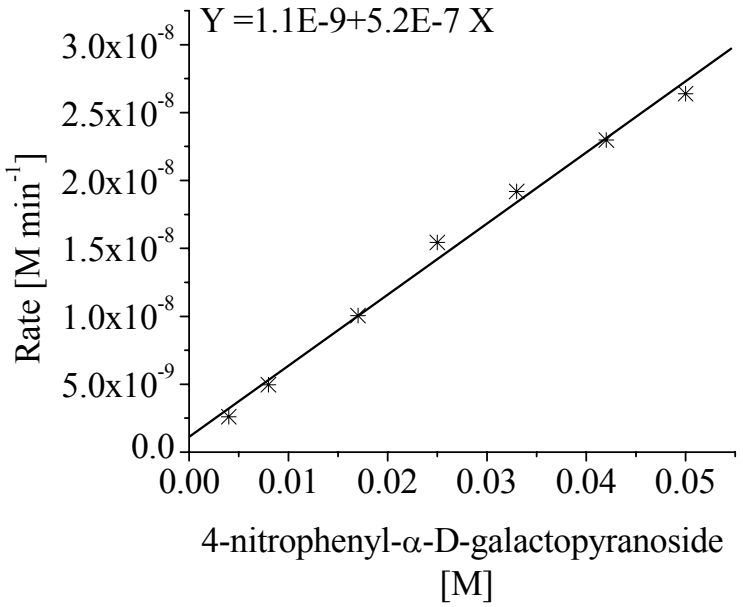

A PLOT OF RATE VS CONCENTRATION FOR NON-CATALYTIC HYDROLYSIS OF 4-NITROPHENYL-α-D-GALACTOPYRANOSIDE IN BORATE BUFFER AT pH 9.0.